Géographie physique et Quaternaire

Pingo Growth and collapse, Tuktoyaktuk Peninsula Area, Western Arctic Coast, Canada: a long-term field study

Croissance et affaissement des pingos de la péninsule de Tuktoyaktuk, côte occidentale de l'Arctique, Canada : une étude à long terme

Pingowachstum und Pingoeinsturz, Tuktoyaktuk Halbinsel, westarktische Küste, Kanada: Eine Langzeitgeländestudie.

J. Ross Mackay

Volume 52, numéro 3, 1998

URI : https://id.erudit.org/iderudit/004847ar
DOI : https://doi.org/10.7202/004847ar

Aller au sommaire du numéro

Éditeur(s)

Les Presses de l'Université de Montréal

ISSN

0705-7199 (imprimé)
1492-143X (numérique)

Découvrir la revue

Citer cet article

Mackay, J. R. (1998). Pingo Growth and collapse, Tuktoyaktuk Peninsula Area, Western Arctic Coast, Canada: a long-term field study. *Géographie physique et Quaternaire*, *52*(3), 271–323. https://doi.org/10.7202/004847ar

Résumé de l'article

Onze pingos ont fait l'objet d'une étude qui comprend des données de croissance et des relevés détaillés pour des périodes allant de 20 à 26 ans. La majorité des 1350 pingos, qui constituent peut-être le quart du total mondial, se sont développés dans des fonds de lacs asséchés, sous lesquels se trouvent des dépôts de sable. L'expansion du pergélisol dans ces dépressions lacustres asséchées a provoqué l'expulsion de l'eau interstitielle, le rejet des solutés sous le front de gel, une diminution du point de congélation et l'écoulement, à des températures sous 0° C, de l'eau souterraine vers des mares résiduelles, là où croissent les pingos. Sous de nombreux pingos en expansion se trouvent des lentilles d'eau. La glace pure qui se forme lors de la progression du ront de gel dans la lentille d'eau peut comporter des bandes de croissance saisonnières qui, tout comme les anneaux de croissance des arbres, peuvent être utiles à l'étude des paléoclimats. Les pingos en expansion comportant des lentilles d'eau sous jacentes peuvent souvent être identifiés à l'aide des caractéristiques suivantes : la rupture en périphérie du pingo, l'écoulement printanier, la croissance de buttes cryogènes, des failles normales et des oscillations de la hauteur du pingo. Ces caractéristiques, ainsi que d'autres, sont associées à la fracturation hydraulique et la perte en eau de la lentille sous-jacente. Certaines données dérivées de l'étude à long terme de la croissance des pingos sont utiles à l'identification des structures d'affaissement, structures que l'on associe à des paléo-pingos dans des régions actuellement sans pergélisol.

Géographie physique et Quaternaire, 1998, vol. 52, n° 3, p. 1- 53, 67 fig., 7 tabl.

PINGO GROWTH AND COLLAPSE, TUKTOYAKTUK PENINSULA AREA, WESTERN ARCTIC COAST, CANADA: A LONG-TERM FIELD STUDY*

J. Ross MACKAY, Department of Geography, University of British Columbia, Vancouver, British Columbia, V6T 1Z2.

Manuscrit reçu le 7 juillet 1997 ; manuscrit révisé et accepté le 25 novembre 1997

ABSTRACT Growth data from precise surveys have been obtained for 11 pingos for periods ranging from 20 to 26 years. Most of the 1350 pingos, perhaps one quarter of the world's total, have grown up in the bottoms of drained lakes underlain by sands. Permafrost aggradation on the drained lake bottoms has resulted in pore water expulsion, solute rejection below the freezing front, a freezing point depression, and groundwater flow at below 0°C to one or more residual ponds, the sites of pingo growth. Sub-pingo water lenses underlie many growing pingos. The pure ice which grows by downward freezing in a sub-pingo water lens may be composed of seasonal growth bands which, like tree rings, are of potential use in the study of past climates. Growing pingos underlain by sub-pingo water lenses can often be identified by features such as peripheral pingo rupture, spring flow, frost mound growth, normal faulting, and oscillations in pingo height. Such features, and others, are associated with hydrofracturing and water loss from a sub-pingo water lens. Some of the data derived from the long-term study of pingo growth are relevant to the identification of collapse features, interpreted as paleo-pingos, in areas now without permafrost.

RÉSUMÉ *Croissance et affaissement des pingos de la péninsule de Tuktoyaktuk, côte occidentale de l'Arctique, Canada : une étude à long terme.* Onze pingos ont fait l'objet d'une étude qui comprend des données de croissance et des relevés détaillés pour des périodes allant de 20 à 26 ans. La majorité des 1350 pingos, qui constituent peut-être le quart du total mondial, se sont développés dans des fonds de lacs asséchés, sous lesquels se trouvent des dépôts de sable. L'expansion du pergélisol dans ces dépressions lacustres asséchées a provoqué l'expulsion de l'eau interstitielle, le rejet des solutés sous le front de gel, une diminution du point de congélation et l'écoulement, à des températures sous 0 °C, de l'eau souterraine vers des mares résiduelles, là où croissent les pingos. Sous de nombreux pingos en expansion se trouvent des lentilles d'eau. La glace pure qui se forme lors de la progression du front de gel dans la lentille d'eau peut comporter des bandes de croissance saisonnières qui, tout comme les anneaux de croissance des arbres, peuvent être utiles à l'étude des paléoclimats. Les pingos en expansion comportant des lentilles d'eau sous-jacentes peuvent souvent être identifiés à l'aide des caractéristiques suivantes : la rupture en périphérie du pingo, l'écoulement printanier, la croissance de buttes cryogènes, des failles normales et des oscillations de la hauteur du pingo. Ces caractéristiques, ainsi que d'autres, sont associées à la fracturation hydraulique et la perte en eau de la lentille sous-jacente. Certaines données dérivées de l'étude à long terme de la croissance des pingos sont utiles à l'identification des structures d'affaissement, structures que l'on associe à des paléo-pingos dans des régions actuellement sans pergélisol.

ZUSAMMENFASSUNG *Pingowachstum und Pingoeinsturz, Tuktoyaktuk Halbinsel, westarktische Küste, Kanada: Eine Langzeitgeländestudie.* Wachstumsdaten wurden durch exakte Vermessungen für 11 Pingos über Zeiträume von 20 bis 26 Jahren gewonnen. Die meisten der 1350 Pingos, was vielleicht einem Viertel aller Pingos weltweit entspricht, sind in entwässerten Seen mit Sandgrund entstanden. Die Entstehung von Permafrost am Grunde dieser Seen hat Porenwasserausschleuderung, Lösungsverhinderung unter dem Gefrierpunkt, Gefrierpunktserniedrigung und Grundwasserströmung unter 0 °C zu einem oder mehreren zurückgebliebenen Tümpel, die der Pingoenstehung dienen, zur Folge. Linsenförmige Wassereinschlüsse unterlagern vielen Pingos während deren Entstehung. Das reine Eis, das durch tiefengerichtetes Gefrieren in den Wassereinschlüssen unter einem Pingo entsteht, kann mit säsonalen Wachstumsbändern durchsetzt sein. Diese können, ähnlich wie Baumringe, in der Paläoklimaforschung Verwendung finden. Enstehende Pingos, die von linsenförmigen Wasserlinsen unterlagert sind, sind oft durch Randriß, Quellfluß, Frosthügelwuchs, Verwerfungen und Schwankungen in der Pingohöhe gekennzeichnet. Diese und andere Foremen sind mit Wasserdruckriß und Wasserverlust der unterlagernden Wasserkammer verbunden. Ein Teil der durch die Langzeitstudie des Pingowuchses gewonnenen Daten dienen der Erkennung von Einsturzformen, die in Gebieten die heute keinen Permafrost mehr aufweisen als Paläopingos interpretiert werden.

* Polar Continental Shelf Contribution 01297

INTRODUCTION

Pingos are intrapermafrost ice-cored hills, typically conical in shape, that can grow and persist only in a permafrost environment. There are about 1350 pingos in the Tuktoyaktuk Peninsula Area, Western Arctic Coast, this comprising the greatest pingo concentration in the world (Fig. 1). The Tuktoyaktuk Peninsula Area (Fig. 2), which includes Richards Island, Tuktoyaktuk Peninsula and the coastal strip south of the Eskimo Lakes, forms part of the Pleistocene Coastal Plain of the Western Arctic Coast. Most of the Tuktoyaktuk Peninsula Area is underlain by a thick sequence of sands (Young *et al.*, 1976; Rampton, 1988). The depth of undisturbed permafrost ranges from about 500 to 800 m (Taylor and Judge, 1977; Judge *et al.*, 1979; Allen *et al.*, 1988). The great majority of the Tuktoyaktuk Peninsula Area pingos have grown up in the bottoms of lakes that probably drained catastrophically (Mackay, 1988a) if not very rapidly. About 80 pingos have grown up in the seaward part of the Mackenzie Delta to the west of Richards Island (Fig. 1). Because the majority of the Mackenzie Delta pingos differ in their genesis, growth, and collapse from those of the Tuktoyaktuk Peninsula Area (Mackay, 1963, 1966a; Mackay and Stager, 1966), the Mackenzie Delta pingos are not discussed in this paper. In addition to the pingos of the Tuktoyaktuk Peninsula and Mackenzie Delta areas, numerous pingo-like features, of uncertain origin, dot the bottom of the Beaufort Sea (Shearer *et al.*, 1971; Poley, 1982; Pelletier, 1987). Elsewhere in Canada there are about 500 pingos in the Yukon (*e.g.* Hughes, 1969; Geurts and Dewez, 1985); scattered pingos in the District of Mackenzie (*e.g.* Anderson, 1913; Mackay, 1958; Craig, 1959; St-Onge and Pissart, 1990); a few pingos in the District of Keewatin (*e.g.* Tarnocai and Netterville, 1976); many pingos in the islands of the District of Franklin (*e.g.* Pissart, 1967; Brown and Péwé, 1973; Balkwill *et al.*, 1974; Pissart and French, 1976; French and Dutkiewicz, 1976; Washburn, 1980; Scotter, 1985; Gurney and Worsley, 1997); and in the Province of Québec (Seppälä, 1988). There are about 1500 pingos in Alaska (*e.g.* Holmes *et al.*, 1968; Carter and Galloway, 1979; Hamilton and Obi, 1982; Walker *et al.*, 1985; Ferrians, 1988; Walker *et al.*, 1996); an unknown number, possibly 1000 or more in the former USSR (*e.g.* Shumskii and Vtyurin, 1966; Vtyurin, 1975); and at least several hundred in other parts of the world such as Fennoscandia (*e.g.* Lagerbäck and Rodhe, 1986; Åkerman and Malmström, 1986); Spitsbergen (*e.g.* Yoshikawa and Harada, 1995), Greenland (*e.g.* Müller, 1959; Worsley and Gurney, 1996), Mongolia (*e.g.* Babinski, 1982, 1994), and the high altitude Tibetan Plateau of China (An, 1980; Wang and Yao, 1981; Cui, 1982; Wang and French, 1995). The occurrence of pingos in Antarctica (Pickard, 1983) has been questioned (Fitzsimons, 1989). As an estimate, there are probably 5000 or more pingos in the world and of these about 1350, or about one quarter, are concentrated in the Tuktoyaktuk Peninsula Area (Stager, 1956; Mackay, 1962). Furthermore, pingos are not only of current interest but also of geologic interest, because numerous more or less circular collapse features, interpreted to be pingo remnants, most being of Holocene age, have been described in many non-permafrost areas of the world, such as in the United Kingdom (*e.g.* Watson, 1977), Ireland (*e.g.* Mitchell, 1971), many countries in northwest Europe (*e.g.* De Gans, 1988), Canada (*e.g.* Bik, 1969), the northern United States (*e.g.* Flemal, 1976; Marsh, 1987) and China (Song and Xia, 1988). The oldest reported pingo-like remnants are associated with Late Ordovician glacial deposits, more than 400 million years old, which extend eastward from Sierra Leone, across northern Africa into Saudi Arabia (Beuf *et al.*, 1971; Biju-Duval *et al.*, 1981; Vaslet, 1990; Abed *et al.*, 1993). Therefore, if these paleo-pingo like remnants can be identified, with confidence, as those of collapsed pingos, such remnants provide one of the very few known proofs of the former existence of permafrost.

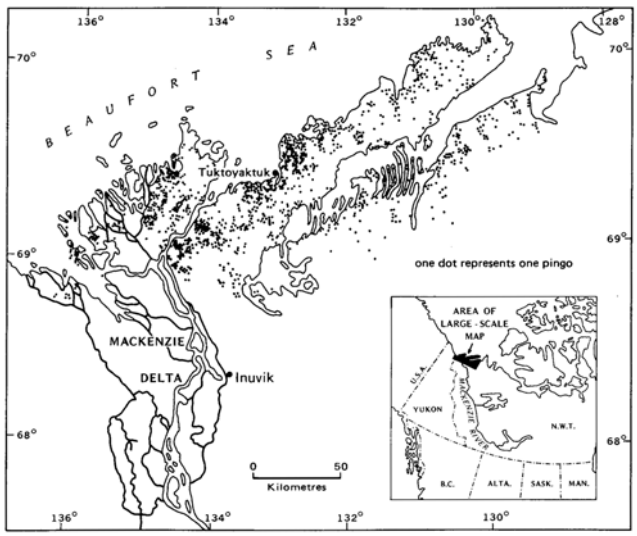

FIGURE 1. Pingo distribution in the Tuktoyaktuk Peninsula and Mackenzie Delta Areas, Western Arctic Coast (Mackay, 1962, Fig. 1).
Répartition des pingos dans la région de la péninsule de Tuktoyaktuk et du delta du Mackenzie, sur la côte ouest de l'Arctique.

Despite the widespread distribution and abundant literature on pingos in permafrost areas of the world, data on pingo growth are remarkably scarce. In the former USSR there have been several estimates, but no known measurements, of pingo growth (*e.g.* Bobov, 1969; Shumskii, 1964; Soloviev, 1973). In China, growth of one pingo in the high altitude Qinghai-Xizang plateau region of Tibet has been estimated by comparing air photos taken in 1956 and 1974 (Cui, 1982). Although it has long been common knowledge among inhabitants of the Western Arctic Coast that pingos grow (*e.g.* Leffingwell, 1919, citing Stefánsson, p. 153; Porsild, 1938) the writer, despite numerous enquiries made since 1951, has been unable to find a single example of a pingo, reportedly growing.

In view of the abundance and variety of pingos along the Western Arctic Coast, in 1969 a long-term study on the growth of pingos was started by installing and surveying bench marks on pingos that appeared to range in age from young growing pingos to old pingos that had long ceased growing. In 1979 a lengthy paper was published in this jour-

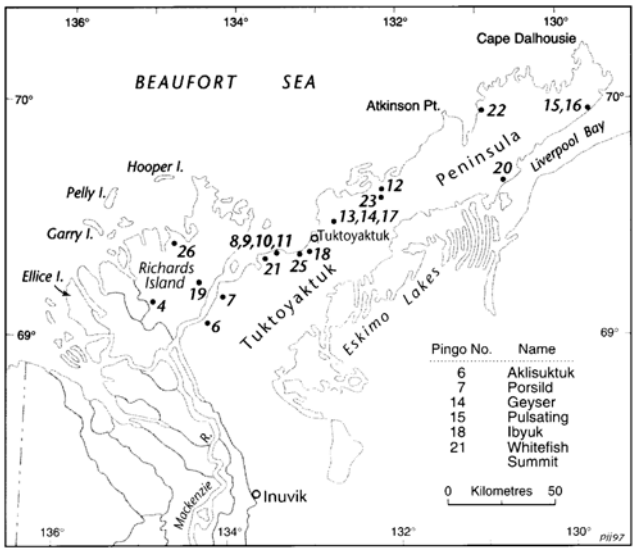

FIGURE 2. The Tuktoyaktuk Peninsula Area includes Richards Island in the west, Tuktoyaktuk Peninsula to the east, and the coastal region south of the Eskimo Lakes. Pingos are referred to by number and also name, where available.

La région de la péninsule de Tuktoyaktuk comprend Richards Island à l'ouest, la péninsule de Tuktoyaktuk vers l'est et la région côtière au sud des Eskimo Lakes. Les pingos sont identifiés par des chiffres et parfois aussi par un nom.

nal on the 1969 to 1978 growth of more than 10 pingos (Mackay, 1979). The 1969 to 1978 pingo surveys have been continued to 1996, although the frequency and duration of the surveys have varied greatly from pingo to pingo. To the best of the writer's knowledge, the growth data previously reported and added to in this paper comprise the only measured pingo growth data in existence, anywhere and for any length of time. In view of the preceding, the main purposes of this paper are to discuss: pingo genesis; the role of pore water expulsion when saturated sands freeze; long-term pingo growth data; sub-pingo water lenses; hydrofracturing, peripheral faulting, and spring flow; pingo collapse; and suggestions for the recognition of features interpreted as paleopingos now in non-permafrost environments.

PINGO NAMES

When the pingo surveys were started in 1969, only Ibyuk Pingo, several kilometres southwest of Tuktoyaktuk, N.W.T. and Whitefish Summit Pingo farther west along the coast had names approved by the Canadian Permanent Committee for Geographical Names (Fig. 2). Therefore, in the general absence of names, the pingos are referred to by numbers as in previous publications (*e.g.* Mackay, 1973, 1977a, 1978, 1979). In 1979, the Canadian Permanent Committee for Geographical Names approved names for four of the numbered pingos (Mackay, 1979, p. 61), these being Aklisuktuk Pingo (Pingo 6); Porsild Pingo (Pingo 7); Geyser Pingo (Pingo 14); and Pulsating Pingo (Pingo 15).

TERMINOLOGY

PERMAFROST

"Ground (soil or rock) that remains at or below 0°C for at least two years" (Harris *et al.*, 1988, p. 63). The definition is based upon time and temperature, without reference to the presence or absence of ice.

1. Ice-bonded permafrost

Ice-bonded or ice-bearing permafrost is permafrost in which the soil particles are cemented together by ice. When permafrost aggrades downward in a drained lake bottom underlain by sands, the typical site for pingo growth in the Tuktoyaktuk Peninsula Area, solute rejection from the growing ice crystals at the freezing front causes a freezing point depression in the pore water below the freezing front. Permafrost in the zone with a freezing point depression is then unbonded and ice-free. The magnitude of the freezing point depression that has been measured at the sites with growing pingos has varied greatly, but it has usually been in the range of - 0.1°C to - 0.5°C. In the Tuktoyaktuk Peninsula Area the pore water beneath ice-bonded permafrost is frequently under such a high pressure that the hydraulic head or potentiometric surface is usually many metres above ground level. Therefore, when a drill hole penetrates ice-bonded permafrost, the depth at which there is the first drill-hole flow to the surface delimits the depth of the ice-bonded permafrost, the water temperature gives the magnitude of the freezing point depression, and the water quality provides data on the solute rejection process (Hallet, 1978; Marion, 1995).

2. Saline permafrost (cryopeg)

When the zone with a freezing point depression persists for two or more years, it is, by definition, permafrost and the unbonded zone, without pore ice, is commonly referred to as a cryopeg (Tolstikhin and Tolstikhin, 1974) or saline permafrost (Harris *et al.*, 1988).

PINGOS AND FROST MOUNDS

A pingo is "a perennial *frost mound* consisting of a core of *massive ice*, produced primarily by injection of water, and covered with soil and vegetation" (Harris *et al.*, 1988, p. 71). The Russian equivalent is bulgunniakh. A frost mound is "any mound-shaped landform produced by ground freezing combined with groundwater movement or the migration of soil moisture" (Harris *et al.*, 1988, p. 36). Muller (1945, p. 220) suggested long ago that the term pingo should be restricted to frost mounds that are of relatively large dimensions, a recommendation that will be followed here to avoid terminological problems with small perennial frost mounds. For example, small perennial ice-cored mounds 5 to 20 m in diameter and up to 1 m in height frequently grow in sedgy drained lake flats near pingos in the freeze-back period by the injection of water into the bottom of the active layer, especially where there is considerable local variation in the downward rate of freezing. These perennial frost mounds are excluded from the definition of pingos, as recommended

by Muller (1945), because of their small size. To complicate the pingo and frost mound terminology, many frost mounds have grown by hydrofracturing and rupture at the periphery of a pingo with intrusion of water into permafrost to form perennial ice-cored frost mounds, the water source being the adjacent pingo. These pingo-associated ice-cored frost mounds can persist for decades and so are, in a sense "baby pingos". However, these relatively small perennial ice-cored mounds will be referred to in this paper as frost mounds and not pingos, to avoid terminological confusion.

ACTIVE LAYER

The active layer, as used conventionally and as defined in this paper, is the top layer of ground above the permafrost table that thaws in summer and refreezes in winter (Muller, 1945; Brown and Kupsch, 1974). The transition between freezing and thawing is considered, for practical purposes, to take place at 0°C. In the *Glossary of Permafrost and Related Ground-Ice Terms* (Harris *et al.*, 1988, p. 13) the active layer is defined as including the upper part of permafrost wherever freezing takes place below 0°C, such as in saline soils or clay soils with a high unfrozen water content at a temperature below 0°C. Because the below 0°C definition at which freezing and thawing takes place is impractical for field use (Mackay, 1995), the conventional definition of the active layer, as defined by the 0°C isotherm, is used in this paper.

FIELD METHODS

In the summer of 1969 a variety of pingos, inferred from field observations to range from young to old, were selected for a long-term study of pingo growth and collapse in the Tuktoyaktuk Peninsula Area. The Tuktoyaktuk Peninsula Area was chosen because the coasts were accessible by freight canoe, then the usual mode of transport. Different criteria were used for pingo selection, such as the estimated age of the drained lake bottom in which the pingo had grown up, the vegetation on both the drained lake bottom and on the pingo itself, the apparent freshness of the summit and radial dilation cracks that crossed the pingo, the degree of development of ice-wedge polygons on the surrounding drained lake flat, the size and apparent freshness of the outlet stream, the nature of the delta, if any, built downstream into either a lake or stream valley, and so forth. In summary, bench marks were installed in 18 pingos in the 1969 to 1973 period. Pingo 6 (Aklisuktuk Pingo) was chosen because of its historical interest (Richardson 1851; Porsild 1938) and Pingo 18 (Ibyuk Pingo) because it was probably the largest in Canada and one of the largest in the world. The other pingos were chosen to cover an inferred age spectrum ranging from young pingos that were probably growing to old pingos that had ceased growing long ago. In retrospect, subsequent surveys have confirmed the initial field estimates as to age, because all pingos thought to be growing were growing and those whose appearances suggested that they were not growing were not growing within the precision of survey measurements. As a result of the long-term field studies, it is now known that the ages of the pingos selected for study ranged from the youngest at about 20 years (Pingo 8) to the oldest of an unknown age. Therefore, a good estimate can be made as to whether a pingo is or is not growing from a knowledge of the geomorphology, permafrost conditions, and vegetation of both the pingo and the drained lake bottom within which the pingo has grown up.

BENCH MARK SURVEYS

Pingo growth, starting in 1969, has been determined by installing and surveying numerous bench marks (BM) on pingos. The pingo bench marks have been referenced to one or more datum bench marks located on stable land inland from the pre-drainage lake shoreline, because the datum bench marks were then in areas with thick permafrost and so would be virtually unaffected by lake drainage (Mackay, 1973). The first bench marks were steel pipes with the lower end installed where possible to a 2 m depth below ground level, this being the depth limit of the portable drilling equipment then usable in stony permafrost. Later, with improved equipment, longer bench marks, of steel or aluminum, with closely spaced anti-heave rings welded onto the pipes, were installed to a greater depth to minimize the possibility of heave. Where bench mark heave was likely, three datum bench marks were usually installed so that a comparison among the bench marks could be used to assess bench mark stability. In areas of sand, where the active layer depth usually exceeded 1 m and deep drilling was difficult, some datum bench marks heaved so their data have been discarded. In contrast, at sites with a thin active layer, such as in the peat of ice-wedge polygons, bench marks have been remarkably stable. A Wild NA 2 automatic engineer's level with a parallel plate micrometer reading to 0.01 cm and Wild GPLE 3 m matching invar staves with supporting struts were used for levelling. All surveys were closed at least once. At Pingo 6 (Aklisuktuk) and Pingo 18 (Ibyuk), the slopes were so steep that a Wild T2 theodolite, mounted on a rigid bench mark, was used to complement the levelling surveys.

CONTOUR MAPS

Contour maps were made of the pingos by plane table survey with a Wild RK-1 self-reducing alidade. Some of the pingos were contoured many times over a period of years in order to study the processes involved in pingo growth, rupture, and collapse.

BENCH MARK TILTS

Bench mark tilts on six pingos were measured with an electronic tiltmeter (Slope Indicator Company Sensor Model 50322, Indicator Model 50306). A vertical alignment key was attached securely to each bench mark so that the alignment of the tiltmeter sensor would correspond to that of the bench mark. Tilt angles were measured upslope, across the slope, and downslope and the downslope or upslope tilts and the resultants calculated. All tiltmeter readings were repeated at least twice.

PRESSURE TRANSDUCERS

Sturdy oceanographic pressure transducers were installed in the sub-pingo water lenses beneath Pingos 9, 14, and 15 to measure sub-pingo water pressures.

WATER QUALITY

Water quality and isotope (oxygen 18, deuterium, and tritium) analyses were carried out by several different laboratories on ice and water samples to help in the study of pingo growth processes. Samples of pingo ice (water) were collected from natural exposures and from drill holes. Water samples were collected from spring flow, which occurred when pingos ruptured, and from drill-hole flow from sub-pingo water lenses, frost mounds, and beneath ice-bonded permafrost. Soil salinity cells were installed in the sub-pingo water lens of Pingo 9 to monitor the changing salinity of the sub-pingo water lens.

TEMPERATURE MEASUREMENTS

Temperature cables with either thermistors or thermocouples were installed vertically into several pingos, including their sub-pingo water lenses, in order to study freezing processes. In addition, a few temperature cables were installed in drill holes in the lake bottoms surrounding several pingos.

PINGO TYPES

Numerous theories have been proposed for the origin of pingos. For the pingos of the Western Arctic Coast theories have included a cursory mention of deposition from drifting sand (Richardson, 1828); hydraulic pressure as for similar pingos in Alaska (Leffingwell, 1919); freezing in a closed system (Porsild, 1938); freezing and expansion of a mud-filled lake after an especially hot summer (Taylor, 1945); piercement domes from the burial of glacial ice (Gussow, 1954, 1962); gradual shoaling by the deposition of sediment and organic material in a lake over a period of many centuries (Müller, 1959); pore water expulsion from permafrost aggradation in saturated sands (Mackay, 1962); water expulsion in a region of sedimentation subject to subsidence (Bostrom, 1967); freezing from a water supply via contraction cracks (Bleich, 1974); and growth in the active layer (sic) from melting of the ice core at the top and freezing at the bottom (Ryckborst, 1975). In summary, the growth processes described by Leffingwell and Porsild, with appropriate modifications, are now widely accepted for the origin of the two basic types of pingos found in permafrost areas of the world. Müller (1959) proposed the terms “open system” pingos for the type described by Leffingwell (1919) in Alaska and “closed system” pingos for that described earlier by Tsytovich and Sumgin (1937) for similar pingos in the USSR and later by Porsild (1938) for those of the Tuktoyaktuk Peninsula Area. Mackay (1979) proposed the terms “hydraulic system” pingos in preference to “open system” pingos and “hydrostatic system” pingos in preference to “closed system” pingos. The terms hydraulic system and hydrostatic system pingos will be used in this paper rather than open and closed system pingos for two reasons. First, the adjectives “hydraulic” and “hydrostatic” identify the source of the water pressure that initiates and sustains pingo growth, *i.e.* hydraulic system pingos derive their water pressure from a topographic gradient and hydrostatic system pingos derive their water pressure from pore water expulsion beneath aggrading permafrost in saturated sand. Second, in many freezing experiments (*e.g.* Taber, 1930; Beskow, 1935; Muller, 1945; McRoberts and Morgenstern, 1975) the terms “open” and “closed” have opposite meanings from those in Müller’s “open” and “closed” system pingos, so the use of the terms in opposite senses is confusing.

HYDRAULIC (OPEN) SYSTEM PINGOS

Hydraulic (open) system pingos grow where intrapermafrost or subpermafrost groundwater flows downslope, under an hydraulic gradient, to the site of pingo growth. Consequently, hydraulic system pingos grow in areas with topographic relief, such as on lower hillslopes as in interior Alaska (Holmes *et al.*, 1968) and adjacent Yukon (Hughes, 1969), on alluvial fans (Scotter, 1985), or in the alluvium of valley bottoms, as in Greenland and Spitsbergen. Although the hydraulic pressure for open system pingos has long been attributed to flow under an hydraulic gradient, the fact that many pingos grow in areas of coarse grained alluvial sediments where permafrost may be aggradating downward suggests that the water pressure, for some pingos, may be derived from pore water expulsion as in hydrostatic pingos. Despite the decades of field studies by many individuals on hydraulic (open) system pingos, particularly in Greenland and Spitsbergen, there are no surveyed growth data, anywhere, on even one pingo, to the writer’s knowledge.

HYDROSTATIC (CLOSED) SYSTEM PINGOS

The groundwater flow for the genesis, growth, and rupture of hydrostatic (closed) system pingos results from pore water expulsion caused by permafrost aggradation beneath the bottoms of drained lakes that are underlain by saturated sands. Within the pingo region of Figure 1, there are local pingo clusters where drainage has resulted primarily from coastal retreat or the headward erosion of rivers when sea level was lower (Hill *et al.*, 1985, 1993). In areas without pingo clusters many lakes have drained rapidly, at times within a few days, by the erosion of ice wedges at their outlets (Mackay, 1988a). The high concentration of hydrostatic system pingos in the Tuktoyaktuk Peninsula Area has been the result of a combination of favorable physical conditions, namely permafrost some hundreds of metres deep, extensive areas underlain predominantly by coarse grained sediments, and numerous large thermokarst lakes with easily eroded ice-wedge polygons at their outlets (Mackay, 1992a).

PORE WATER EXPULSION

1. LABORATORY AND FIELD STUDIES

Numerous laboratory experiments and field studies, many in the former USSR, have shown that when saturated sands are frozen downward the surface will either not heave or heave very little, given free drainage, because the 9% vol-

ume expansion of pore water to pore ice results in some pore water expulsion with flow in the direction of a lower water pressure (*e.g.* Taber, 1930; Beskow, 1935; Tsytovich and Sumgin, 1937; Tsytovich, 1955, 1959, 1975; Khakimov, 1957; Balduzzi, 1959; Shumskii, 1959, 1964; McRoberts and Morgenstern, 1975; Arvidson and Morgenstern, 1977; Fotiev, 1978; Takashi *et al.*, 1978; Chen *et al*., 1980; Zhestkova, 1982; Mackay, 1997). To quote Beskow (1935, p. 32): "From the tests shown in the table we can thus conclude the following: Coarse soils – medium sands and coarse silts – act as an open system and do not expand upon freezing; instead the water is forced out and the amount is about 1/10 of the quantity of frozen water. But as a closed system these sands have an expansion upon freezing an amount up to 1/10 of the contained water." The preceding quotation from Beskow illustrates that "open" and "closed" in a freezing experiment are used in the opposite context from that in "open" and "closed" system pingos as defined by Müller (1959).

2. THEORY AND OBSERVATIONS

When permafrost aggrades downward in a drained lake bottom underlain by saturated sand the normal stress (σ) at depth (z) (see Table I for nomenclature) is:

$$\sigma_z = \gamma_s z \qquad [1]$$

The effective stress (σ') at depth (z) is:

$$\sigma'_z = \sigma_z - \mu_z \qquad [2]$$

where (μ) is the pore water pressure and (μ_z) the pore water pressure at depth (z).

If all of the pore water in a saturated sands freezes in place as permafrost aggrades downward, *i.e*. the entire system is "closed", the lake bottom will heave an amount approximately equal to the 9% volume expansion of the pore water that freezes to become pore ice. Therefore, in order for pore ice to grow in place in a closed system with a 9% volume expansion, the pore ice must both separate and uplift many of the soil particles that are in grain to grain contact with the result that the local effective stress in the freezing zone [2] must approach zero (Miller, 1980, p. 290). In sands, which have negligible amounts of unfrozen pore water at temperatures just below 0°C, the pore water in the freezing zone is continuous with the pore water in the unfrozen zone beneath. Therefore the pore water pressure beneath the freezing zone in a closed system will approach the total normal stress [1]. However, if freezing is in an open system, with free drainage in at least one direction, some if not all of the 9% volume expansion of pore water to pore ice will be expelled to move as groundwater flow. Consequently, the heave of the lake bottom, which can be determined by long-term precise survey, will be less than the 9% volume expansion of the pore water frozen to become pore ice. The water pressure beneath the freezing zone will then range upward from hydrostatic, if drainage is unimpeded in an open system, to the total normal stress in a closed system. The pore water pressure beneath ice-bonded permafrost has been measured at three growing pingo sites by means of pressure transducers. At each of the three sites the pore water pressure has been about 75% of the total normal stress and long-term surveys have shown that lake bottom heave has been minimal (Mackay, 1987). The growth of pore ice that leads to pore water expulsion has been studied, under the microscope, in frozen sand (Zhestkova, 1982). As the mineral grains and pore water cool, the first stable crystals of ice are formed on the surface of the chilled grains of sand. Then, as the ice gradually grows inward from the sand grains to the pore water in the inter-grain zone, pore water is expelled by the growing crystals away from the front of crystallization. Tsytovich (1955) has estimated that pore water expulsion can occur if the hydraulic conductivity (K) exceeds about 10 to 20 cm/d which is far below that of most sands. Furthermore, in the former USSR, field experiments on the freezing of saturated sands have demonstrated that pore water expulsion, with groundwater flow, has contributed excess water to cause damage to certain types of construction facilities (*e.g.* Khakimov, 1957; Tsytovich, 1975). Finally, in 1978, Illisarvik Lake on Richards Island was artificially drained to study, among other factors, pore water expulsion from permafrost aggradation in saturated lake bottom sands (Mackay, 1997). The field results (1978 to 1995) show conclusively that, if lake bottom heave is minimal as permafrost aggrades downward in saturated sands, pore water is expelled to move as groundwater flow beneath the ice-bonded aggrading permafrost. In summary, the driving mechanism for the growth of hydrostatic system pingos is pore water expulsion from the downward growth of

TABLE I

Nomenclature

Symbol	Definition
A	amplitude of temperature wave at ground surface
A_z	amplitude of temperature wave at depth z
B	Stefan's b
E	exponential e
K	thermal conductivity
K	hydraulic conductivity
L	volumetric latent heat of fusion
P	period
T	time
T_z	lag in time (t) of temperature wave at depth z
T	temperature
T_g	mean annual ground surface temperature
Z	thickness, depth
Z_i	thickness of ice-bonded permafrost
α	thermal diffusivity
γ	bulk unit weight
γ_s	bulk unit weight of frozen sand
λ	pore water pressure
λ_z	pore water pressure at depth z
σ	normal stress
σ_z	normal stress at depth z
σ'	effective stress
σ'_z	effective stress at depth z

permafrost in saturated sands under conditions such that the expelled pore water can move as groundwater flow to a residual pond, the usual site of pingo growth.

PERMAFROST GROWTH

1. THEORY

The depth (z) of ice or ice-bonded sands frozen, in time (t) can be approximated, with simplifying assumptions, by Stefan's solution (Ingersoll *et al.*, 1954).

$$z = \sqrt{-2Tkt / I} = b\sqrt{t} \qquad [3]$$

The value for (b), the constant for Stefan's solution for saturated sands in the Tuktoyaktuk Peninsula Area, is about 3 $m/\alpha^{1/2}$ and that for ice about 1.5 $m/\alpha^{1/2}$ or half that of saturated sands (Fig. 4). Therefore, the thickness of aggrading ice-bonded permafrost (z_i) beneath the lake bottom surrounding a pingo tends to be, approximately, twice the thickness of the pingo ice core (Fig. 3).

The annual increment (z) at the bottom of ice-bonded permafrost, in finite form, with (t) in years, is

$$\frac{\Delta z}{\Delta t} = \frac{b}{2}\sqrt{t} \qquad [4]$$

The amplitude of the surface temperature wave (A) at depth (z) below the ground surface (Ingersoll *et al.*, 1954) is given by

$$A_z = Ae^{-z\sqrt{\pi/\alpha P}} \qquad [5]$$

The time lag (t_z) of the temperature wave with depth (z) is given by

$$t_z = \frac{z}{2}\sqrt{P/\pi\alpha} \qquad [6]$$

2. UNFROZEN BASINS (TALIKS) BENEATH LAKES

The maximum thickness of lake ice in the Tuktoyaktuk Peninsula Area is about 2 m so all lake bottoms where water depths exceed about 2 m will be underlain by an unfrozen basin or talik all year. However, since the maximum thickness of lake ice lasts for only a brief period in the spring, field studies in the Tuktoyaktuk Peninsula Area have shown that an unfrozen basin tends to underlie those lake areas where water depths exceed about 2/3 of the maximum ice thickness. This means that unfrozen basins of varying shape and depth tend to underlie most of the large lakes in the Tuktoyaktuk Peninsula Area (Fig. 4a), and, as discussed previously, most of the lake bottom sediments are sands. Consequently, when such lakes drain, pore water will be expelled beneath the aggrading permafrost (Fig. 4b). The next sequence of events depends upon the sizes and depths of any residual ponds that might remain on the drained lake bottom. If there is at least one large and relatively deep residual pond without permafrost directly beneath it, then expelled pore water, moving as groundwater flow, can discharge upward into the unfrozen basin that underlies the pond and a pingo is unlikely to grow. However, if there is at least one residual pond of sufficient size and critical depth so that the bottom sediments gradually freeze downward, the pressure exerted by the groundwater flow from the surrounding large lake bottom area of aggrading permafrost acts like an hydraulic jack (Gasanov, 1978) on the much smaller area of the frozen bottom of the residual pond to dome it up and so to initiate pingo growth (Fig. 4b, 4c). The overburden thickness above the top of the pingo ice is then the thickness of the uplifted pond sediments when pingo growth started. Here it should be stressed that a pingo will not grow in every residual pond because many ponds are too large, too small, too deep, too shallow, and so forth.

PINGO GROWTH

SUB-PINGO WATER LENSES

If, as a pingo grows, the addition of water to the bottom of the pingo ice exceeds the downward rate of freezing, a sub-pingo water lens will underlie the pingo ice (Fig. 4c). When a pingo is underlain by a sub-pingo water lens, the hydraulic head is then above the top of the pingo (Fig. 5), because the pressure in the water lens is sufficient to uplift and deform the pingo ice core with its superincumbent frozen overburden (Mackay, 1973, 1978, 1983). Many growing pingos in the Tuktoyaktuk Peninsula Area are underlain by sub-pingo water lenses.

PINGO ICE

When pure ice is seen in a pingo exposure (Fig. 6) or encountered by drilling, then the ice has usually grown from downward freezing at the top of a sub-pingo water lens. The ice is referred to as intrusive or injection ice, although it is water that is intruded or injected and then freezes, not, of course, ice. If the pingo ice core is composed almost entirely

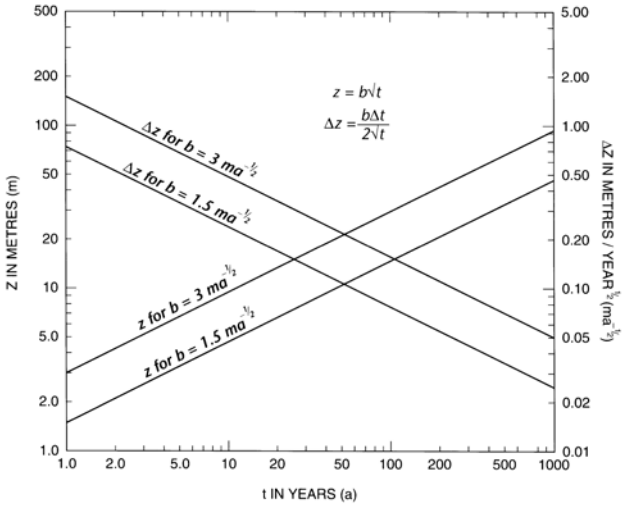

FIGURE 3. Nomograph for the growth of permafrost (z) and rate of growth (Δz) given two typical freezing conditions for the Tuktoyaktuk Peninsula Area. See text.

Nomogramme de l'expansion du pergélisol (z) et taux de croissance (Δz) compte tenu de deux types d'engel caractéristiques de la région de la péninsule de Tuktoyaktuk.

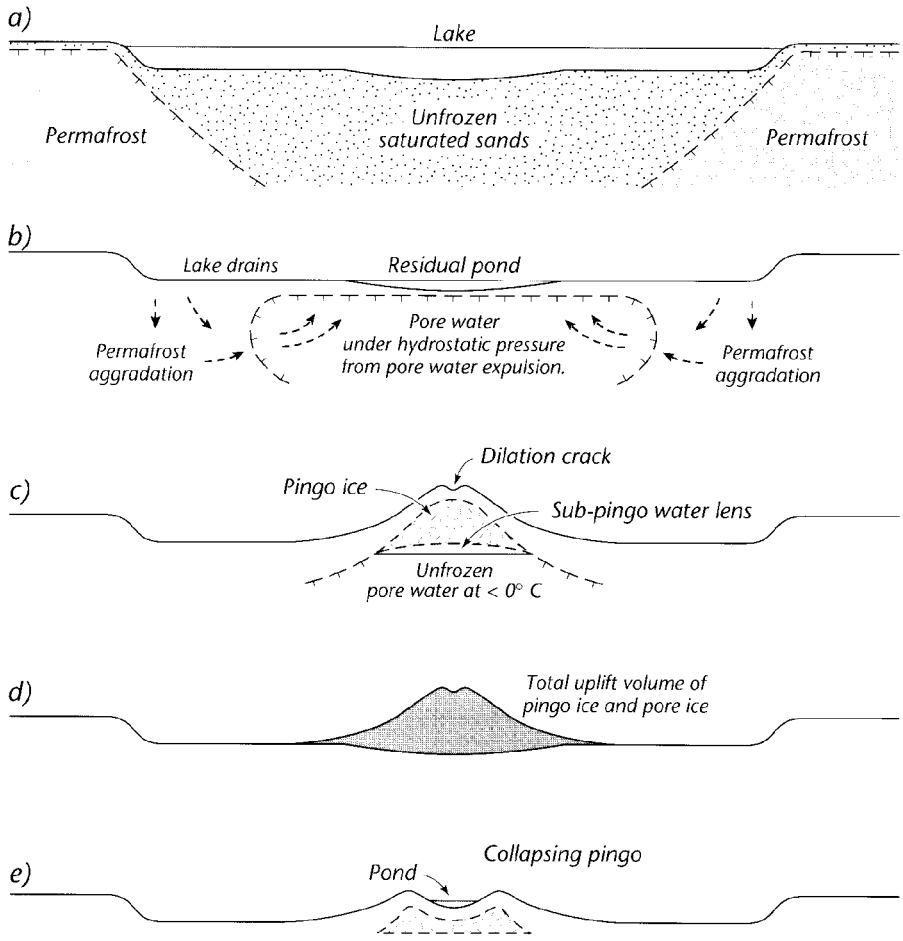

FIGURE 4. Diagrams illustrating the genesis and growth of the Tuktoyaktuk Peninsula Area pingos. a) a large lake underlain by a basin of unfrozen saturated sands; b) the lake after rapid drainage with permafrost aggradation, pore water expulsion, and the development of an hydrostatic pressure beneath a residual pond where there is thin permafrost; c) a growing pingo underlain by a sub-pingo water lens whose downward freezing results in intrusive ice which may become banded from the downward propagation of the cold and warm seasonal temperature waves. The pore water in the unfrozen and unbonded sands beneath the water lens is at a below 0°C temperature because of a freezing point depression; d) the total volume of ice required to grow a pingo is equal to the pingo volume above that of the bottom of the residual pond in which growth commenced; and e) pingo collapse from partial thaw of pingo ice beneath a central pond that is surrounded by a pingo rampart.

Diagrammes montrant la genèse et la croissance des pingos de la région de Tuktoyaktuk. a) Bassin de sables saturés non gelés sous-jacents à un grand lac ; b) lac après assèchement rapide et progression du pergélisol, expulsion de l'eau interstitielle et développement de pression hydrostatique sous une mare résiduelle où il y a une mince couche de pergélisol ; c) pingo en voie de croissance avec lentille d'eau sous-jacente dont l'engel entraîne la formation d'une glace intrusive qui peut comprendre des bandes en raison de la propagation descendante du froid et de vagues saisonnières de températures chaudes. L'eau interstitielle dans le sable non gelé et non cimenté est à -0 °C à cause d'une baisse du point de congélation ; d) Le volume total de glace requis pour permettre la croissance d'un pingo est égal au volume du pingo au-dessus du fond de la mare résiduelle où la croissance s'est amorcée ; e) affaissement d'un pingo en raison de la fonte partielle de la glace du pingo située sous une mare centrale entourée d'une levée.

of intrusive ice, then the depth of the bottom of the ice core below that of the adjacent lake flat remains essentially unchanged during pingo growth. In pingos where the temperature amplitude (A_z) at the top of the water lens varies appreciably during the year, the ice may be seasonally banded (Fig. 7) in a manner similar to growth rings in a tree or varves in lake sediments (Mackay, 1990). Furthermore, if the thicknesses of the seasonal bands are relatively large compared to the depth of water beneath, the salinity of the water and the intrusive ice frozen from it, should also vary seasonally.

If some of the sub-lake bottom sediments at the site of pingo growth are fine-grained frost susceptible soils, ice lenses may grow to form segregated ice. In such cases, the water may be in suction (*e.g.* Williams and Smith, 1989). In addition, segregated ice can also grow in sands provided that there is a high uplift pressure (Rampton and Mackay, 1971; Konrad, 1990; Mackay and Dallimore, 1992). If a pingo contains segregated ice, the bottom of the ice core is at a greater depth below the adjacent lake flats than it was when growth commenced.

BASAL AREA

The basal area of a pingo is established in the first few years of its growth primarily by the characteristics of the residual pond in which growth commenced, for afterwards, a pingo grows higher but with minimal increase in its basal area (Fig. 4c). This is because a pingo grows in an upward direction with reference to the bottom of the ice core, whereas the depth of the surrounding ice-bonded permafrost (z_i) grows downward with reference to the ground surface, so that an increase in the basal area of the bottom of the pingo ice would require the rupture of the surrounding ever thickening permafrost. Therefore, a pingo with a small basal area can grow in a suitable portion of a large residual pond (*e.g.* Pingo 9) but a pingo with a large basal area (*e.g.* Pingo 18) cannot grow in a small residual pond.

FIGURE 6. In August, 1955, the seaward face of Pingo 22 (Fig. 2) was wave-eroded during a storm surge to expose a vertical section of the ice core. Prior to erosion Pingo 22 was about 90 m long and 7 to 10 m high. The ice core, of intrusive ice, formed by downward freezing in a sub-pingo water lens. The 1.2 to 1.5 m thick overburden was of brownish lacustrine sand. The bottom of the ice core was below the bottom of the ice in the photograph. Several ice wedges, as wide as 1 m in true section, penetrated downward into the pingo core thus suggesting that the pingo was at least several hundred years old.

En août 1955, la face du pingo n^{o} 22 (fig. 2) du côté de la mer a été, au cours d'une tempête, érodée et une partie du noyau de glace a été exposée. Avant cet événement, le pingo n^{o} 22 mesurait 90 m de long et 7 à 10 m de haut. Le noyau composé de glace intrusive s'est formé par engel descendant dans la lentille d'eau sous-jacente. La couverture de dépôts meubles de 1,2 à 1,5 m d'épaisseur était composée de sable lacustre brunâtre. La base du noyau était située sous la base de la glace sur la photographie. Plusieurs fentes de glace pouvant atteindre 1 m de largeur ont pénétré dans le cœur du pingo indiquant ainsi que le pingo avait au moins plusieurs centaines d'années.

FIGURE 5. Drill-hole flow from Pingo 14 in 1976 (see Figs. 35 and 36 for location). The gusher that rose to a maximum height of 2.6 m issued from a 7.5 cm diameter hole from a depth of 22 m. The water temperature was about - 0.1°C (Mackay, 1979).

Écoulement en jet d'un trou de forage dans le pingo n^{o} 14, en 1976 (localisation aux fig. 35 et 36). L'eau a jailli d'une profondeur de 22 m jusqu'à une hauteur de 2,6 m par un trou de 7,5 cm de diamètre. La température de l'eau était à environ 0,1 °C (Mackay, 1979).

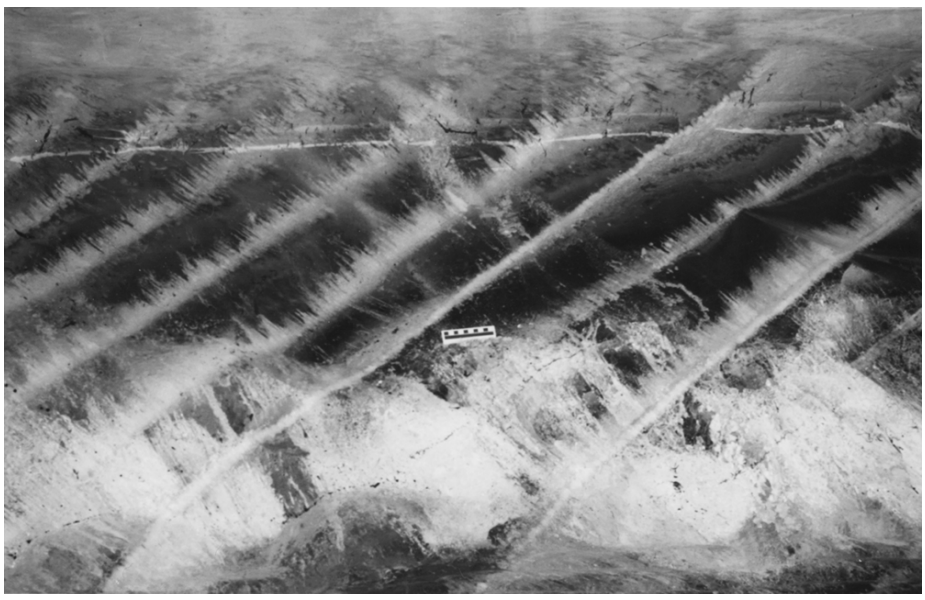

FIGURE 7. Seasonal growth bands in Pingo 20 that resulted from the downward propagation of the warm and cold temperature waves. Note the 10 cm scale in the middle of the photograph. (Mackay, 1990).

Bandes de croissance saisonnières au pingo n^{o} 20 résultant de la propagation descendante des températures, chaudes ou froides selon les saisons. Noter l'échelle de 10 cm au centre (Mackay, 1990).

MECHANICALLY INDUCED FAILURE

When the frozen bottom of a residual pond is domed to form a pingo the mineral and organic overburden must either stretch in response to the increase in surface area or fail in tension. Overburden stretching usually results in summit failure, as seen in vertical cross section through the pingo summit, in circumferential failure, as seen in horizontal cross section, and frequently in peripheral failure if the pingo is underlain by a sub-pingo water lens. In addition to the mechanically induced failure of the pingo overburden, the pingo ice itself is also deformed by creeping, faulting, and the wedging effect of dilation crack ice, and, to a lesser extent, of ice-wedge ice.

1. Summit failure

Most pingos that are more than several metres in height are crossed by a summit crack, here referred to as a dilation crack, because it is formed by the dilation of a once concave upward to flattish pond bottom (Fig. 8). The dilation cracks propagate downward through the frozen pingo overburden usually into pingo ice. As a pingo continues to grow the distance between the sides of a dilation crack increase so that the summit cracks soon range in shape between flat-floored trenches and V-shaped gullies. The widths of the summit cracks tend to reflect the stretch as measured in vertical profile (Fig. 8). Because of dilation cracking, any point "a" initially on the bottom of the residual pond tends to be uplifted to point "b" to give a radially outward displacement of "ΔL". The outward displacement is enhanced, during pingo growth, by downhill creep and mass wasting. Furthermore, as the summit dilation cracks widen, the overburden at the bottom of the crack depression becomes spread thinner and thinner over a greater and greater area until some of the pingo ice beneath may be exposed to thaw and thus produce the so-called pingo crater. Because the stresses that result in dilation cracking are mechanically induced by pingo growth, dilation cracking can occur at any time of the year, in contrast to ice-wedge cracking which occurs only in winter. Dilation crack ice is formed when water and sometimes mineral or organic matter infills an open crack and then freezes (Mackay, 1979, p. 47-48).

2. Circumferential failure

The increase in circumference of a pingo at any given height tends to be relieved by radial dilation cracks that trend downslope from the pingo summit. Because summit dilation cracks usually form first and the radial cracks second, the junctions are often orthogonal (Lachenbruch, 1962). Many of the downslope trending radial dilation cracks continue beyond the pingo periphery onto the adjacent lake flats where they may grade into ice-wedge systems (Fig. 9). The radial cracks, like the summit cracks, can become infilled with surface water to form dilation crack ice. Neither the summit nor radial dilation cracks tend to develop raised rims, like those bordering many ice-wedge systems, but many radial cracks that extend onto the lake flats develop raised rims as they grade into and become ice-wedge systems with raised rims. Because the radial dilation cracks result primarily from a mechanically induced tensional stress whereas ice-wedge cracks result from a thermally induced tensional stress, the gradation of one into the other is an interesting problem that has not yet been investigated.

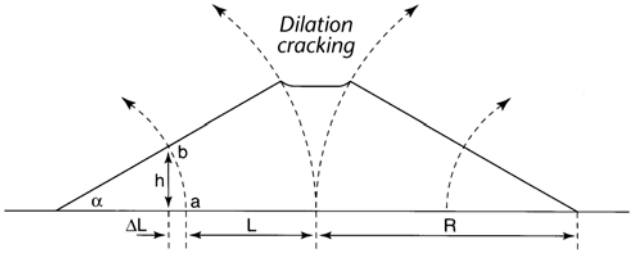

FIGURE 8. Diagrammatic sketch of the growth of a pingo, circular in plan view, as seen in vertical section. Location "a" on the bottom of the residual pond, of radius "R" and distance "L" from the pond centre, is uplifted by pingo growth to location "b". The radially outward displacement of "a" is, then, approximately ΔL. The stretch of the pingo overburden is relieved primarily by dilation cracking at the pingo summit. (Mackay, 1987).

Schéma de croissance d'un pingo vu en coupe. L'emplacement de « a » sur le fond de la mare résiduelle, du rayon « R » et de la distance « L » à partir du centre de la mare ont été haussés en raison de la croissance du pingo à l'emplacement de « b ». Le déplacement radial vers l'extérieur de « a » est alors d'environ ΔL. L'étirement de la couverture de dépôts sur le pingo s'est relâché en raison de l'apparition de fissures de dilatation au sommet (Mackay 1989).

3. Hydrofractures and peripheral failure

The periphery of a pingo, like its geologic counterpart the laccolith (Pollard, 1968, 1973; Gretener, 1969; Pollard and Johnston, 1973; Corry, 1988) has many features that result from hydrofracturing of the surrounding material. To para-

FIGURE 9. Photograph of Pingo 15 showing radial dilation cracks extending downslope from the summit. Some of the cracks have propagated beyond the pingo periphery onto the drained lake flat where they have merged into ice-wedge cracks.

Photographie du pingo n^{o} 15 montrant des fissures de dilatation radiales qui s'étendaient du sommet au bas de la pente. Certaines fissures se sont étendues au-delà de la périphérie du pingo jusqu'au fond du lac asséché où elles ont fusionné pour devenir fentes de gel.

phrase Guth *et al.* (1982, p. 606) with respect to pingos, the phenomenon of hydrofracture occurs whenever the fluid pressure within a sub-pingo water lens exceeds the tensile strength of the enclosing frozen material plus the least compressive principal total stress with compression positive. The least compressive principal total stress in a sub-pingo water lens will depend upon a variety of local factors such as the pingo shape, material, ground temperatures, and stresses on the surrounding drained lake bottom. The pingo hydrofractures then result from failure at sites of local stress concentrations (*e.g.*, Gretener, 1969; Guth *et al.*, 1982; Rummel, 1987; Middleton and Wilcock, 1994). Most pingo hydrofractures appear to originate at the periphery of a sub-pingo water lens from where the fracture propagates both upward and outward towards the pingo periphery. The field evidence for hydrofracturing comes from spring flow at the pingo periphery, the intrusion of water into the active layer or top of permafrost, and the growth of both ephemeral and perennial frost mounds. In some pingos the hydrofractures have propagated upward into the pingo ice to form ice dikes. Sites of local stress concentration that lead to hydrofracturing are affected not only by the characteristics of the sub-pingo water lens but also by the planimetric shape of the pingo. Hydrofracturing has occurred in about one quarter of the pingos discussed in this paper during the observation period of about two decades.

PINGO 4

When Pingo 4 was first seen in June 1967 (Fig. 10a) it was distinctive in several respects: in plan view, the pingo was crescent-shaped with a length of about 200 m and a width of about 50 m, rather than being approximately circular; in profile, a steep central plug was flanked by a curving ridge on each side, here referred to as the Left and Right ridge (Fig. 10a,b); and the central plug was partially surrounded by a moat 1 m or more in width and 0.5 to 1 m in depth (Fig. 11). The moat suggested an episodic up-and-down motion of the central plug with respect to the adjoining Left and Right ridges. The unstable surface of the plug was covered with large semi-detached slump blocks, a metre or more in diameter. The pingo had grown in a partially drained lake about 600 m long and 400 m wide. A reconstruction of pingo growth suggests the following sequence of events: first, growth of the crescent-shaped pingo started before 1890, as dated by the oldest willows on the Left and Right ridges; second, the central plug collapsed; third, regrowth of the central plug commenced prior to 1935, because the pingo appeared as a low mound on a 1935 air photo (A5020-39L); and fourth, the central plug has oscillated up-and-down from episodic pingo rupture, spring flow, and the growth of frost mounds. The collapse in the centre is attributed to the greater mechanical instability of an elongated crescent-shaped pingo as compared to a more circular-shaped pingo (Mackay,1987).

PINGO RUPTURE

In June 1969, datum bench marks (BM 14, 15, 16) were installed on higher land inland from the former lake shoreline and three bench marks (BM 17, 18, 19) were installed from the bottom to the top of the central pingo plug (Fig. 10a). From 1969 to 1978 pingo growth increased yearly with bench mark height (Fig. 12). Therefore no survey was made in 1979, because it was evident that a continuation of the growth trend would result in pingo rupture. When the pingo was next surveyed in 1980 the pingo had, indeed, ruptured, a frost mound had grown at the pond side of the Right ridge, and the adjacent pond bottom with its aquatic plants had been uplifted 1 m by mound growth (Fig. 10b). The frost mound was drilled to a depth of 1.2 m, which was below the maximum depth of the active layer, without ice being encountered, so the intrusion of water to grow the frost mound was below the top of permafrost. In addition to the growth of the frost mound, there had been spring flow the preceding winter issuing from several sites in Right ridge, as shown by dead willows, stained a rusty brown, and flow marks to a height of 0.3 m above ground level, an indication that flow had been over snowbanks. The volume of the frost mound was about 800 m^3 or about one third of the 2500 m^3 volume of the central plug. Therefore, the water source for the frost mound could not have come from a sub-pingo water lens beneath the central plug, because if it had, the central plug would have decreased substantially in height from 1978 to 1980 instead of the height remaining nearly constant. By 1981, the top of the pingo had decreased slightly in height but the frost mound, although remaining unchanged in area, had grown about 0.2 m in height. There was also evidence of spring flow over snowbanks in the winter of 1980/81 as in the preceding winter. Thus water loss from the groundwater system beneath Pingo 4 provides the explanation for the up-and-down movement of the central plug (Fig. 12) and, presumably, the existence of the encircling moat (Fig. 11). In view of the erratic growth of Pingo 4, no surveys were made until 1989 when the survey showed that BM 17 was lower than it was 20 years earlier and both BM 18 and BM 19 had lost height compared to 1981 (Fig. 12). However, in the 1980 to 1989 period, the frost mound had increased in both area and height. Drilling of the frost mound in 1989 showed that there was an organic rich clay from the surface down to a depth of about 1.0 m; clay with ice lenses down to 1.5 m; a brownish silt with little visible ice from 1.5 m to 1.9 m; intrusive ice from 1.9 m to about 2.7 m; and an icy sand beneath the intrusive ice. The evidence suggests that the intrusion of water was probably in early winter after the active layer had frozen through but before the downward propagating cold winter temperature wave (t_z) had cooled the upper part of permafrost to well below 0°C, because the resistance to fracture generally decreases with temperature.

A hole drilled at the pingo summit penetrated first an organic ice-rich clay down to 2.2 m, then a brownish ice-rich silty clay to the bottom of the hole at 3.7 m. As no pingo ice was encountered to a depth of 3.7 m and as the top of the pingo rose only about 7 to 8 m above pond level in the 1969 to 1992 period, the top of the ice core could not have been more than several metres above pond level. By 1992, the last year of survey, all three bench marks on the pingo had not only increased in

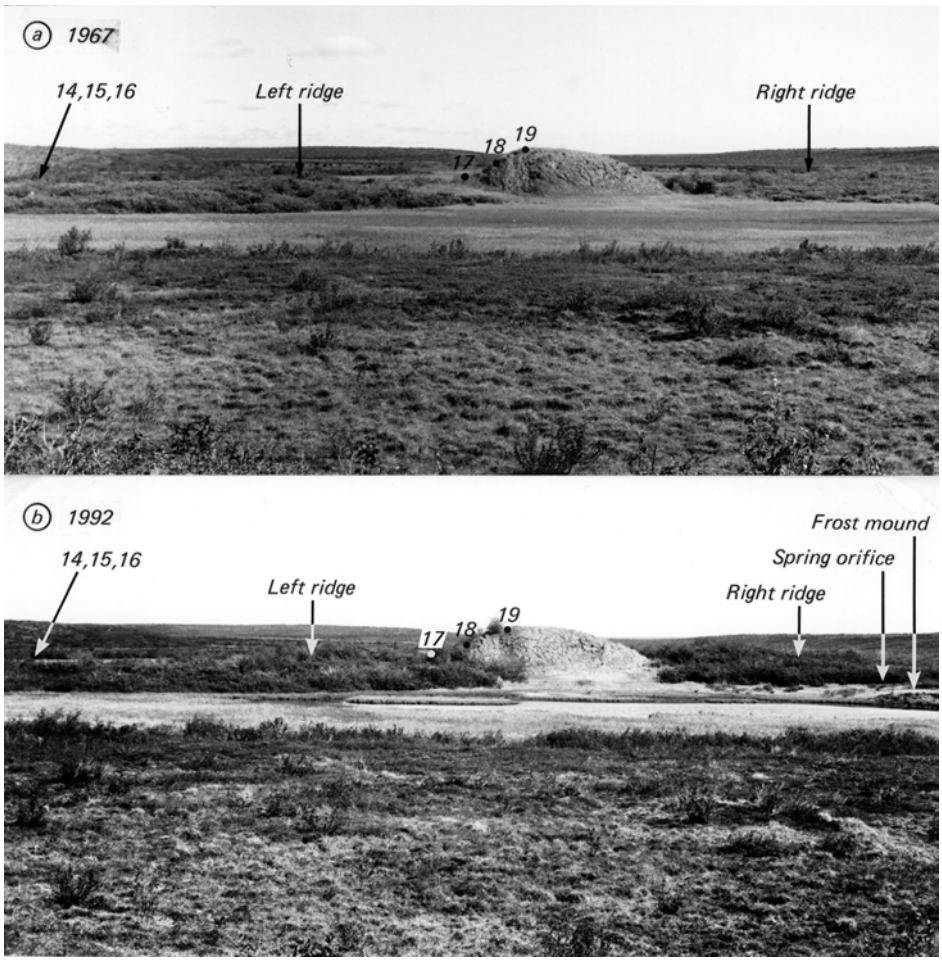

FIGURE 10. a) Photograph of Pingo 4 taken in 1967. The datum bench marks, BM 14, 15, and 16, are on higher land inland from the shoreline of the drained lake and BM 17, 18, and 19 are on the central pingo plug. b) Photograph of Pingo 4 taken in 1992 with the same camera and from the same site as in the 1967 photograph above it. See text.

a) Photographie du pingo n^{o} 4 en 1967. Les répères de nivellement 14,15 et 16 sont situés sur un terrain plus élevé vers l'intérieur à partir de la rive du lac asséché et les repères 17, 18 et 19 sont situés sur le bouchon central du pingo. b) Photographie du pingo n^{o} 4 prise en 1992 avec le même appareil et à partir du même emplacement.

height since 1989, but all were higher than they were in 1969 (Fig. 12). Meanwhile the frost mound had increased in area from about 1500 m^2 in 1980 to 2000 m^2 in 1992 and the volume from about 800 m^3 in 1980 to 1500 m^3 in 1992. The total volume of sub-pingo water lost by spring flow between 1969 and 1992 is unknown, but when the unknown volume of water lost from spring flow is combined with that intruded to grow the frost mound, the total water loss from beneath the Right ridge was undoubtedly far in excess of 1500 m^3. In addition, in the 1969 to 1992 period there was normal faulting with an uplift of about 1 m along the far side of the Right ridge (Fig. 10a, b).

PHOTOGRAPHIC COMPARISON: 1967-1992

The major changes in Pingo 4 from 1967 to 1992 can be seen by comparing the photo taken on 27 June 1967 (Fig. 10a) with the photo taken on 29 June 1992 (Fig. 10b) from the same site and with the same camera. In the intervening 25 years, the Left and Right ridges appear higher in 1992 than in 1967 but the increase in height can be attributed more to the growth of willows than to the growth of the ridges. The base of the central plug had broadened slightly between 1967 and 1992. Although hardly detectable in the photos, the pond in the foreground decreased in area from 1967 to 1992. The vegetation in the foreground had changed little, as can be seen by comparing the same plants in each photograph, but the vegetation appeared to be much more lush in 1992 than in 1967. Thus, although Pingo 4 probably commenced growth before 1890, even after more than 100 years following lake drainage, pore water was still being expelled, there was groundwater flow, and the water pressure below ice-bonded permafrost was sufficiently high to rupture permafrost, grow a frost mound, issue as spring flow, and uplift the Right ridge.

PINGO 6 (AKLISUKTUK PINGO)

John Richardson, in the narrative of his boat voyage down East Channel of Mackenzie River to the Beaufort Sea in 1848, described an eminence (Aklisuktuk Pingo) as follows: "About three miles further on, we had a distant view of an eminence lying to the eastward, which resembled an artificial barrow, having a conical form, with very steep sides and a truncated summit. This summit, in some points of view, presented three small points, in others, only two, divided from one another by an acute notch" (Richardson, 1851, p. 234-235). Figure 13a shows the 1848 sketch of the eminence Richardson described. In 1932, Dr. A.E. Porsild, in describing the pingo seen by Richardson, stated that the pingo had two local names: the common name being Agdlissartoq (now spelt Aklisuktuk) meaning "the one that is growing" and a second name Pingorssarajuk meaning "the poor thing that is getting to be a pingo" (Porsild, 1938). In

FIGURE 11. The moat that partially surrounds the central plug of Pingo 4 on which BM 17, 18, and 19 are located, has resulted from episodic up-and-down movement from pingo growth, water loss below the pingo, and then growth with water gain at depth below the pingo.

La dépression qui entoure partiellement le bouchon central du pingo n^{o} 4 où sont situés les repères 17, 18 et 19 résulte d'une croissance irrégulière du pingo, d'une perte d'eau sous le pingo puis d'une croissance avec augmentation en profondeur de la quantité d'eau sous le pingo.

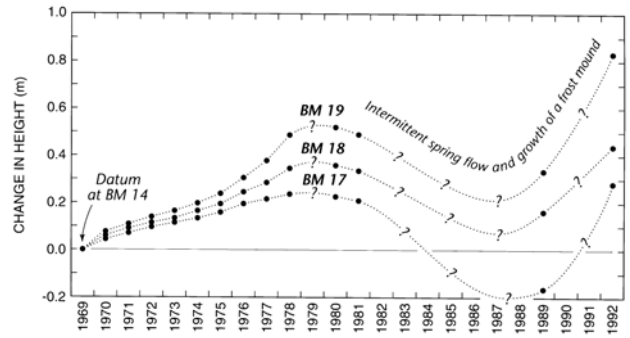

FIGURE 12. Graph showing the change in height of BM 17, 18, and 19 on the central plug of Pingo 4 from 1969 to 1992.

Graphique montrant les différences d'altitude entre les repères 17,18 et 19 situés sur le bouchon central du pingo n^{o} 4 de 1969 à 1992.

local tradition, as recounted to Porsild, the pingo at one time was not visible from the adjacent river (*i.e.* the East Branch of Mackenzie River) but the information given to Porsild had come from older men, long dead. In the absence of written records, the rapid growth of Aklisuktuk Pingo must have taken place within the memory of at least one individual.

SURVEYS

In 1972 a long-term study was started of Aklisuktuk by installing bench marks extending from a datum bench mark inland from the drained lake shore to the pingo top. Yearly surveys from 1972 to 1979 showed that the pingo was slowly subsiding (Mackay, 1979, 1981) so no further surveys were carried out until 1992. Unfortunately, in the 1972 to 1992 period, some of the bench marks between the datum bench mark and the pingo periphery had frost heaved, so all data involving those bench marks have been discarded. The bench marks from BM 85 at the pingo periphery to the pingo top (Fig. 14) have either not heaved or heaved very little, as shown by the consistency of the survey results. Therefore, BM 85 at the pingo periphery has been used as the local datum for the 1972 to 1992 surveys. Here it should be noted that in the 1972 to 1992 period there was, as would be expected, downslope creep of the active layer past BM 87 and BM 88 on the steep pingo slope, because BM 87 had a 2 cm diameter cavity on the downslope side of the bench mark and BM 88 a 3 cm cavity. The three hilltop bench marks (BM 89, 90, and 91) being in flat areas, lacked cavities. The 1972 to 1992 survey data indicated that Aklisuktuk was slowly losing altitude, with decreases, referenced to BM 85, ranging from about 5 cm for BM 91 on the highest peak down to 2 cm at BM 87 on mid slope. The decreases in altitude probably resulted from slow downslope creep of the frozen overburden and ice core beneath.

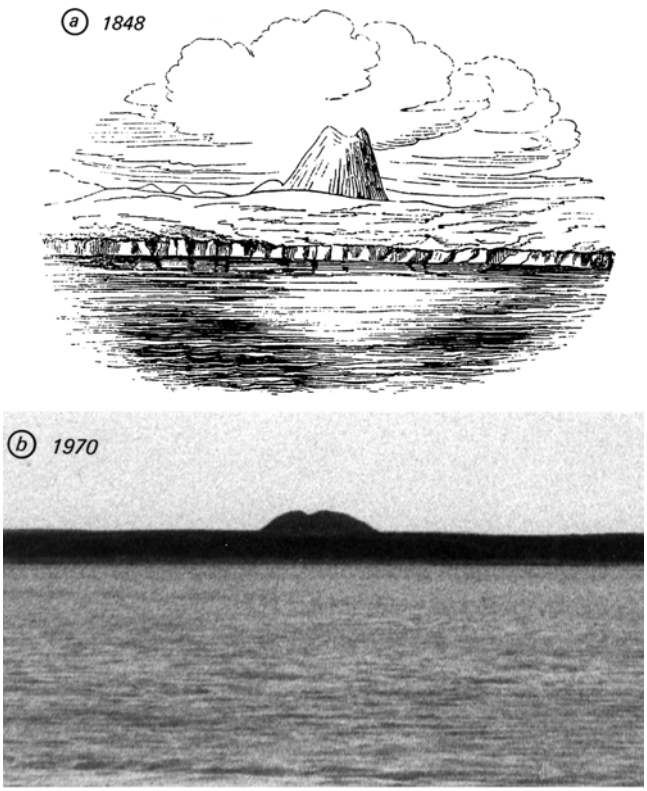

FIGURE 13. a) An 1848 sketch of Pingo 6 (Aklisuktuk Pingo) from East Channel, Mackenzie River (Richardson, 1851, p. 230). b) Photograph of Pingo 6 (Aklisuktuk Pingo) taken from East Channel, Mackenzie River in 1970.

a) Dessin du pingo n° 6 réalisé en 1848 (Aklisuktuk) à partir de l'East Channel, delta du Mackenzie (Richardson, 1851, p. 230). b) Photographie du pingo n° 6 (Aklisuktuk) prise en 1970 à partir de l'East Channel, delta du Mackenzie.

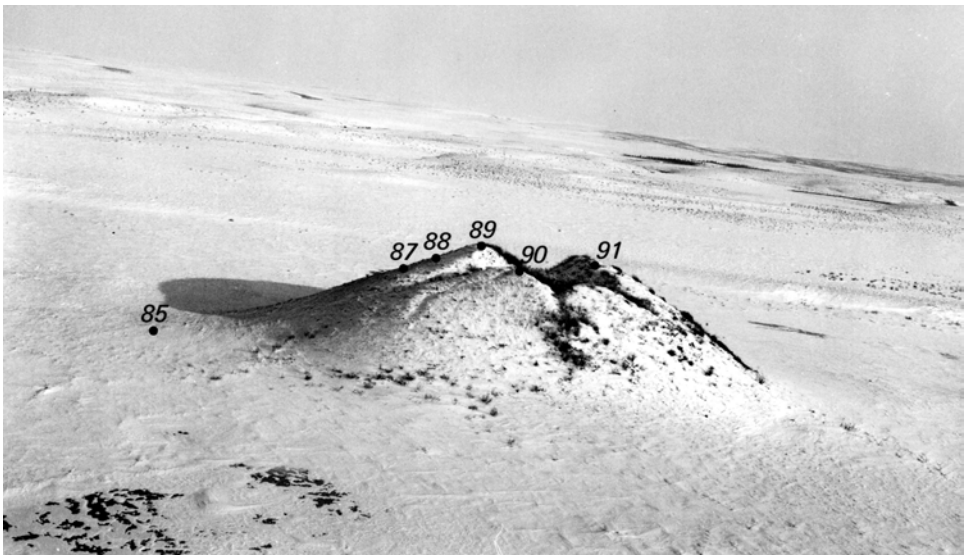

FIGURE 14. Pingo 6 (Aklisuktuk Pingo) rises about 31 m above the surrounding drained lake flats. BM 85 is near the pingo periphery; BM 87 and 88 are on the pingo slope; and BM 89, 90, and 91 are on three of the four pingo peaks.

Le pingo n^{o} 6 (Aklisuktuk) domine de 31 m le lac asséché environnant. Le repère 85 est situé à la périphérie du pingo ; les repères 87 et 88 sont sur le versant du pingo et les repères 89, 90 et 91 sont sur trois des quatre sommets du pingo.

SUB-PINGO WATER LENS

Aklisuktuk, like most large pingos, has a summit crater formed by dilation cracking of the overburden during growth. In 1954, two holes were drilled into Aklisuktuk, the first in the summit crater, the second at the pingo periphery (Pihlainen *et al.*, 1956). Pingo ice was encountered in the summit crater hole from a depth of 1.1 m, or just below the bottom of the active layer, to the bottom of the hole at a depth of 9.8 m. The ice, being pure, was intrusive ice formed by the downward freezing of a sub-pingo water lens. The drill hole on the periphery penetrated 5 m of lake sediments and then fine sand to the bottom of the hole at a depth of 8.3 m, the stratigraphy being identical with that exposed on the sides of the summit crater (Porsild, 1938). One radiocarbon date obtained by the writer in lacustrine sediments near the pingo top at a depth of 0.5 m below the surface yielded an uncorrected radiocarbon date of 6.73 ka BP (GSC 1797). Therefore, as about 5 m of lacustrine sediments were beneath the sample, the pre-drainage lake was much older than 7 ka. The drilling data from the periphery suggest that the thickness of the overburden, when Aklisuktuk started to grow, was about 10 m. If the residual pond in which the pingo grew is assumed to have been 1 m deep and the thickness of the pingo overburden 10 m, then the bottom of the present pingo ice core, if composed of pure intrusive ice, would be about 11 m below the surrounding lake flat and even deeper, if segregation ice is also present below the intrusive ice in the ice core.

The most favorable line-of-sight from East Channel of the Mackenzie River to Aklisuktuk Pingo, which lies 5 km inland from the right bank of East Channel, shows that the pingo was probably more than 7 m high before the top would be noticeable from the river (Mackay, 1981). Therefore, at the 7 m height the pingo was underlain by a sub-pingo water lens as shown by the presence of intrusive ice as discussed above. It is significant to note that Richardson's 1848 description and sketch (Fig. 13a) depict Aklisuktuk as a very steep conical hill which contrasts with the present subdued profile (Fig. 13b). In Richardson's time, artistic licence was frequently used in Arctic drawings, as shown by the pingo slopes of 60 to 70° in Figure 13a. Such steep slopes could not have existed, even for a few years, because if they had, the pingo periphery would now be blanketed with old slumped debris from mass wasting, which it is not. In view of the preceding data, the oral tradition of "the one that is growing" (*i.e.* Aklisuktuk) could be explained by a rapid increase in the depth of the sub-pingo water lens within the memory of an individual. The subsequent reduction in height and steepness might then be attributed to pingo rupture and spring flow after 1848.

VEGETATION CHANGES

In May 1932, the inside slopes of the crater were scantily covered with vegetation and there was a huge snowdrift in the crater (Porsild, 1938). In 1954, when the pingo was drilled, the drilling tripod was placed in the centre of the crater where there was a pool measuring about 3 m wide and 10 m long. Although there was no mention of vegetation in the published report a field sketch showed very few willow thickets (Pihlainen *et al.*, 1956). In the 1972 to 1992 survey period, the willows in the crater grew so rapidly that, by 1992, it was difficult to carry the surveying equipment through the willows in the crater. Since Aklisuktuk Pingo was probably full grown in 1848, if not even higher than at present, the rapid growth of willows in the crater since 1954, particularly since 1972, suggests climate change.

PINGO 7 (PORSILD PINGO)

In May 1935, Porsild (1938) photographed an unusual frost mound that had grown the previous winter in the bottom of a drained lake. The frost mound, whose ice core was exposed by a summit dilation crack, grew from rupture of permafrost and intrusion of water into the active layer (Mackay, 1988b). Pingo 7 has grown up at the site of the 1935 frost mound. Pingo 7 (Porsild Pingo) has been named after Porsild and the name has been approved by the Canadian Permanent Committee on Geographical names (Mackay, 1979, p. 61) in recognition of the contributions to northern science of the late Dr. A.E. Porsild (1901-1977). Porsild Pingo is circular, about 150 m in diameter, and it has grown up in the bottom of a drained lake measuring

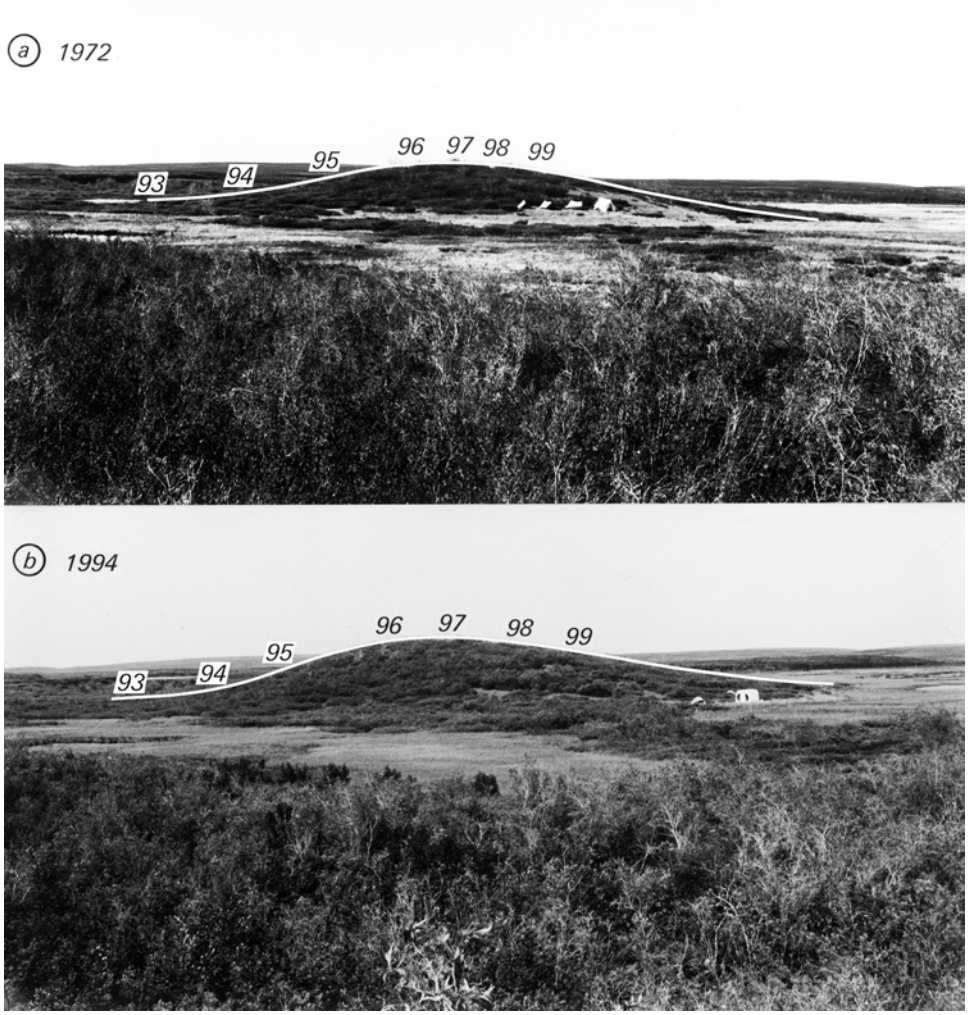

FIGURE 15. a) 1972 photograph of Pingo 7 (Porsild Pingo). Datum BM 92 is off the left side of the photograph. BM 93 to 99 are on the pingo. b) 1994 photograph taken from essentially the same site as the 1972 photograph. A comparison of the 1972 and 1994 photographs shows a combination of both pingo and willow growth. See text.

a) Photographie datant de 1972 du pingo n^{o} 7 (Porsild). Le repère de niveau 92 est à gauche, en dehors de la photographie. Les repères 93 à 99 sont sur le pingo-même ; b) photographie de 1994 prise à peu près du même endroit. La comparaison entre les deux photographies montre une croissance à la fois du pingo et des saules (voir texte).

about 700 m in width and 1100 m in length. In 1972 bench marks were installed from the former lake shore to the pingo top (Fig. 15a, b). The results of the 1972 to 1987 surveys have been published (Mackay, 1988b). The pingo was resurveyed in 1992 and 1994 to give a 22 year record of pingo growth (Fig. 16). The lake drained in about 1900, as estimated from the ages of willows. Drainage was catastrophic as shown by a greatly oversized flat-floored outlet channel, 25 m in width at the top and 6 m in depth, and also by a 4 m high former waterfall *within* the drained lake basin, proof of a torrential flow (Mackay, 1988b, Fig. 3). By 1935 the pingo site, *i.e.* the site of the seasonal frost mound, was dry enough to support willow growth. In the summer of 1935 (air photo A5022-52R) the seasonal frost mound photographed by Porsild in the spring shows up as a white dot. By 1950 (air photo A12918-165) a small pingo was growing at the site and by 1972 (Fig. 15a) Porsild Pingo was large enough to be seen from a distance of many kilometres.

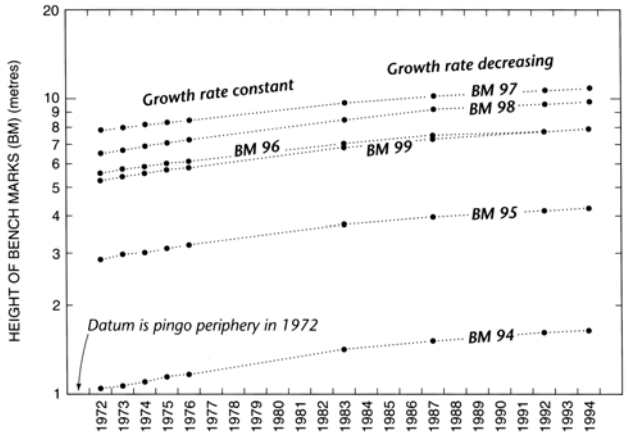

FIGURE 16. The heights of the bench marks of Pingo 7 are plotted on a logarithmic scale to facilitate the comparison of growth rates during the 1972 to 1994 period. Datum is the pingo periphery in the 1972 survey.

Altitudes des repères du pingo n^{o} 7 reportées à échelle logarithmique afin de faciliter la comparaison des taux de croissance au cours de la période 1972-1994. En 1972, la périphérie du pingo représente le niveau de base.

PINGO GROWTH

Pingo growth from 1972 to 1994, omitting the minute height change of BM 93, is plotted in Figure 16. In the 1972 to 1976 period, when the bench marks were surveyed each summer, the yearly growth rates, when pro-rated for the number of days

between surveys, were remarkably constant for all bench marks. Between the next two survey periods, 1983 to 1987, and 1987 to 1992, the growth rates for all bench marks decreased. However, in the last period of 1992 to 1994 the growth rates for BM 94, 95, and 96 on the west slope of the pingo continued to decline, the growth rate for BM 97 on the pingo top remained unchanged, bw% the growth rates for BM 98 and 99 on the southeast slope increased.

BENCH MARK TILTS

In 1987, 1992, and 1994 the tilts of BM 94 to BM 99 were measured with an electronic tiltmeter. From 1987 to 1994 the bench marks tilted downslope, the increases in decimal degrees being: BM 94, 0.18°; BM 95, 0.58°; BM 96, 0.64°; BM 97, 0.67°; BM 98, 0.23°; and BM 99, 0.26° When the downslope increases in tilt are plotted against increases in height, the data for the west slope from BM 94 to BM 97 lie on a smooth curve, quite different from that of BM 98 and BM 99 on the southeast slope. The differences in the tilt patterns between the west and southeast slopes correspond to the differences in their growth patterns for the same period. The growth of Porsild Pingo is then asymmetric with a more rapid growth on the southeast side, probably because freeze-through would have been earlier on the shoreward (*i.e.* west) side than on the southeast (*i.e.* lakeward) side, similar to what happened with Pingos 8, 9 and 10, to be discussed later. Porsild Pingo has not been drilled so there is no information as to whether the ice core is of intrusive ice, segregation ice, or a combination of both.

DILATION CRACKS

Porsild Pingo, unlike many pingos of its size, lacks a large summit dilation crack but it has, instead, a spider-like pattern of cracks that start at the summit and then trend downslope (Mackay, 1979, Fig. 18; 1988b, Fig. 4). Some of the summit dilation cracks have matching sides, an indication that the pingo is growing. In the period from 1972 to 1994 the dilation crack between BM 96 and BM 97 on the west slope, and BM 97 and BM 98 on the southeast slope, each widened from about 1 m to 2 m. The rate of widening was then about 5 cm/a, a probable indication of the dilation crack widths.

PHOTOGRAPHIC COMPARISON (1972-1994)

Photographs taken from essentially the same position in 1972 and 1994 are shown in Figure 15a,b. In the 22 year interval the periphery remained unchanged in height, as shown by survey, but the top at BM 97 grew about 3 m, a substantial amount. However, the visual impression of pingo growth is misleading, because in the intervening 22 years the willows grew taller, thicker, and willow growth spread from the upper bare pingo slopes down to the periphery and onto the adjacent lake flats. Nevertheless, with allowance for willow growth, a comparison of the 1972 and 1994 profiles, marked with solid lines, against the background horizon profile provides clear evidence of substantial pingo growth.

PINGO 8

LAKE DRAINAGE

The best known evidence for the genesis of the Tuktoyaktuk Peninsula Area pingos from the sequence of rapid lake drainage, permafrost aggradation on the drained lake bottom, pore water expulsion, groundwater flow, and pingo genesis in residual ponds comes from the growth of Pingos 8, 9, 10, and 11. The evidence, fortuitously discovered after field studies commenced in 1969, has come from air photos taken before, the year of, and after the beginning of pingo growth (Mackay, 1973, 1979). The before coverage, a 1935 air photo (A5026-35R) of the coastal area about 20 km southwest of Tuktoyaktuk showed three lakes (Lakes A, B, and C) inland from the coast (Fig. 17). By 1950 (air photo A12918-246) Lake A had been drained by coastal retreat. The drop in water level in Lake A caused Lakes B and C to drain, because the three lakes were interconnected by creeks.

PINGO GENESIS

The 1950 air photo (A12918-246) of drained Lake B shows several residual ponds with the top of Pingo 8 emerging in one of the ponds and, within the brief span of about 5 years, Pingos 9, 10, and 11 had also commenced growth in three other residual ponds (Mackay, 1973). The years in which Lakes A and B drained are unknown but they can be

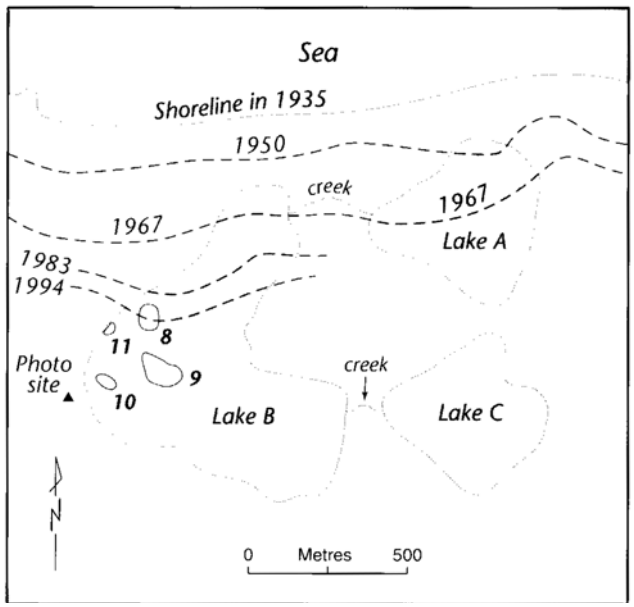

FIGURE 17. In 1935 (air photo A5026-35R) lakes A, B, and C were inland from the coast; by 1950 (air photo A12918-246) coastal retreat had drained, successively, Lakes A, B, and C leaving residual ponds on the bottom of Lake B; by 1967 (air photo A19978-18) Pingos 8, 9, 10, and 11 had grown up in four of the 1950 residual ponds.

En 1935 (photo A5026-35R), les lacs A, B et C étaient à l'intérieur des terres ; en 1950 (photo A12918-246), le retrait de la mer avait provoqué l'assèchement des lacs A, B et C, laissant des mares résiduelles au fond du lac B ; en 1967 (photo A19978-18), les pingos n^{os} 8, 9, 10 et 11 se sont développés dans quatre des mares résiduelles de 1950.

estimated, with reasonable confidence, to within a time span of about 5 years. Lake A, which was 200 m inland in 1935, probably drained a few years after 1940, as estimated from long-term rates of coastal retreat (Mackay, 1986a). Lake B could not have drained much later than about 1945 in order for there to have been time, by 1950, for: permafrost aggradation on the exposed drained lake bottom; pore water expulsion beneath ice-bonded permafrost; groundwater flow to the birth site of Pingo 8; and an hydrostatic pressure of sufficient magnitude to intrude a sub-pingo water lens, as shown by the presence of intrusive ice, beneath nearly 2 m of frozen pond sediments and to initiate pingo growth.

PINGO GROWTH

When Pingo 8 was first seen in 1969, the freshness of the dilation cracks with matching sides and the vegetation suggested that the pingo was young and growing. Pingo 8 was then 6 m high, circular in plan view, with a diameter of 75 m, and about 100 m inland from the rapidly eroding coast (Fig. 18). Pingo 8 was surveyed each summer from 1969 to 1981 (Fig. 19). However the surveys were discontinued after 1981, because storm waves, as a result of rapid coastal recession, were beginning to erode the seaward perimeter of the pingo. In contrast to the 6 m pingo growth from 1950 to 1969, the pingo top grew only 1 m from 1969 to 1981 (Fig. 19). Nevertheless, neither the height of Pingo 8 nor its growth rate can be equated with the growth of pingo ice, because the variations in depth of the sub-pingo water lens beneath Pingo 8 are unknown. The rapid decrease in the growth rate resulted from its proximity to the shoreline of pre-drainage Lake B. In most lakes the top of permafrost beneath the unfrozen basin dips lakeward (Fig. 4a). Therefore, upon drainage, downward freeze-through of aggrading permafrost normally occurs first closest to the former lake shore and last towards mid-lake where the pre-drainage depth to permafrost was the greatest. In support of the preceding, in April 1973, a hole was drilled (Geological Survey of Canada under the supervision of Dr. V.N. Rampton) 10 m lakeward from the middle of the periphery of Pingo 8. Ice-bonded permafrost (z_i) was penetrated at a depth of 17 m and water from beneath the ice-bonded permafrost flowed to the surface with a 0.3 m head. As the drill hole was 110 m from the former lake shoreline and the depth to the bottom of unbonded permafrost exceeded 17 m, the lakeward slope of the permafrost surface was 10° or steeper. Therefore, freeze-through of permafrost would have occurred first on the landward side of Pingo 8, closest to the former lake shoreline, and last on the lakeward side which was farther away (Fig. 18). To illustrate, although BM 302 and BM 304 were both on the lower pingo slope and not much different in height above the pingo periphery in 1969, the growth of BM 304 was less than that of BM 302 (Fig. 19), probably because it was closer to the former lake shore than BM 302.

PINGO ICE

In the period from the early 1980's, when waves began to erode Pingo 8, to 1996, when only about a fifth of the sectioned pingo still remained, pingo ice was exposed continuously beneath the overburden (Fig. 20). The thickness of the overburden at the pingo top varied, but it was typically about 2 m and it increased downslope to the pingo

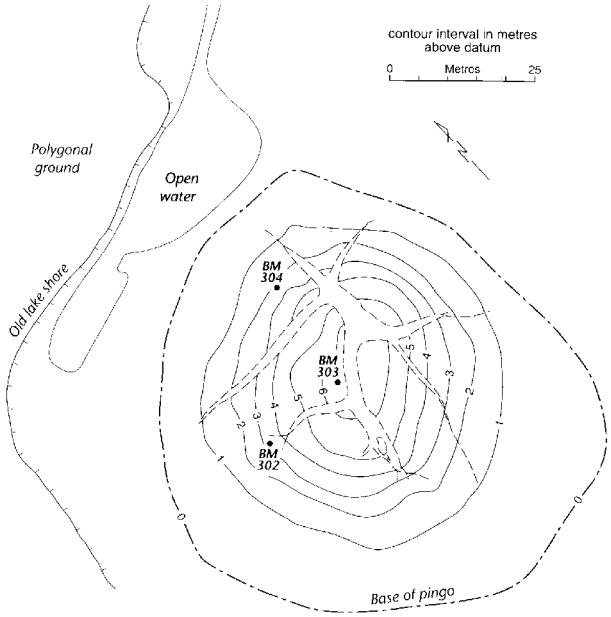

FIGURE 18. Contour map of Pingo 8 in 1975 when it was 25 years old. Growth started in 1950 (air photo A12918-246) when the pingo top can be seen emerging in the centre of a shallow residual pond.

Courbes de niveau du pingo n^{o} 18, qui a 25 ans d'existence en 1975. La croissance a commencé en 1950 (air photo A12918-246) alors que le sommet du pingo émergeait du centre d'une mare résiduelle peu profonde.

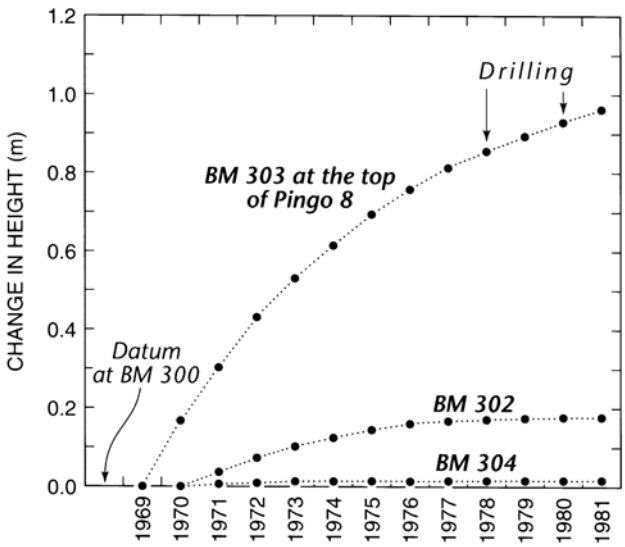

FIGURE 19. Graph for Pingo 8 showing the change in height of BM 302, 303, and 304 for the 1969 to 1981 period. By 1981 the seaward periphery was being wave-eroded from coastal retreat so no further height surveys were carried out.

Graphique du pingo n^{o} 8 montrant les différences d'altitude des repères 302, 303 et 304 au cours de la période 1969-1981. En 1981, la partie périphérique exposée à la mer a été emportée et aucune autre mesure n'a été effectuée depuis.

periphery. The pond depth in which Pingo 8 grew is unknown, but if a depth of 1 m is assumed, then the top of pingo ice when growth commenced was about 3 m below the adjacent lake flat. Furthermore, as all exposures seen

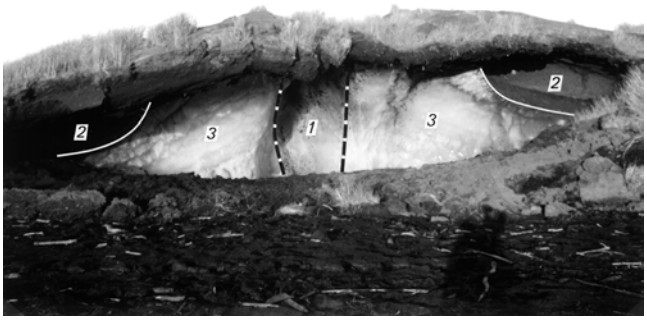

FIGURE 20. Wave-eroded Pingo 8 in 1987. The peaty overburden at the top was about 1.8 m thick. 1) Mostly vertically banded dilation crack ice. 2) Stony clay, about 1 m or more in thickness, beneath the overburden peat to either side of the summit dilation crack. 3) Intrusive ice, formed from downward freezing of the sub-pingo water lens, with seasonal bands of clear and bubbly ice formed by the downward propagation of the cold and warm temperature waves.

Le pingo n^o 8 érodé par la mer en 1987. La couverture de dépôts tourbeux sur le sommet fait 1,8 m d'épaisseur. 1) Fissure de dilatation remplie de glace en grande partie rubannée verticalement. 2) Argile pierreuse, d'environ 1 m d'épaisseur, sous la tourbe de recouvrement, de chaque côté de la fissure de dilatation du sommet. 3) Glace intrusive, formée par l'engel de la lentille de glace sous-jacente au pingo, avec bandes saisonnières de glace claire contenant des bulles, qui se sont formées en raison de la propagation descendante des températures, chaudes ou froides selon les saisons.

during the erosion of Pingo 8 were of intrusive and dilation crack ice, except for the lower portion of an ice wedge, the bottom of the ice core during the growth period was then about 3 m below the adjacent lake flat.

The contact between the pingo overburden and the underlying intrusive ice was so sharp that it was delimited within 1 cm in many exposures (Fig. 21). Bubble trains, oriented normal to the contact, frequently extended downwards, in discontinuous alignment, for several metres. The ice, upon exposure to radiation, usually developed into "candle ice" similar to that often seen in lake and river ice (Hobbs, 1974; Michel and Ramseier, 1971; Danilov, 1983). A nearly complete vertical section of Pingo 8 is shown in Figure 20. Vertically banded orangish dilation crack ice penetrated downward beneath the summit dilation crack (Fig. 20, no. 1). On either side of the pingo the overburden peat was underlain by as much as 1 m or more of stony clay (Fig. 20, no. 2) below which there was intrusive ice (Fig. 20, no. 3). The intrusive ice was composed of alternating bands of clear and bubbly ice, the banding paralleling the pingo slope. The thickness of each band pair of clear and bubbly ice represented one year's growth of ice [4], the alternating clear and bubble bands, as in Figure 7, resulting from differences in freezing rates from the downward propagation of the seasonal cold and warm temperature waves (Mackay, 1990). The band thicknesses were difficult to measure where exposed to prolonged radiation, but at a depth of 3.5 m below the overburden, near the pingo centre, the widths of four successive band pairs, measured in the downward direction, were: 0.35 m, 0.33 m, 0.26 m and 0.24 m. Solving

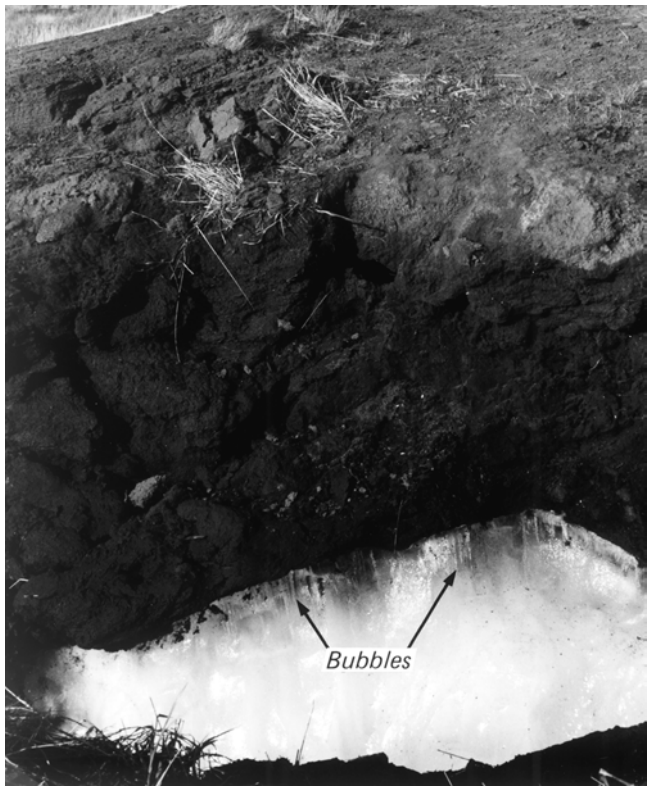

FIGURE 21. The contact between the peaty overburden and underlying ice of Pingo 8 was often so sharp that it could be delineated within one centimetre as in this 1983 photograph. Bubble trains, oriented normal to the contact, usually extended downwards, in discontinuous alignment, for several metres and, upon exposure to radiation, often "candle ice" developed as in lake and river ice.

Le contact entre la couverture tourbeuse et la glace sous-jacente au pingo n^o 8 était parfois si net qu'il pouvait être retracé au centimètre près comme sur cette photographie de 1983. Des trains de bulles s'étirent vers le bas en alignements discontinus de plusieurs mètres ; en raison de l'exposition au rayonnement, il se forme de la glace d'exsudation comme dans les lacs et et les rivières.

for "t" using [4] and the four measured values for "Δz" give a value of "t" of about years 5, 6, 7, and 8 for the four bands The annual growth of ice [4] in much of the Tuktoyaktuk Peninsula Area can be estimated, reasonably well, using $b = 1.5 m/a^{1/2}$ and Figure 4 (Mackay, 1985a, 1985b). If the first band grew in year 5, the four measured band thicknesses show good agreement with the plotted values in Figure 3, thus confirming the former existence of a sub-pingo water lens.

WATER QUALITY

Data on the water quality of pingo ice are given in Table II. Samples 1, 2, and 3 of ice were collected 0.3, 1.8, and 3.5 m below the top of pingo ice where the overburden was 1.7 m thick. The analyses in Table II show a rapid increase in solute concentrations from sample 2 to 3 with depth as a result of solute rejection from downward freezing combined with recharge of increasingly saline groundwater from beneath the surrounding ice-bonded permafrost (Mackay, 1990).

TABLE II

Water quality analyses for ice samples collected on July 2, 1983, from a vertical exposure of ice in Pingo 8. The peaty overburden above the ice was 1.7 m thick. Analyses by the Inland Waters Directorate, Environment Canada.

Sample	pH	Total Hardness mg/L $CaCO_3$	Conductivity λS/cm	Chloride dissolved mg/L	Silica mg/L SiO_2	Ca dissolved mg/L	Mg dissolved mg/L	Na dissolved mg/L	K dissolved mg/L
1. Ice 0.3 m below the top of pingo ice	5.4	12.8	54.7	4.1	0.2	3.3	1.1	2.2	0.5
2. Ice 1.8 m below the top of pingo ice	5.5	13.4	54.2	4.7	0.2	3.7	1.0	2.3	0.2
3. Ice 3.5 m below the top of pingo ice	6.4	55.1	172	24.5	0.4	9.8	7.5	12.5	0.8

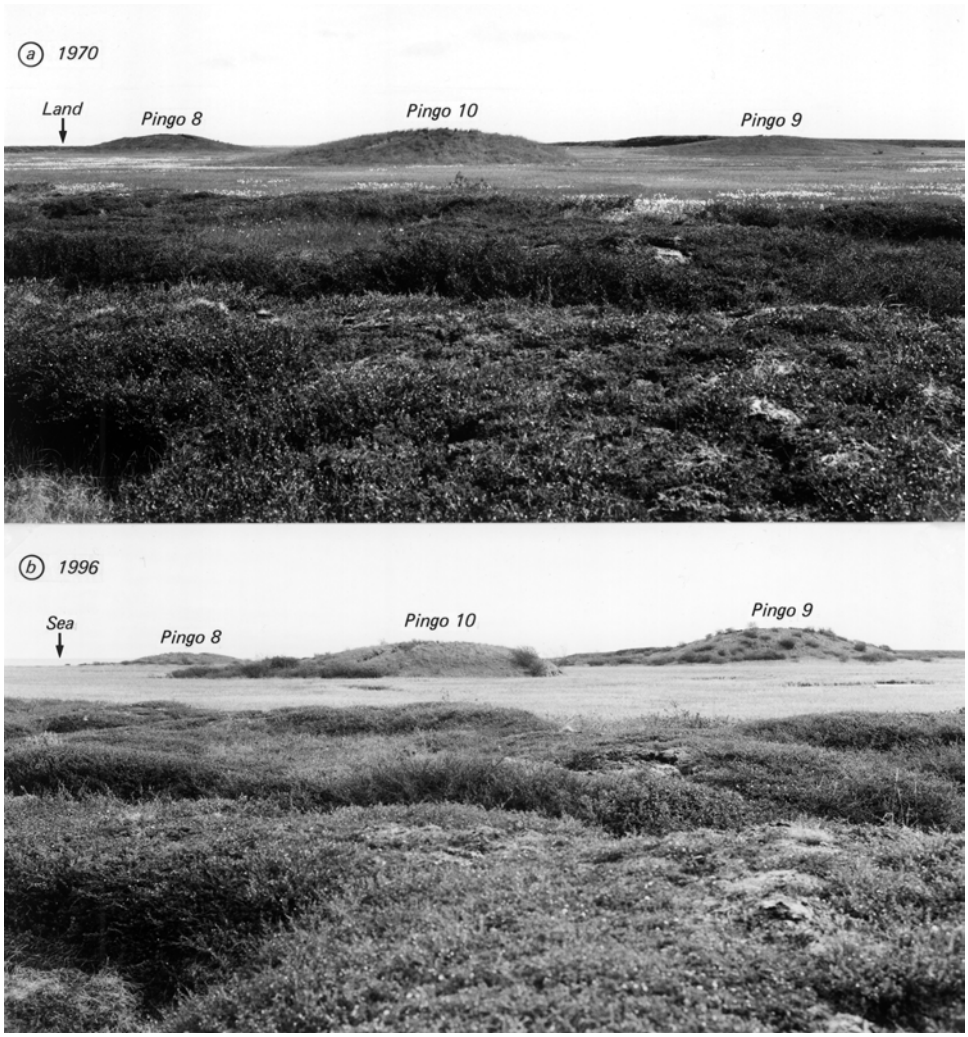

FIGURE 22. a) A 1970 photograph of Pingos 8, 9, and 10. In 1970, there was "Land," so labelled, between Pingo 8 and the sea (the photo site is shown in Fig. 17). b) A 1996 photograph of Pingos 8, 9, and 10 taken with the same camera and from the same site as for the 1970 photograph. By 1996, coastal recession had eroded the "Land," in the 1970 photograph, to be replaced by the "Sea." The growth of Pingo 9 was substantial as can be seen by comparing the 1970 pingo outline, with respect to the background profile, with that in 1996. There was negligible growth of Pingo 10. Between 1970 and 1996 there was considerable willow growth on both Pingos 9 and 10.

a) Photographie prise en 1970 des pingos n^{os} 8, 9, et 10. En 1970, il y avait de la « terre » entre le pingo n^{o} 8 et la mer (emplacement de la prise de vue à la fig. 17) ; b) photographie datant de 1996 des pingos n^{os} 8, 9 et 10 prise du même endroit et avec le même appareil. La mer a alors remplacé la terre en raison du recul de la côte. La comparaison entre les deux photographies montre que la croissance du pingo n^{o} 9 a été considérable et celle du pingo n^{o} 10 a été négligeable. La croissance des saules a quant à elle été forte sur les pingos n^{os} 9 et 10.

PHOTOGRAPHIC COMPARISON: 1970 to 1996

The major changes in Pingo 8 can be seen by comparing the 1970 and 1996 photographs (Fig. 22a,b) that were taken with the same camera and from the same site (see Fig. 17 for the photo site location). In the 1970 photograph, "Land" can be seen on the seaward side of Pingo 8. By 1996 the "Land" on the seaward side of the 1970 photograph had been completely eroded away and Pingo 8 was smaller, because much of the pingo had been wave-eroded. The vegetation of the peaty polygons in the immediate foreground showed little change in the 26 year period.

PINGO 9

Pingo 9 (Fig. 23a,b) has grown up in a residual pond in the same drained lake bottom as Pingos 8, 10, and 11. In 1950 (air photo A12918-246) the growth site of Pingo 9 was occupied by a large residual pond and by 1957, age dating shows that willows were growing on the periphery of Pingo 9. Because it would probably have taken at least one or two years after pingo growth started before willows could have become established on the pingo periphery, pingo growth will be assumed to have begun in 1953, a date intermediate between 1950 and 1957.

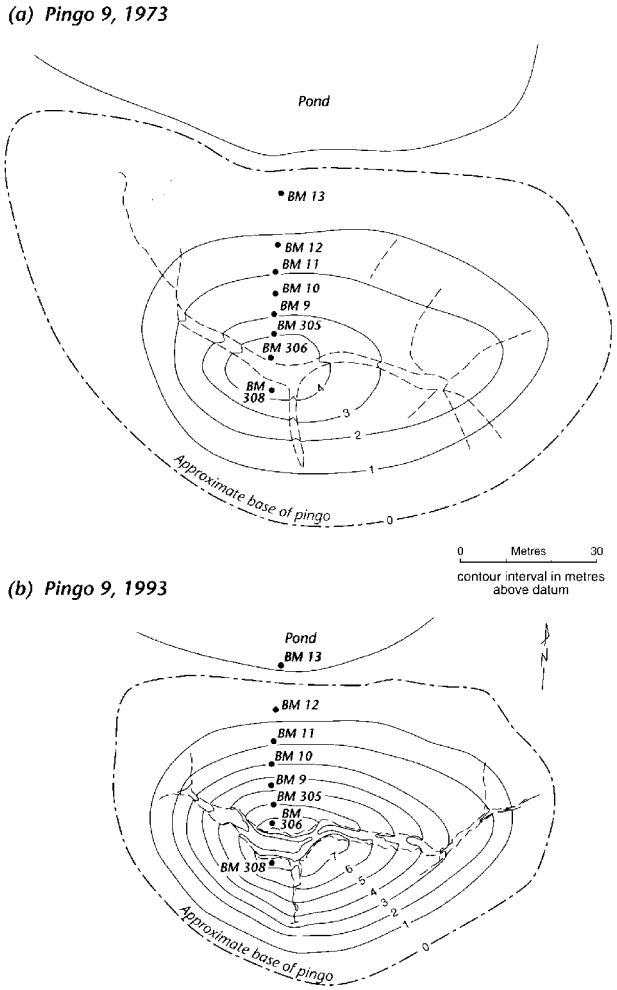

FIGURE 23. Contour maps of Pingo 9 for 1973 and 1993. The contours are based upon a local datum whereas the datum used for levelling was inland from the lake shore.

Topographie du pingo n^{o} 9 en 1973 et en 1993. Les courbes de niveau ont été tracées à partir d'un niveau de base local, le nivellement ayant été fait à partir d'un niveau de base situé à l'intérieur par rapport à la rive du lac.

STRATIGRAPHY

The stratigraphy, as determined from drilling (Fig. 24) from the surface downward was: a 1 to 2 m layer of peat and icy clay, an ice-bonded sand, and then unbonded sand with

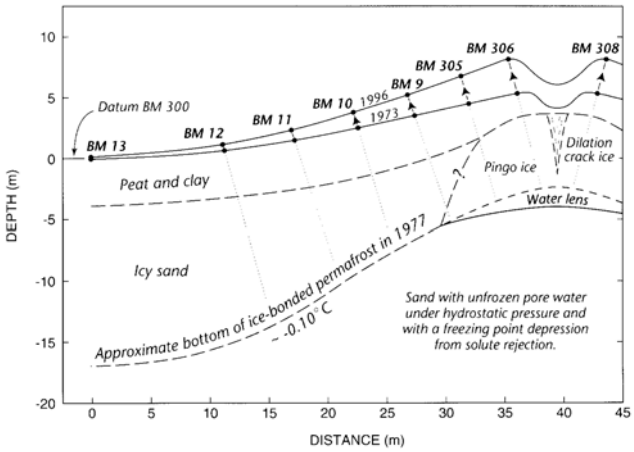

FIGURE 24. Vertical cross section of Pingo 9 based partly upon 1977 drilling showing: the approximate boundary between ice-bonded permafrost and unbonded permafrost; the pingo ice core; the sub-pingo water lens; dilation crack ice; and the locations of the bench marks on the pingo.

Coupe du pingo n^{o} 9 réalisée en partie d'après le sondage de 1977 montrant la limite approximative entre le pergélisol cimenté par la glace et le pergélisol non cimenté, le noyau de glace, la lentille d'eau sous-jacente, la fissure de dilatation et l'emplacement des repères sur le pingo.

a freezing point depression of about - 0.1°C. The surface peat was derived from the thermokarst enlargement of Lake B into the surrounding area of peaty ice-wedge polygons which now border about two-thirds of the drained lake shoreline. The clay beneath the peat came from the fine-grained sediments that underlie the ice-wedge polygons. The sands at depth are typical of the glaciofluvial sediments of the Tuktoyaktuk area.

PINGO GROWTH

In 1970 BM 305 and 306 were installed near the top of Pingo 9 and in 1973 BM 9, 10, 11, 12, and 13 were added on the north facing slope and BM 308 at the top (Fig. 23a,b). The datum bench marks were inland from the former lake shore. After installation, all bench marks were surveyed each summer until 1996, except for 1995 because of logistic problems. In the period between 1970 and 1996 Pingo 9 grew higher, as determined by survey, but the pingo periphery, which had been mapped subjectively by noting both the break in slope and vegetation change between the pingo and the adjacent lake flats, decreased (Fig. 23a,b). In 1973, BM 13 was about 7.6 m south of the well defined pond shoreline to the north but, by 1993, BM 13 was within the pond and north of the ill defined base of the pingo. The reduction in the basal pingo area resulted from about 0.15 m of lake bottom heave coupled with a slight rise of pond level from partial blockage of lake bottom drainage to the sea.

HEIGHT INCREASE

In 1970, when Pingo 9 was about 17 years old, the top of the pingo was 4 m above the surrounding lake flat and in 1996, when the pingo was about 43 years old, the top was 7.5 m above the lake flat for a growth of about 3.5 m in 26

years. The depth of the residual pond in which Pingo 9 commenced growth is unknown, but if it was about 1 m, the top of the pingo had been uplifted 5 m by 1970 and 8.5 m by 1996. The change in height of BM 306, at the top of Pingo 9, is shown for the 1970 to 1996 period and also height changes for BM 9, 11, and 13 for the 1973 to 1996 period in Figure 25. The growth rates for the bench marks gradually decreased to 1977, prior to 1977 drilling. The rates after 1977 were affected also by water loss from the sub-pingo water lens by drilling in 1980, 1982, and 1985.

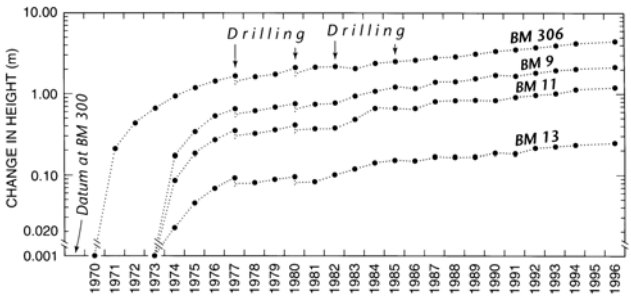

FIGURE 25. Graph showing the change in height, on a logarithmic scale, of some bench marks on Pingo 9: i.e. BM 306 for 1970 to 1996 and BM 9, 11, and 13 for 1973 to 1996. The pingo subsided slightly from water loss from the sub-pingo water lens each time that the pingo was drilled.

Graphique illustrant les différentes altitudes, à échelle logarithmique, de certains repères du pingo n^{o} 9 : le repère 306 de 1970 à 1996 et les repères 9, 11 et 13 de 1973 à 1996. Lorsqu'il y avait forage, le pingo s'affaissait légèrement en raison d'une perte d'eau provenant de la lentille d'eau sous-jacente.

VOLUME INCREASE

The volume of Pingo 9 above the lake flat has been estimated from contour maps drawn in 1970, 1986, 1990, and 1993. In 1970, when Pingo 9 was about 17 years old, the volume was about 6000 m^3; in 1986, 10,000 m^3; in 1990, 11,000 m^3; and in 1993, 12,000 m^3. Thus, the volume increase averaged about 250 to 300 m^3/a.

SUB-PINGO WATER LENS

In July 1977 ten holes were drilled in a line across Pingo 9 in order to delineate the configuration of permafrost and pingo ice. The first and last holes were on the lake flat just beyond the pingo perimeter, six holes were on the sides and top of the pingo, and two were in the summit dilation crack. The holes near the pingo top penetrated a sub-pingo water lens which was 2.2 m deep in the middle, 30 m in basal diameter, and the top and bottom of the water lens were concave downward with the general curvature being sub-parallel to the ground surface (Mackay, 1978). Strong drill-hole flow of clear water at a temperature of about - 0.1°C welled up from each of the four drill holes that penetrated the water lens, with heads of 0.05 to 0.1 m above ground level. The drill holes on the pingo slopes and adjacent lake flats first penetrated through ice-bonded permafrost and then into unbonded permafrost, at a temperature of - 0.1°C, from which water flowed to the surface with much entrained sand. As a result of water loss from the sub-pingo water lens, the pingo began to subside, the amounts from 6 July 1977, prior to drilling, to 13 July 1977, one week after drilling but not before all drill-hole flow had ceased were: BM 13, 0.70 cm; BM 12, 0.97 cm; BM 11, 1.29 cm; BM 10, 1.56 cm; BM 9, 1.82 cm; BM 305, 2.09 cm; BM 306, 2.23 cm; and BM 308, 2.35 cm, the subsidences increasing from BM 13 at the pingo periphery to BM 306 and BM 308 at the pingo top. The pingo was re-drilled in 1980 and the subsidences from 24 to 28 June 1980 were: BM 13, 0.99 cm; BM 12, 1.17 cm; BM 11, 1.35 cm; BM 10, 1.57 cm; BM 9, 1.79 cm; BM 305, 2.15 cm; BM 306, 2.20 cm; and BM 308, 2.35 cm. The 1980 subsidence pattern was similar to that of 1977 with the subsidence increasing from the side to the top, thus indicating not only greater subsidence for bench marks underlain by the sub-pingo water lens but also subsidence for bench marks which were not underlain by the water lens (Fig. 24). In late June 1980, a hole was drilled through ice-bonded permafrost about 150 m north of Pingo 9 and near Pingo 8 (Fig. 17). The drill hole yielded substantial flow and, as a result, within less than half an hour, which was the shortest time that could be made from the drill hole to Pingo 9, the water pressure at Pingo 9 had begun to decrease. The pressure continued to decrease until flow at the drill hole 150 m to the north had ceased. The rapid drop in pressure for the two sites which were 150 m apart shows not only that both sites were in the same groundwater system but also the fact that water is virtually incompressible. Pingo 9 was drilled again in 1985, for the installation of equipment, and the depth of the sub-pingo water lens was about 2 m, or similar to the 2.2 m depth in 1977, despite the drilling in previous years. As a consequence of the drilling, the growth curves for the bench marks are saw-toothed, and, for some bench marks, it was several years before the bench mark heights recovered from the drilling (Fig. 25).

RATE OF PINGO GROWTH

Although the pingo growth can be measured by precise survey, the growth of intrusive ice by downward freezing at the top of the water lens remains unknown without additional data. For example, the top of Pingo 9 grew about 4.5 m from 1970 to 1996 (Fig. 25) but the growth of the ice at the bottom of the ice core is unknown. This is because the growth of a pingo that is underlain by a water lens depends upon two factors, first the 9% volume increase in the growth of ice by freezing at the top of the water lens, and second, the addition and/or loss of water to or from the water lens. Since only the sum of the two variables is known from survey, the contribution of each factor remains unknown without additional data (Mackay, 1978). With respect to Pingo 9, a temperature cable installed vertically in the centre for the 1987 to 1992 period has provided the additional data to compute the growth rate of pingo ice (Parameswaran and Mackay, 1996). From 1987 to 1992, the pingo top grew 67 cm, as determined by survey, and the ice-water freezing front descended 75 cm, as determined from temperature and electrical potential measurements. When the 9% volume expansion of water to ice is taken into account, the 75 cm of ice represented the downward freezing of 68 cm of water at the top of the water

lens. Therefore, as only 7 cm of the 67 cm of pingo growth can be attributed to the 9% volume expansion of water to ice, the water lens was recharged by about 60 cm of water. If there had been no recharge, the pingo growth would have been only 7 cm. The 75 cm of ice that grew in the 1987 to 1992 period represented a growth rate of 15 cm/a. Pingo 9 was about 34 years old in 1987 and 39 years old in 1992. From Figure 4 with b = 1.5 m/$a^{1/2}$ and a time period from 34 to 39 years, the growth rate would be just below 15 cm/a. For Pingo 20, the measured seasonal width of clear and bubble rich bands at year 30 was 15 cm (Mackay, 1990). Therefore, seasonal growth bands of clear and bubble rich ice, as in Figure 7, were probably growing at Pingo 9 from 1987 to 1992 and, quite probably, throughout the previous lifetime of the pingo.

WATER PRESSURES

The pressure in the sub-pingo water lens was measured with pressure transducers from the time of installation in 1977 to 1986, the last year before the connecting cables broke. In 1977 the water pressure dropped after the pressure transducers were installed, because of water loss from drill-hole flow, so no reliable data are available for 1977. The pressures stabilized at about 150 kPa by the summer of 1978. On 23 June 1980 the pressure before drilling was 130 kPa but on 26 June 1980 after drilling it had dropped to 40 kPa. Pressures also dropped after the 1985 drilling. By the summer of 1986 the pressure had risen to 170 kPa or slightly above that of 1978. During the 1977 to 1986 period the pressure transducers, which were at or slightly below the bottom of the sub-pingo water lens, were about 5 m below the adjoining lake flats (Fig. 24). Therefore, in 1986 the hydrostatic head or potentiometric surface was at least 5 m above the pingo top and so about 12 m above the lake flats. In 1977, the depth of ice-bonded permafrost beneath BM 13 was about 17 m (Fig. 24) and it would have been deeper farther from the pingo and even deeper in 1986. Therefore, a 12 m head of water above the surrounding lake flats where ice-bonded permafrost was probably more than 20 m deep is in good agreement with measured pressures in freezing experiments (Balduzzi, 1959) and those observed under field conditions (Mackay, 1987).

BENCH MARK DISPLACEMENT VECTORS

The displacement vectors for the bench marks of Pingo 9, which have been published for the 1973 to 1983 period (Mackay, 1985b) are here extended to 1996 in Figure 24. The upward and outward movements of the bench marks resulted in a change in separation between bench marks. The results of the 1973 to 1996 measurements show that the separations of all bench marks on the north slope (BM 13 to BM 306) decreased whereas those between BM 306 and BM 308 on opposite sides of the summit dilation crack increased (Table III). The displacement vectors in Figure 24 have been plotted from the increases in bench mark heights and decreases in bench mark separations. Significantly, when the upward trends of the displacement vectors are projected downward, they intersect, almost orthogonally, with the bottom of ice-bonded permafrost as it was in 1977. The trends of the displacement vectors indicate that the uplifts of BM 13, 12, 11, 10 and possibly 9 were from the growth of pore and/or segregation ice whereas the uplifts of BM 305, 306, and 308 were from the growth of intrusive ice at the top of a constantly replenished sub-pingo water lens.

BENCH MARK TILTS

The bench mark tilts of Pingo 9, from 24 August 1985 to 1996, are plotted in Figure 26. The first tilt measurements were made on 9 July 1985 just prior to drilling and again on 24 August 1985 six weeks after drilling. The changes in tilt show that all of the bench marks from BM 11 to 306 tilted slightly upslope in response to subsidence from the loss of water from the sub-pingo water lens (note: the data are not plotted in Fig. 26 because tilts had been affected by the recent drilling). In the period between 24 August 1985 (*i.e.*, six weeks after the 1985 drilling) to 1990, all of the bench marks tilted progressively downslope, as would be expected of a growing pingo. Unexpectedly, in 1991, there was a temporary reversal in trend that coincided with a 25 to 35% decrease in the annual uplift of the bench marks, but the decreases were too small to be noticeable on the logarithmic scale used in Figure 25. The reversal in trend suggests that there was water loss from the sub-pingo water lens, as occurred after the 1985 drilling, but no evidence of water loss was seen in the summer of 1991, although water loss could have gone undetected the preceding winter. There was nothing unusual in the 1991 to 1996 trend.

SUMMIT DILATION CRACK

The width of the summit dilation crack between BM 306 and BM 308 increased steadily from 1970 to 1996. In 1970 the crack was 1.45 m wide, the sides were vertical, the trough flat floored, and the active layer was underlain by banded dilation crack ice (Mackay, 1979, Fig. 78). By 1974 the width had increased to 2.8 m; by 1976 to 3.25 m; by 1987 to 4.5 m; by 1992 to 6.0 m; and by 1996 to 6.8 m. The summit dilation crack, in vertical profile, changed from a flat floored 1.15 m deep trough with vertical sides in 1970 to a V-shaped trough 2.20 m deep in 1996. Because the dilation crack widened by the spreading of the overburden on either side, without any addition of material to the middle of the trough, except for whatever slumped in from the sides, some of the dilation crack ice beneath the trough gradually thawed. Measurements show that about 1 m of dilation crack ice thawed beneath the middle of the trough in the 1970 to 1996 period. The 1973 to 1996 distance between BM 306 and BM 308 on either side of the summit dilation crack increased 2.91 m (Table III). The increase in width of the summit dilation crack and the separation between BM 306 and BM 308 can be attributed to frequent summer/winter dilation cracking, the entry of water, and the growth of dilation crack ice at a rate of about 0.12 m/a.

TABLE III

Separations of bench marks at Pingo 9 for 1973 and 1996 as shown in Figure 24

Separation Measured		Separation		Change in Separation	
		1973 (m)	1996 (m)	1973 to 1996 (m)	%
1.	BM 13 to BM 12	10.21	10.02	- 0.19	- 1.86
	BM 12 to BM 11	7.09	6.85	- 0.24	- 3.38
	BM 11 to BM 10	5.38	5.19	- 0.19	- 3.53
	BM 10 to BM 9	4.81	4.69	- 0.12	- 2.49
	BM 9 to BM 305	4.80	4.72	- 0.08	- 1.67
	BM 305 to BM 306	4.30	4.28	- 0.02	- 0.46
2.	BM 13 to BM 306	36.69	35.75	- 0.84	- 2.30
3.	BM 306 to BM 308	6.30	9.21	+ 2.91	+ 46.19

PHOTOGRAPHIC CHANGES: 1970-1996

As discussed with Pingo 8, the 1970 and 1996 photographs in Figure 22a,b were taken 26 years apart with the same camera and from the same photographic site. In the intervening 26 years, Pingo 9 grew substantially in height, as can be seen from the change in profile with reference to that of the stable terrain in the background. There was also an increase in the growth and spread of willows.

PINGO 10

Pingo 10 (Fig. 27) has grown up in a residual pond in the bottom of the same drained lake as Pingos 8, 9, and 11. The planimetric outline of Pingo 10 conforms precisely with that of the residual pond in which the pingo grew, as shown by the outline of the residual pond in a 1950 air photo (A12918-246), taken before growth commenced, with that of Pingo 10 in a 1967 air photo (A19978-18) taken after growth had nearly ceased (Mackay, 1973, 1979). Aging of willows suggests that growth started shortly before 1957. In 1970, BM 307 was installed near the top of Pingo 10 (Fig. 27). Although Pingo 10 had grown to a height of more than 3 m by 1970, growth by then had virtually stopped. The height of BM 307 was remeasured in 1983 and 1989. By 1994 the changes from 1989 were too small to show in Figure 28 and so have been omitted. The brief growth span of Pingo 10 was expected, first, because the pingo was only 60 m from the former lake shore so that an early downward freeze-through to the sub-lake bottom permafrost was expected, and second, Pingo 10 was so small, being only 45 m in length and 30 m in width, that inward freezing from the periphery would have encroached gradually upon the unfrozen zone beneath the pingo and so have hastened freeze-through to permafrost beneath.

Pingo 10, like Pingos 8 and 9, was photographed in 1970 and 1996 (Fig. 22a,b) with the same camera and from the same site. In the 26 year interval, the growth of Pingo 10 was too small to detect on the photos except, perhaps, for a slight bulging of the lower slope on the side towards Pingo 9.

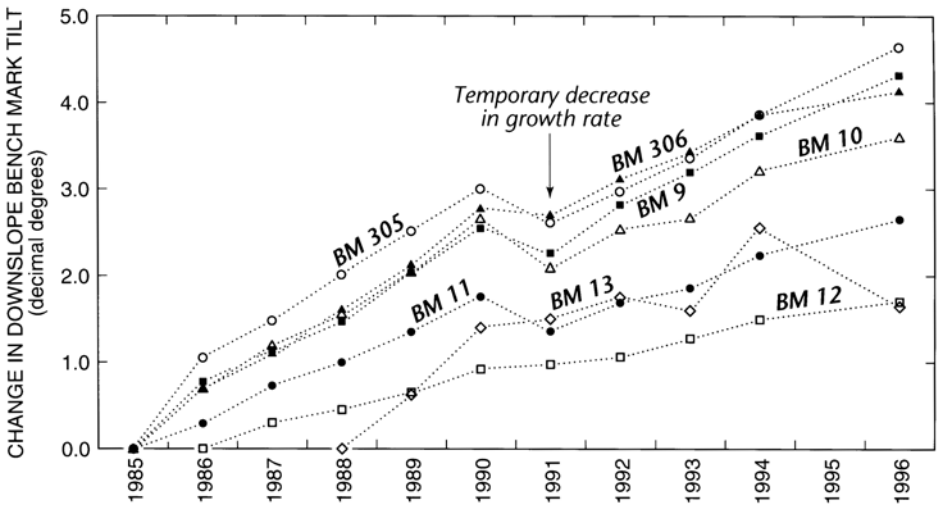

FIGURE 26. Graph showing the change in downslope tilt of the Pingo 9 bench marks for the 1985 to 1996 period. The first tilt measurement for BM 13 was in 1988. The bench marks tended to tilt progressively downslope with pingo growth except for 1991 when there was an unexpected and unexplained reversal in trend.

Graphique montrant les différences d'inclinaison des repères du pingo n^{o} 9 de 1985 à 1996. La première mesure de l'inclinaison du repère 13 a été faite en 1988. Les repères ont tendance à s'incliner vers le bas de la pente avec la croissance du pingo, sauf en 1991 où il y eut un renversement de situation à la fois inattendu et inexpliqué.

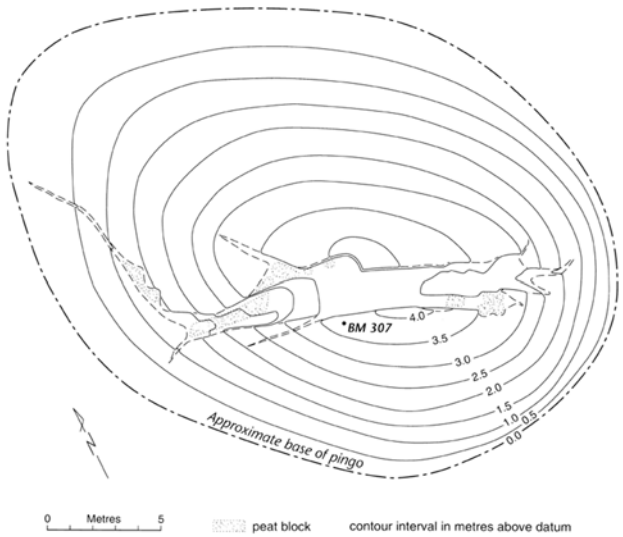

FIGURE 27. Contour map of Pingo 10 prepared in 1994.

Topographie du pingo n^{o} 10 établie en 1994.

PINGO 11

Pingo 11 grew up in a tiny residual pond in the same drained lake bottom as Pingos 8, 9, and 10 (Fig. 17). Growth started before 1957 and the pingo shape conforms precisely to the small pond in which it grew. Pingo 11, the smallest of the four pingos, is only 20 m in length, 10 m in width, and 1.5 m in height. In 1973 two holes were drilled into the pingo to depths of 3.1 m, one hole on the top and the other on one side. The hole on the top penetrated 1.2 m of nearly ice-free peat; then 0.8 m of alternating peat and ice layers that graded downward into pure intrusive ice to the bottom of the core at 3.1 m (Gell, 1976). Bench marks were installed in the two drill holes. Surveys since 1973 have shown that the two bench marks have been stable with reference to datum bench marks inland from the former lake shore, the reason being that Pingo 11, at its nearest point, was only 6 m from the former shore so freeze-through to the underlying perma-

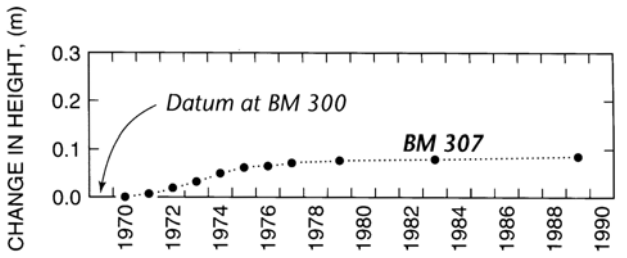

FIGURE 28. Change in height of BM 307 at the top of Pingo 10 for the 1970 to 1989 period.

Différences d'altitude du repère 307 au sommet du pingo n^{o} 10 de 1970 à 1989.

PINGO 12

In 1935 (air photo A5025-49C) there was a lake at the site of Pingo 12 (Fig. 29a); within a few years the lake had drained and Pingo 12 showed up clearly on a 1943 air photo (3025-300R-49); and by 1947 (air photo A10988-111) Pingo 12 had collapsed, leaving a faint rampart (Fig. 29b). Thus, the maximum period between the existence of the lake and pingo collapse was barely 12 years. Since it was most unlikely that lake drainage occurred immediately after the 1935 photo was taken, and that pingo collapse occurred just before the 1947 photo was taken, the interval between lake drainage and pingo collapse was probably considerably less than 12 years. If mid-dates between successive photos are used for the times of lake drainage and pingo collapse, then lake drainage took place about 1939 and pingo collapse about 1945, for an approximate 6 year interval between lake drainage, pingo growth, and pingo collapse.

PINGO REMNANTS

In plan view, Pingo 12 was about 200 m long, 50 m wide, and crescent-shaped (Fig. 30). The convex side that faces the former lake shore is flattish whereas the concave side that faces the former lake centre comprises a series of irregularly

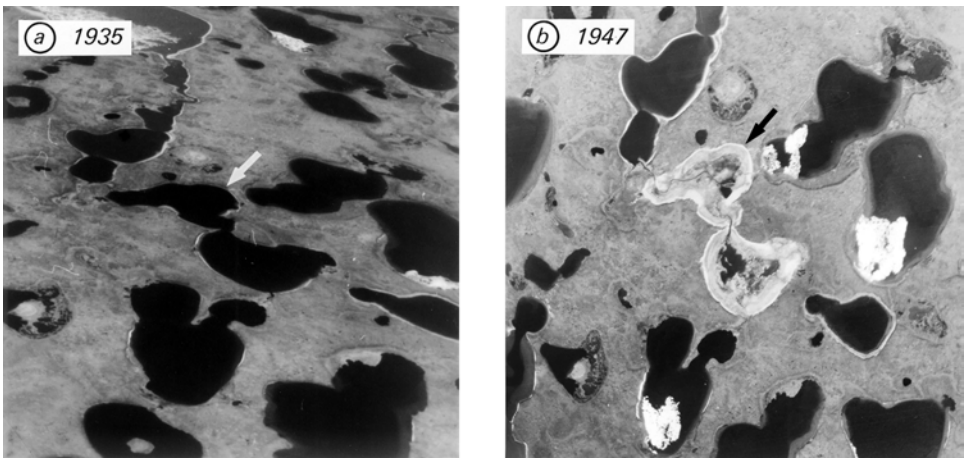

FIGURE 29. a) A 1935 air photo (A5025-49C) showing the lake in which Pingo 12 grew prior to drainage. b) A 1947 air photo (A10988-111) showing collapsed Pingo 12 in the lake which drained between 1935 and 1943 (air photo 3025-300R-49). The two air photographs, ©Her Majesty the Queen in Right of Canada, are reproduced in part from the collection of the National Air Photo Library with permission of Natural Resources Canada.

a) Photographie aérienne (A5025-49C) montrant le lac avant assèchement dans lequel le pingo n^{o} 12 s'est développé. b) Photographie de 1947 (A10988-111) montrant le pingo n^{o} 12 affaissé dans le lac qui s'est asséché entre 1935 et 1943 (photo 3025-300R-49) (reproduction partielle des photographies avec la permission de Ressources naturelles Canada).

shaped ice-cored mounds with intervening depressions, most being the sites of small ponds. The maximum topographic relief is about 1.5 m (Mackay, 1987, 1988c). The collapse of Pingo 12 when it was only a few years old probably resulted from the pingo's crescent shape, like Pingo 4, because crescent-shaped pingos are more likely to rupture than pingos of a more circular shape (Mackay, 1987). In 1971, when it was discovered that Pingo 12 was still hydrologically active, summer and winter field trips were made to observe the types of pingo activity, the last field trip being in 1992. Drilling in the pingo remnants showed that the soil beneath the active layer to a depth of 2.5 m was composed mainly of an ice-rich silt, locally peaty, which, when thawed in a cylinder, yielded about two thirds supernatant water above one third saturated soil. Because the relative relief of the Pingo 12 remnants is only about 1.5 m, the remnants would again become part of the lake bottom if the upper several metres of permafrost were to thaw.

FIGURE 31. The intrusive ice was formed by the rupture of ice-bonded permafrost and the injection of sub-permafrost water into the active layer during the autumn freeze-back of 1985. The scale is given by the handle of a 1 m long shovel, marked with an arrow. Water quality analyses for the 5 ice samples, collected at 10 cm intervals, are given in Table IV.

La glace intrusive s'est formée en raison de la rupture du pergélisol cimenté par la glace et de l'injection d'eau localisée sous le pergélisol dans la couche active au cours d'un regel à l'automne 1985. L'échelle est donnée par le manche de la pelle de 1 m pointée par la flèche. Les résultats de l'analyse des cinq échantillons de glace, recueillis à 10 cm d'intervalle, sont donnés au tableau IV.

INTRUSIVE ICE

The indication that Pingo 12 was still hydrologically active at least 30 years after pingo collapse came from: summer observations of intrusive ice, formed the previous winter in the active layer (Fig. 31); large dilation cracks in the active layer above intrusive ice; and winter observations of icings from water overflowing onto snowbanks and pond ice. The water quality analyses in Table IV came from ice samples collected at 10 cm intervals from the intrusive ice of Figure 31. The analyses show the increase in dissolved solids, total hardness, and conductivity typically associated with the downward freezing of confined bulk water with solute rejection from the growing ice crystals.

ICE-BONDED PERMAFROST

Because Pingo 12 continued to be hydrologically active for decades after it had collapsed, a series of holes were drilled in a line across Pingo 12 starting near the lakeward side and ending near the former lake shore (Fig. 30, Profile A to B). All drill holes first penetrated ice-bonded permafrost (Fig. 32) and then, at variable depths, unbonded permafrost from where there was strong drill-hole flow carrying much entrained sand to the surface. In vertical profile, the lower surface of ice-bonded permafrost was concave down directly beneath the Pingo 12 remnant. The drill-hole flows were initially as much as 1 L/s, but the amounts soon diminished to a trickle, although some flows continued for several days. The water temperature was usually about - 0.1°C, and for some holes, slightly colder. Six temperature cables were installed in drill

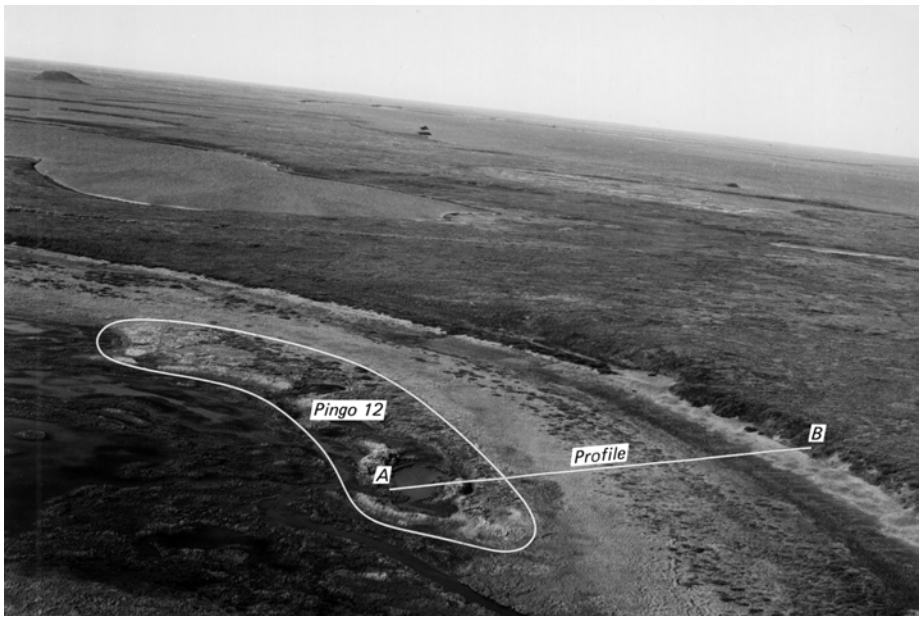

FIGURE 30. Aerial view of part of the drained lake of Figure 29b showing the outline of collapsed Pingo 12. The vertical profile from A to B, as determined from drilling, is given in Figure 32.

Vue aérienne d'une partie du lac asséché de la figure 29b montrant les pourtours du pingo n^{o} 12 affaissé. La coupe de A à B, déterminée à partir des forages, apparaît à la figure 32.

TABLE IV

Water quality analyses for intrusive ice (Samples 1 to 5) and for drill-hole flow (Samples 6 and 7) at Pingo 12. Samples 1 to 5 came from the intrusive ice, formed in the winter of 1985/86, as shown in Figure 31. Samples of drill-hole flow came from below ice-bonded permafrost from beneath the pond shown in Figure 32. Analyses by Chemex Labs Ltd., Vancouver, B.C.

Sample		PH	Total hardness mg/L $CaCO_3$	Conductivity λS/cm	Chloride dissolved mg/L	Silica mg/L SiO_2	Ca dissolved mg/L	Mg dissolved mg/L	Na dissolved mg/L	K dissolved mg/L
1.	Intrusive ice at depth of 5 cm	7.5	15	280	34	0.5	24	8	20	0.7
2.	Intrusive ice at depth of 15 cm	7.4	49	470	50	0.5	36	19	30	0.9
3.	Intrusive ice at depth of 25 cm	7.3	73	710	74	19	52	28	49	1.6
4.	Intrusive ice at depth of 35 cm	7.4	100	950	142	5	67	36	79	2.2
5.	Intrusive ice at depth of 45 cm	7.3	200	1500	284	1	82	50	167	4.1
6.	Drill-hole flow beneath 7.8 m of ice-bonded permafrost at a temperature of - 0.11°C, July 19, 1986	6.9	450	3000	480	2.5	270	100	250	10
7.	Drill-hole flow beneath 8.7 m of ice-bonded permafrost at a temperature of - 0.10°C, June 13, 1987	6.9	1170	2970	650	8.3	240	130	260	9.6

holes. The temperatures in the unbonded permafrost gradually decreased after 1988, when the last holes were drilled, to 1992, when the last temperature measurements were made. The temperature decreases varied with depth and location, but temperatures were as low as - 0.2°C for some holes. No intrusive ice in the active layer was observed in 1990, 1991, and 1992. Perhaps the loss of water from drill-hole flow in previous years had so depleted the relatively warm water in the unbonded permafrost beneath ice-bonded permafrost and reduced the hydrostatic pressure that it was insufficient to rupture the ice-bonded permafrost above it.

PERMAFROST TEMPERATURES

Temperature data from all the cables show that, at any given depth, such as 5 or 10 m, permafrost temperatures were warmer beneath the Pingo 12 remnants, including the pond shown in Figure 32, than in the deeper permafrost to either side. The pond was certainly a warming factor, because it reduced the temperature amplitude (A_z) and delayed the downward penetration (t_z) of the cold winter temperature wave beneath the pond. In order to assess the role of topography on ground temperatures, six minimum thermometers were installed at a depth of 0.5 m at sites that ranged from the top of a mound, to the depression between two mounds, to the lake flat on the landward side of Pingo 12. For three winters the minimums at 0.5 m ranged from - 8°C for the areas with a deep snow cover, *e.g.* 1 m, to - 17°C for windblown sites with a thin snow cover, *e.g.* 0.1 m. Therefore, three factors probably helped to account for the warmer temperatures beneath the Pingo 12 remnants: the warming effect of the pond, the greater depth of snow trapped by the irregular mound topography by the pond, and the frequent growth of intrusive ice and icings, because the release of the latent heat of fusion retarded the downward penetration of the winter cold wave wherever intrusive ice and/or icings occurred.

PINGO 13

Sometime prior to 1890 (minimum age from willows) a long narrow lake about 20 km east of Tuktoyaktuk, N.W.T. drained and Pingos 13, 14, 17 (Fig. 2), and several much smaller pingos, have grown up in the drained lake bottom. Pingos 13, 14, and 17 were already large in 1935 (air photo A5025-40C)

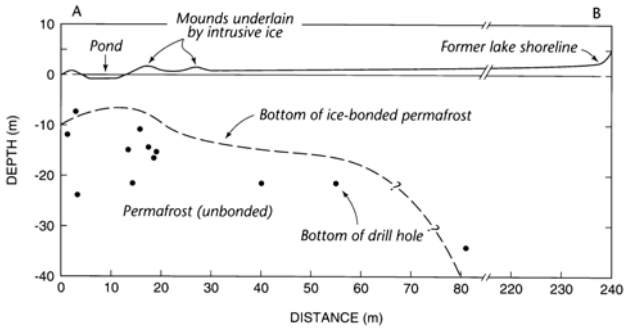

FIGURE 32. Vertical profile from A to B (Fig. 30) as determined by drilling. There was drill-hole flow from unbonded permafrost whenever the drill holes penetrated the bottom of ice-bonded permafrost. The temperature of the drill-hole flow ranged from about - 0.1 to - 0.2°C because of the freezing point depression that accompanied permafrost aggradation and solute rejection.

Coupe AB (fig. 30) déterminée à partir des forages. Il y a eu écoulement dans le trou de forage à partir du pergélisol non cimenté toutes les fois que les trous perçaient le pergélisol cimenté par la glace. La température de l'eau écoulée variait de -0,1 à -0,2 °C, en raison de l'abaissement du point de congélation qui accompagnait la progression du pergélisol et le rejet de solution.

when they looked much the same then as they do now, so growth probably started decades before 1890. In 1971 datum BM 37 was installed on the north side of the lake above the former lake shoreline and BM 55 at the top of Pingo 13 (Fig. 33). Pingo 13 has a steep sided 4 m deep summit crater. The height of BM 55, in 1971, was about 11.9 m above BM 41, another stable BM, on the adjoining flat. The pingo height increased to about 12.5 m above BM41 by 1982, then decreased to about 12.3 m by 1987, and then increased again, but only by a few centimetres, to 1991. The pattern of height change was similar to that of Pingos 14 and 17 (Fig. 34), partly because all three pingos shared the same groundwater system. The changes in tilt of BM 55, at the pingo top, were measured each time that the pingo was surveyed from 1985 to 1991. Although the height changes from 1985 to 1991 were only a few centimetres, the tilt changes were away from the crater when the pingo grew several centimetres and, conversely, the tilt was towards the crater when there was slight subsidence. Some of the increase in bench mark tilt away from the crater probably resulted from the growth of dilation crack ice. To illustrate, on 5 May 1978, a snow pit dug in the crater exposed a 5 cm wide dilation crack. The crack depth exceeded 5.1 m, the limit of measurement, and as the crater was 4 m deep, the bottom of the crack was at least 9 m below the pingo top or less than 3 m above the general level of the adjacent lake flat. However, since the angle subtended by the dilation crack was about 0.30° whereas the maximum range in BM 55 tilt from 1985 to 1991 was only 0.13°, the wedging effect of the growth of dilation crack ice, if the pingo deformed as a semi-rigid body, would have been much greater than the measured change in tilt.

PINGO 14 (GEYSER PINGO)

Pingo 14 is a large, broad-based, flat-topped pingo that has grown up in the bottom of the same drained lake as Pingos 13 and 17. The north to south cross section of the drained lake bottom with Pingo 14 in the centre (Fig. 35) has been compiled from: 1970 drilling by Imperial Oil Canada Ltd.; 1973 drilling by the Geological Survey of Canada (under the supervision of Dr. V.N. Rampton); drilling in 1976 and 1977 and a resistivity survey by the writer (Mackay, 1975a). All of the drill holes, except for the hole which was closest to the former lake shore where permafrost was deepest, yielded strong drill-hole flow with much entrained sand. In addition, at least four other drill holes several kilometres off the line of section in Figure 35 also yielded strong drill-hole flow. The lake bottom stratigraphy, from the drill holes, comprised 5 to 10 m of icy clay with medium grained sand and gravel beneath. The first bench marks were installed in 1971 with additional bench marks in 1973.

SUB-PINGO WATER LENS

Pingo 14 is underlain by a large sub-pingo water lens (Fig. 35) as determined by drilling in 1973, 1976, and 1977. In each of the three years the drill rods dropped, when the water lens was penetrated, and there followed an upward flow of water at a temperature from - 0.05 to - 0.10°C. In 1977 the drill-hole flow jetted to a maximum height of 2.6 m above ground level (Fig. 5), and, as a result of water loss, the pingo subsided at least as far away as BM 50 which was 200 m from the drill hole site (Fig. 36). In 1977, the depth of the water lens at the drill hole site, on the pingo slope, was 1.2 m. Because the available evidence suggests that the greatest depth of a water lens is beneath the pingo top, the maximum depth of the water lens at BM 50 in 1977 probably exceeded 2 m.

SUB-PINGO WATER PRESSURE

In 1977, two sturdy oceanographic water pressure transducers, similar to those in the sub-pingo water lens of Pingo 9, were installed at a depth of 22 m below the ground surface at the bottoms of two adjacent drill holes. Because the two pressures were similar, although there was some variation between them, the results have been averaged and plotted for the 1977 to 1991 period in Figure 37. The transducers were about 15 m below the general level of the adjacent flats and about 25 m or more below the pingo summit at BM 50. In the 1977 to 1991 period the water pressure in the sub-pingo water lens always exceeded that of a 30 m column of water. Therefore, the hydraulic head was at least 15 m above the surrounding lake

FIGURE 33. Pingo 13, which is about 13 m high, with BM 55 at the top.

Le pingo n^{o} 13 haut d'environ 13 m et le repère 55 au sommet.

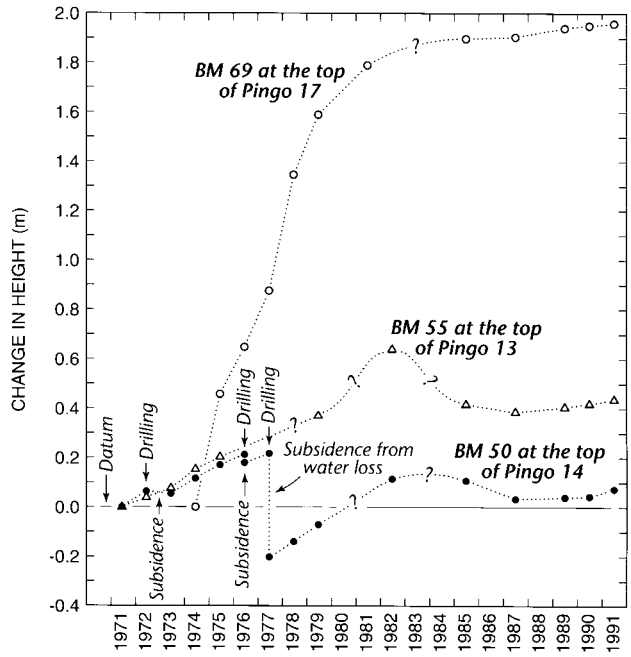

FIGURE 34. The change in height for BM 55 at the top of Pingo 13, BM 50 at the top of Pingo 14, and BM 69 at the top of Pingo 17 for the survey periods as shown. The three pingos are close to each other and they share the same groundwater system.

Les différentes altitudes du repère 55 au sommet du pingo n^o 13, du repère 50 au sommet du pingo n^o 14 et du repère 69 au sommet du pingo n^o 17 pour les périodes données. Les trois pingos sont près les uns des autres et partagent le même réseau d'eau souterraine.

flats. Clearly, the water pressure beneath Pingo 14 was great enough to uplift and deform more than 25 m of superincumbent material (i.e. the frozen pingo overburden and subjacent ice core) so the hydraulic head was well above the top of the pingo.

PINGO GROWTH

The growth of the top of Pingo 14 is shown in Figure 34 for the 1971 to 1991 period. From 1971 to 1977, despite the loss of many hundred cubic metres of water from drill-hole flow in 1973 and 1976 the growth at the top was about 3 cm/a. As a result of the 1976 drilling there was an initial rapid subsidence at BM 50 of 5 cm, then a partial recovery, so that the height in 1977 was similar to that in 1976 (Fig. 34). In 1977, however, there was first a rapid 60 cm subsidence at the top and then a slow recovery of about 20 cm to give a net subsidence of about 40 cm from the 1977 drilling (Figs. 34 and 38). Afterwards, the pingo reached its maximum height between 1982 and 1985. From 1985 to 1991 the bench marks near the pingo periphery (BM 44, 45, and 46) continued to increase in height whereas the bench marks on the pingo slope from BM 47 to BM 50 at the top first decreased in height from 1985 to 1987, and then increased slightly to 1991 (Fig. 39). The pattern of pingo subsidence shown in Figure 39 was identical in shape, though not in degree, to that in Figure 38 where the decrease was the result of drill-hole flow from the sub-pingo water lens. Because there had been no drilling after 1977 the subsidence pattern from 1985 to 1991 for Pingo 14 is indicative of water loss from the sub-pingo water lens but the source of the water loss has not been identified. No evidence could be found of spring flow or the growth of frost mounds as at Pingo 4. However, temperature measurements by the writer and geophysical surveys (Scott, 1975; Scott and Hunter, 1977) suggest that an unfrozen basin may underlie the deepest part of IOL Lake to the west of Pingos 13 and 14 (Fig. 40). It is then possible, although unlikely, that spring flow might have escaped upward into IOL Lake without being detected. In any event, by 1991, the height of the top of Pingo 14 had reverted back to where it was in 1973, just two years after the start of the surveys (Fig. 34). Further support for water loss comes from surveys of numerous bench marks on the drained lake bottom. Surveys before and after the 1976 drilling, showed that the lake bottom had subsided as far as BM 39, which was 300 m from the pingo periphery (Fig. 40). In addition, surveys for the 1982 to 1991 period of BM 52, 53, and 54 on the lake bottom just northeast of the periphery of Pingo 13 showed that the changes in height, although only several centimetres, tended to parallel the trend of BM 55 on the top of Pingo 13. Thus, Pingos 13, 14, and 17 and the surrounding lake flats

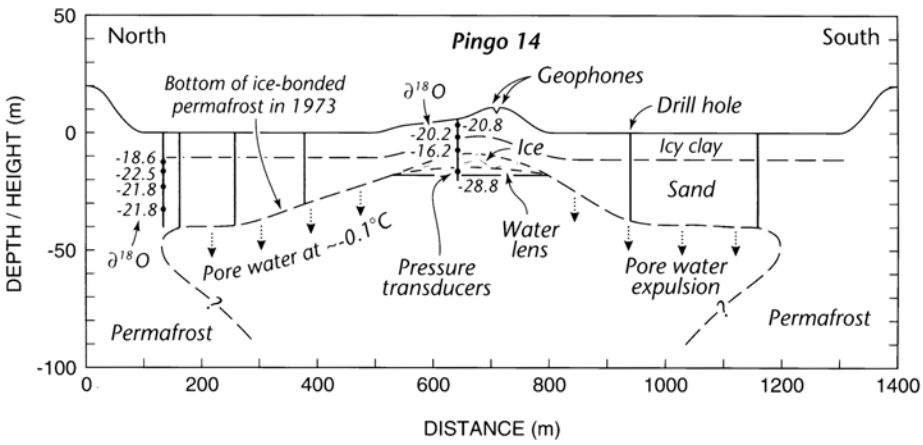

FIGURE 35. Profile through Pingo 14 from the north to south shore of the drained lake. All drill holes, except for the most northerly drill hole, which did not penetrate to the bottom of ice-bonded permafrost, yielded drill-hole flow at a below 0°C temperature because of a pore water freezing point depression. Pingo 14 was underlain by a sub-pingo water lens. Note the $\delta^{18}O$ data.

Coupe du pingo n^o 14 de la rive nord à la rive sud du lac asséché. Tous les trous de forage, sauf le plus nordique qui n'a pas rejoint la base du pergélisol cimenté par la glace, ont eu un écoulement malgré une température située sous 0 °C, en raison d'un abaissement du point de congélation de l'eau interstitielle. Le pingo n^o 14 comprend une lentille d'eau sous-jacente. Noter les données $\delta^{18}O$.

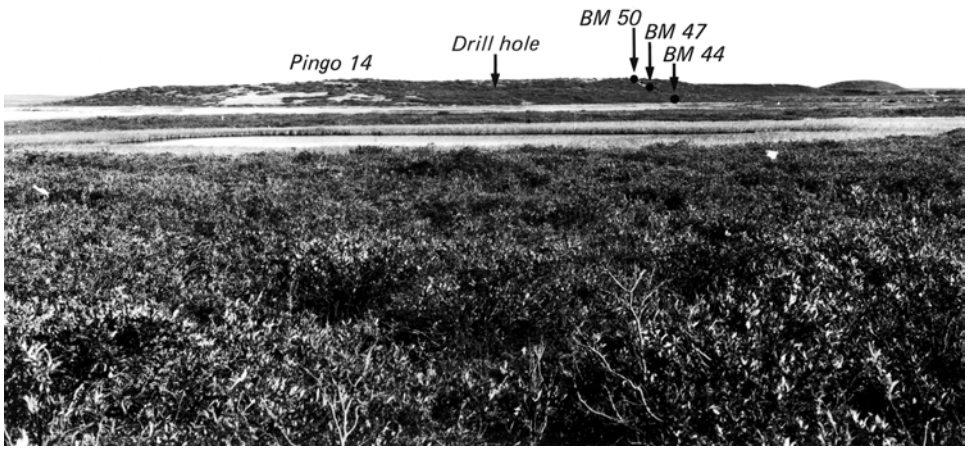

FIGURE 36. Pingo 14 is a broad flat-topped pingo. BM 44 is near the pingo periphery; BM 47 is on mid-slope; and BM 50 is at the top (see Fig. 40). The drill-hole flow for Figure 5 was at the "Drill Hole" on the photograph.

Le pingo n^{o} 14 est un pingo de grande largeur à sommet plat. Le repère 44 est situé près de la périphérie du pingo ; le repère 47 est à mi-pente ; le repère 50 est au sommet (voir la fig. 40). L'écoulement en jet au trou de forage de la figure 5 s'est fait à l'emplacement appelé « Drill hole » sur la photographie.

share the same groundwater system and respond to the gain and loss of groundwater below ice-bonded permafrost.

DILATION CRACKS

The dilation crack pattern of Pingo 14 is unique, because it has not been observed elsewhere. Although four cracks radiate from the summit, which is not unusual, two of the cracks then bifurcate before reaching the pingo periphery and one crack system continues to bifurcate beyond the pingo periphery onto the lake flats (Fig. 40).

TENSION CRACKS

1. Description

The pre-drainage lake in which Pingos 13, 14, and 17 have grown trended east-west with a length of about 7 km and a width of 1 to 2 km. At present, there is a shallow residual lake 3 km long and several hundred metres wide to the east of the three pingos and IOL Lake to the west of the three pingos. The drained lake bottom is crossed by numerous canal-like features here referred to as tension cracks. Some of the cracks can be traced from one side of a pond or lake to the other, as shown by crack alignment and a continuation of the cracks where there are islands (*e.g.* IOL Lake, Fig. 40). Whether the cracks have propagated upward under water, as with some ice-wedge cracks (Mackay, 1984), or whether a rise of pond level has submerged a pre-existing crack system is unknown. Wherever the lake bottom is poorly drained, tension cracks are usually present, as in the area west of IOL Lake (air photos A23422-129 to 133). Many of the tension cracks that are the continuation of pingo dilation cracks bifurcate with angles in the 30 to 45° range. The tension cracks range in width from the barely perceptible to 4 m wide troughs. Many cracks resemble water filled ditches that are bordered by sedges in the wetter areas and sedges with willows in the drier areas. A few tension crack ditches resemble ice-wedge troughs except for the absence of raised rims (Figs. 41, 42). No other cracks comparable in variety, type, and extent to those discussed above have been seen by the writer nor is he aware of any others elsewhere.

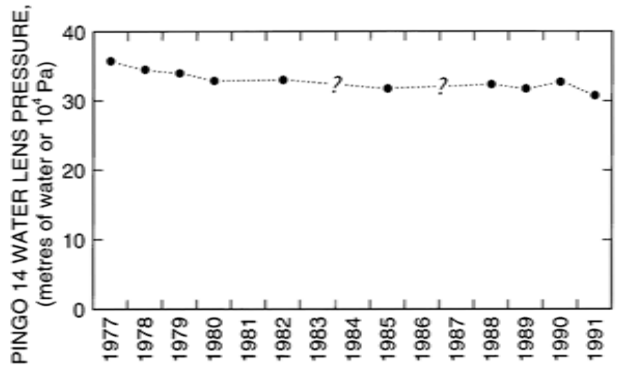

FIGURE 37. The water pressure in the sub-pingo water lens of Pingo 14, as given by the average of two transducers installed in the water lens at the site of the drill hole in Figures 35 and 36, is plotted for the 1977 to 1991 period. The hydraulic head or potentiometric surface was above the top of the pingo (Fig. 5).

La pression de l'eau dans la lentille d'eau sous-jacente au pingo n^{o} 14, mesurée par les deux transducteurs installés dans la lentille à l'emplacement du trou de forage des figures 35 et 36, est donnée pour la période 1977-1991. La surface piézométrique était située au-dessus du sommet du pingo (fig. 5).

2. Breaking cables

In the summer of 1974 fine insulated copper wires, referred to as "breaking cables", were buried near the bottom of the late summer active layer across many tension cracks on the lake flats and also across some dilation cracks on Pingos 14 and 17 in order to monitor the extent of cracking. The "breaking cables" had been used previously to monitor ice-wedge cracking at Garry Island, N.W.T. (Mackay, 1974a). The cables were checked for breakage either electrically, which was done in summer and winter, or manually, which was done only in summer. In total, 70 breaking cables were buried across tension and dilation cracks, the locations of 60 being shown in Figure 40, the other 10 being off the map. In Figure 40 the number "0" identifies those cables that remained unbroken in the first two years of 1974/76; "1" identifies those cables that broke in the first winter of 1974/75; and "2" identifies those cables that broke in the second

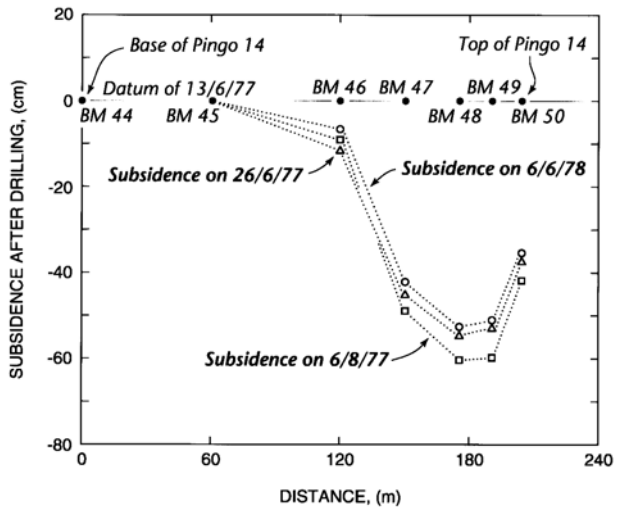

FIGURE 38. Subsidences of BM 46 to 50, from drill-hole flow from the sub-pingo water lens, from June 1977 to June 1978 for selected survey dates.

L'affaissement des repères 46 à 50, en raison de l'écoulement au trou de forage à partir de la lentille d'eau sous-jacente, a été mesuré à certaines dates de juin 1977 à juin 1978.

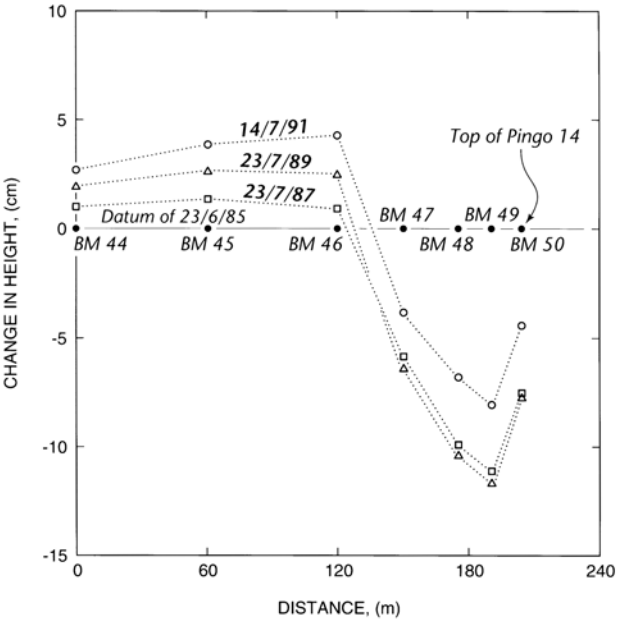

FIGURE 39. Changes in heights of BM 44 to BM 50 for selected dates from 23 June 1985 to 14 July 1991. The changes in heights have a pattern similar to the subsidence pattern of Figure 38, even though there had been no drilling after 1977. The implication is that there had been water loss from the sub-pingo water lens of Pingo 14, perhaps by pingo rupture, after 1985.

Différences d'altitude des repères 44 à 50 à certaines dates du 23 juin 1985 au 14 juillet 1991. Ces différences correspondent au type d'affaissement constaté à la figure 38, bien qu'il n'y ait pas eu de forage après 1977. Une perte d'eau se serait produite à partir de la lentille d'eau sous-jacente au pingo n^{o} 14, probablement en raison d'une rupture survenue après 1985.

winter of 1975/76. In summary, 30 of the 70 cables broke in the first winter of 1974/75. The 30 broken cables were not replaced. In the second winter (1975/76) 19 out of the 40 remaining cables broke. By the end of the fifth winter (1978/79) only 9 cables out of the original 70 remained unbroken.

Two winter trips were made in order to examine the tension cracks. On a visit in March 1974, a fresh crack along the middle of one tension crack was probed to a depth of 4 m. In late April and early May 1978, while the ground was still covered with 30 to 50 cm of snow, 17 breaking cable cross sections on the lake flats and all of the cross sections at the summits of Pingos 13, 14, and 17 were checked for winter cracking. A trench was dug through the snow to frozen ground or ice at each of the 17 breaking cable sites on the lake flats, the widths of cracks measured, and the crack depths probed. Cracking had occurred at 7 out of the 17 sites and of the 7, only one had not cracked in the first two winters after installation. The conclusion is that cracking tends to occur more frequently at some sites than others. Some of the cracks were 5 to 10 cm in width (Fig. 41). Although the cracks appeared to be identical to those seen hundreds of times previously in ice-wedge troughs (Mackay, 1974a, 1992b), none of the cracks could be probed to a depth below that of the late summer active layer (Fig. 42) so there was no way to determine the depth of crack penetration, if any, into permafrost. However, at the time of probing in late April and early May, the spring temperature warming wave [6] would already have caused the upper part of permafrost to expand and thus to close the smaller cracks, as with many ice-wedge cracks.

3. Increase in tension crack width

In order to try to measure the lateral growth of tension cracks, as had been done previously with ice wedges at Garry Island, BM 51 and BM 52 were installed in 1973 on either side of the long tension crack that skirted the north periphery of Pingo 14 and terminated on the east side of Pingo 13 (Fig. 40). The tension crack trough was about 1.5 m below ground level and the bottom width about 1 m. The bottoms of BM 51 and BM 52, of length 2.75 m, were at a depth of 2.35 m below ground level. The bottom ends of the two bench marks were then about 0.85 cm below the bottom of the tension crack trough and therefore below the bottom of the active layer in the trough. In the 1973 to 1991 period the separation was measured 8 times. To summarize, on 12 July 1973 the separation was 8.583 m; on 10 July 1982, the separation was 8.595 m; and on 14 July 1991 the separation was 8.642 m. Therefore, in the first 9 years the increase in separation was only 1.2 cm whereas in the second nine years it was 4.7 cm, for an 18 year increase of about 6 cm. Although the separation increase might have resulted from a tilting away from the tension crack trough of one or both of the bench marks unconnected with the growth of tension crack ice, the fact that the bottoms of the two bench marks were well below that of the active layer of the ditch-like tension crack trough suggests the increase in separation may have resulted from growth of tension crack ice from the infilling of winter cracks, as with ice-wedge growth.

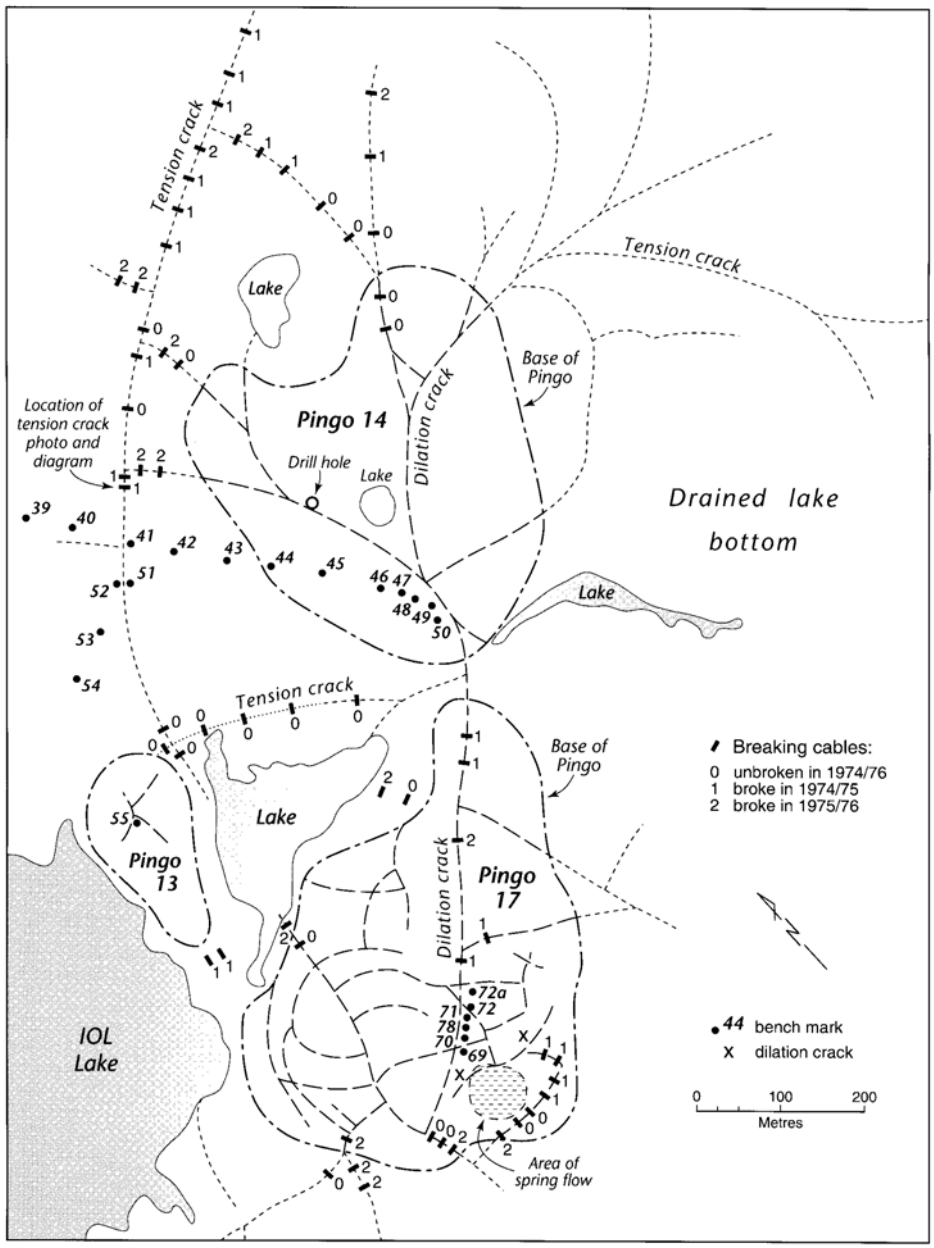

FIGURE 40. Map of Pingos 13, 14, and 17 showing the dilation cracks, the extension of the dilation cracks onto the lake flats as tension cracks, bench mark locations, and the sites of the majority of breaking cables. "Dilation crack x" is north of the "Area of spring flow" on the southerly side of Pingo 17. See text.

Carte des pingos 13,14 et 17 montrant les fissures de dilatation, la prolongation des fissures jusque dans le fond du lac, en tant que fissures de tension, la localisation des repères et les emplacements de la plupart des câbles de rupture. La fissure de dilatation x est située au nord de l'emplacement dit « Area of spring flow » situé dans la partie sud du pingo n^{o} 17.

4. Tension crack propagation

The tension crack pattern shown in Figure 40 is puzzling and its origin uncertain. First, there are two unusually long 900 m tension cracks that can be seen on a 1935 air photo (A5025-40C). The first 900 m long tension crack passes within 10 m of the east side of Pingo 13 (Fig. 40), between BM 51 and BM 52, within 75 m of the periphery of Pingo 14, and then continues for 250 m off the map edge. The fact that the tension crack does not deviate as it passes close to Pingo 13 and then skirts Pingo 14 suggests that the crack predated the growth of both pingos. The second 900 m long crack follows along the summit dilation crack of Pingo 17, then continues to follow the summit dilation crack of Pingo 14 (the Pingo 17 and Pingo 14 cracks are labelled "Dilation crack" in Fig. 40) and then continues beyond the pingo periphery onto the drained lake flat. The observation that the second 900 m long crack follows the summit dilation crack of Pingo 17 and Pingo 14 suggests that the second 900 m long crack was associated with the growth of Pingos 17 and 14. Furthermore, when branching occurs as a tension crack propagates, the branching direction indicates the crack propagation direction (Bahat, 1991). Therefore, the dilation/tension cracks of Pingo 14 propagated outwards from the pingo top to the pingo periphery and then beyond onto the drained lake flat. Because three of the Pingo 14 branching cracks terminate, with orthogonal intersections, at the first 900 m long crack, on the north side of Pingo 14, the branching cracks are younger than the 900 m long tension crack, as Lachenbruch (1962) has shown for similar orthogonal ice-

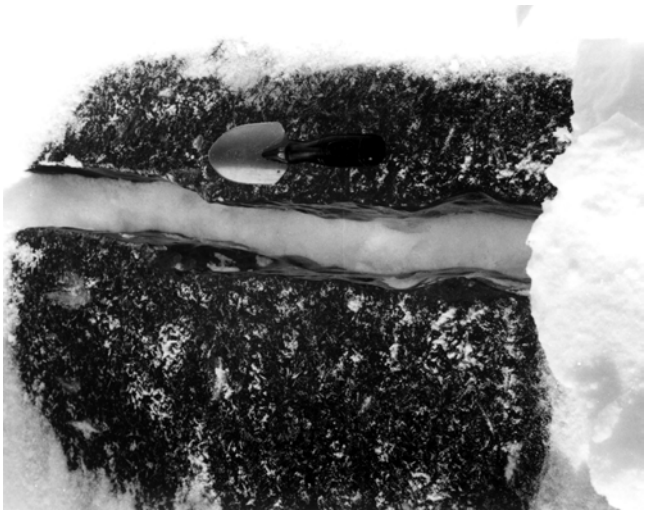

FIGURE 41. Tension crack on the drained lake flat with a 22 cm long trowel for scale.

Fissure de tension sur le fond du lac asséché (la truelle mesure 22 cm de long).

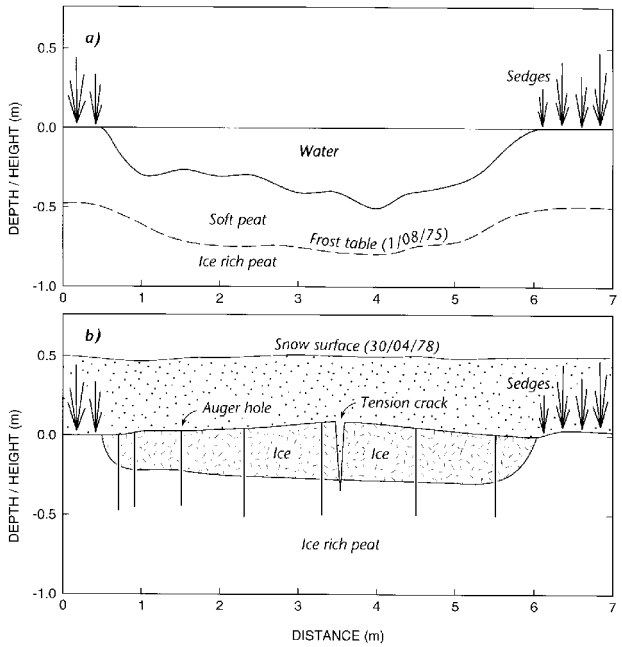

FIGURE 42. a) Summer cross section of the tension crack of Figure 41. b) Late winter cross section of the tension crack of Figure 41.

a) Fissure de tension de la figure 41 en été, vue en coupe ; b) fissure de tension de la figure 41 à la fin de l'hiver, vue en coupe.

wedge intersections. The preceding observations suggest that the first 900 m long tension crack predated the growth of Pingos 13, 14, and 17 whereas the second 900 m long crack probably formed contemporaneously with the growth of Pingos 13, 14, and 17. Two possibilities for the 900 m long crack origins are suggested. First, as permafrost aggraded on the exposed lake bottom, the temperature at any given depth, such as 5 metres, would decrease with time, for example within 10 years, as monitored in an artificially drained lake (Mackay, 1997). Thus thermal contraction of the upper part of permafrost over large areas of the drained lake bottom, if not relieved by creep, might have contributed to tensional failure. Second, the uplift pressure exerted from pore water expulsion beneath a growing pingo might have added to the tensional stresses possibly created from thermal contraction of thin permafrost beneath Pingos 17 and 14 to contribute to the stresses derived from the cooling of the upper part of permafrost.

BENCH MARK TILTS

The bench mark tilts from BM 44 on the pingo periphery to BM 50 on the pingo top were measured in 1985, 1987, 1989, and 1991. In the 1985 to 1991 period both the changes in height and tilt for BM 44 and BM 45 on the lower pingo slope were too small to be significant. What is unusual is that as the bench mark heights increased from BM 46 to BM 50 (Fig. 39), even though all increases were less than 5 cm, the tilt changes were upslope rather than downslope (Fig. 43) as would be expected from measurements at other pingos. There was little change for BM 50 at the top of the pingo. The lack of consistency in the tilt data probably reflects the up-and-down movement of the pingo from water gain, water loss, and ice growth for the same period (Fig. 39).

PINGO 15 (PULSATING PINGO)

Pingos 15 and 16 have grown up in the bottom of a lake that drained catastrophically by the erosion of ice wedges along its outlet creek. The drained lake is almost circular, about 650 m in diameter, and the two pingos have grown up in residual ponds that were located slightly off centre. Lake drainage probably occurred before 1915, as estimated from the ages of willows. By 1935 Pingo 15 was large enough to show up prominently in an air photo (A5024-27L). In 1969 four bench marks (BM 25 to 28) were installed on the pingo and in 1972 eight more bench marks (BM 91 to 98) were added for a total of twelve. Datum BM 91 was located inland from the former lake shore; BM 92 and 93 on the drained lake flat; and BM 94 to 98 from the pingo periphery to the top (Fig. 44a,b). The 3 m thick overburden of Pingo 15, as exposed by ditching downslope on a summit dilation crack, comprised, from the surface downward: sand, blackish lake silts, sand to a depth of about 3 m, and then clear intrusive ice below 3 m.

PINGO GROWTH

The initial growth pattern of Pingo 15 was most puzzling. During the first four years of survey (1969 to 1973) BM 28 at the top (Fig. 45) and BM 27 and BM 26 on the slope oscillated up-and-down, a movement which could not be attributed to survey errors, because all surveys had been closed at least twice (Mackay, 1979). The explanation became clear when, in July 1974, a frost mound, Mound A (Fig. 46) was discovered to have grown up in the previous winter by rupture at the pingo periphery and the intrusion of water into the upper part of permafrost (Mackay, 1977a). In view of the irregular growth pattern of Pingo 15, subsequent surveys

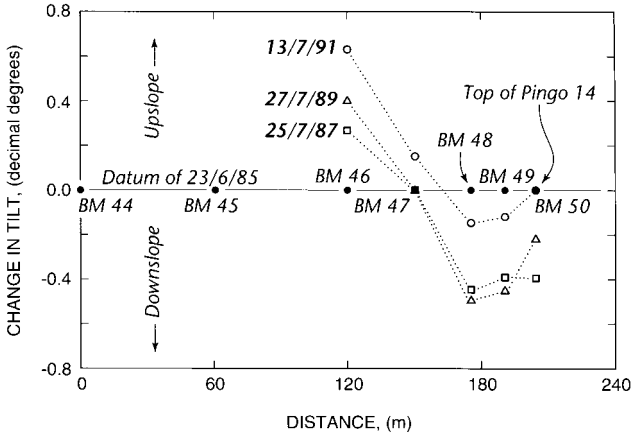

FIGURE 43. Changes in bench mark tilts of BM 46 to BM 50 on Pingo 14 for selected dates for the 1985 to 1991 period.

Différences d'inclinaison des repères 46 à 50 sur le pingo n^{o} 14 à certaines dates choisies au cours de la période 1985-1991.

were spaced at longer intervals. In 1983 a second frost mound, Mound B (Fig. 46) was found to have grown up adjacent to Mound A. Mounds A and B were located on either side of the main summit dilation crack (Fig. 47) thus indicating a failure zone from a local stress concentration in the area of greatest curvature in the pingo periphery (Fig. 44). The oscillations of Pingo 15 resulted from hydrofracturing (Rummel, 1987) at the periphery of the sub-pingo water lens with the upward and outward propagation of tension cracks as associated with the growth of some laccoliths (Pollard and Johnson, 1973, p. 330-337).

1. Sub-pingo water lens

In order to study the peripheral rupture of Pingo 15, on 25 June 1976 the heights of all bench marks were surveyed. On the next day a hole was drilled on the pingo periphery about 20 m to the east of BM 94 (Fig. 44). When ice-bonded permafrost was penetrated at a depth of 23 m there was a strong drill-hole flow, with much entrained sand, to the surface. The flow lasted for three days during which period the water temperature remained nearly constant at about -0.2°C whereas the salinity decreased daily (Mackay, 1977a, 1977b). As a result of the water loss not only did the top of the pingo subside (Fig. 45), but the lake bottom also subsided for a distance of more than 100 m from the pingo (Mackay, 1975b, 1977b). When Pingo 15 was last surveyed in 1992, BM 28 at the top was only 0.64 m higher than in 1969, but despite the 23 year survey record, neither the intrusive ice growth rates nor the fluctuating depths of the sub-pingo water lens are known for reasons previously discussed for Pingo 9.

2. Mound A

Mound A, when first seen in 1974, was about 2.3 m high. The active layer, which had been domed by uplift, was crossed by numerous dilation cracks with widths to 0.5 m and depths to 1 m. Drilling showed that water had been intruded in the preceding winter at depths of 1 to 2 m below

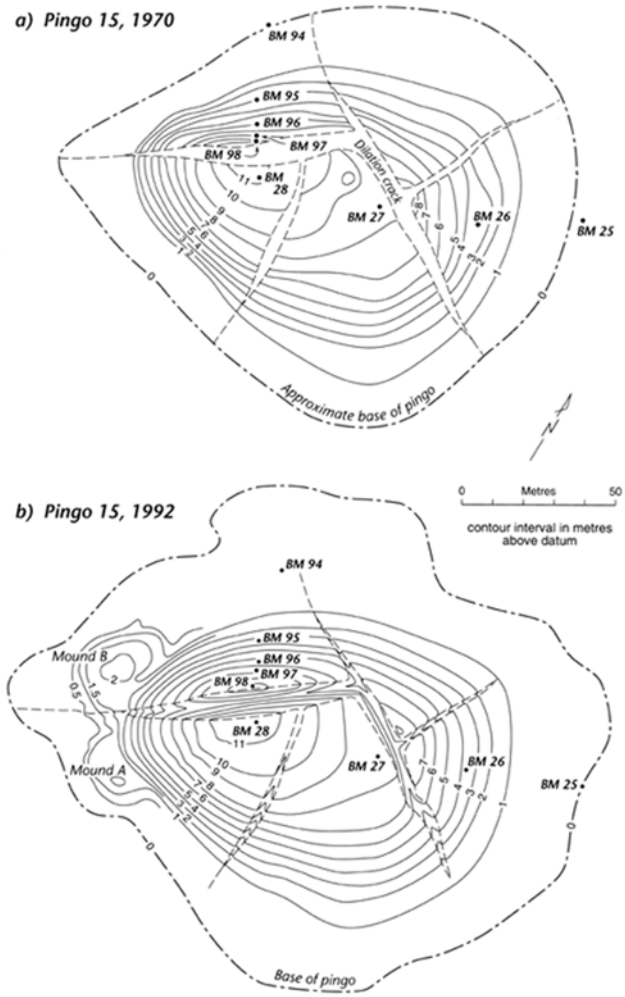

FIGURE 44. a) Contour map of Pingo 15 for 1970. b) Contour map of Pingo 15 for 1992. The approximate base of Pingo 15 in the 1970 and 1992 maps are not identical, because the bases were mapped using the dual criteria of changes in topography and vegetation, the same as was done for Pingo 9 (Fig. 23).

a) Topographie du pingo n^{o} 15 en 1970 ; b) topographie du pingo n^{o} 15 en 1992. Les bases approximatives du pingo sur les deux cartes diffèrent en raison du double critère des changements dans la topographie et dans la végétation, choisi pour effectuer la cartographie de la base, tout comme ce fut le cas pour le pingo n^{o} 9 (fig. 23).

the bottom of the late summer active layer. Therefore, the intrusion of water into permafrost indicates hydrofracturing of permafrost. The thickness of the intrusive ice varied from 1 to 2 m, and the growth of ice was rapid, judging from the small ice crystals (Gell, 1978). Although most of the intruded water had frozen through by the summer of 1974, drilling showed that there were still a few centimetres of very saline water under artesian pressure beneath parts of Mound A and there was still a slight spring flow at the lakeward side of the mound. Since old iron-stained vegetation had been observed in previous years near the site of the spring, the field evidence suggests that there had been intermittent spring flow in previous years. As an estimate, the volume of

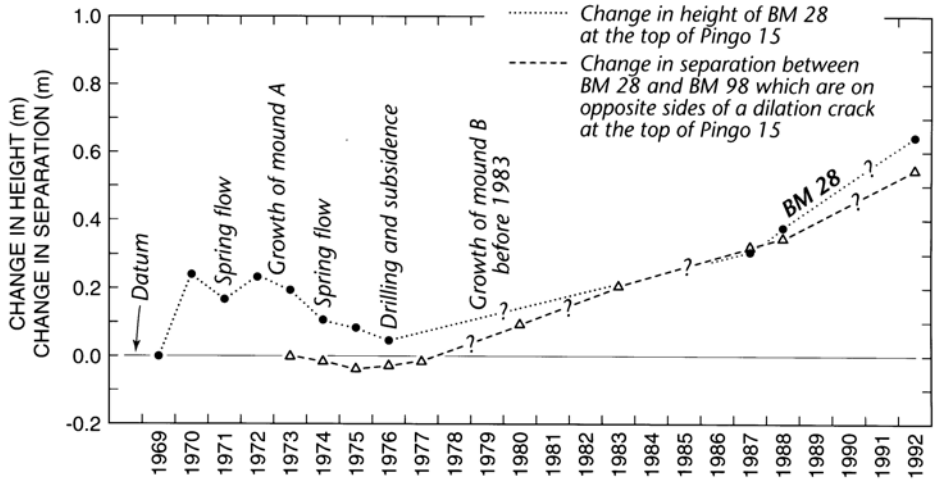

FIGURE 45. Change in height of BM 28 on the top of Pingo 15 for the survey period of 1969 to 1992 and the change in separation between BM 28 and BM 98, on opposite sides of the summit dilation crack for 1973 to 1992. Because the change in bench mark separation paralleled the change in pingo height, measurements of the separation of bench marks across a summit dilation crack can give an indication of pingo growth.

Différences d'altitude du repère 28 au sommet du pingo n^o 15 au cours de la période 1969-1992 et différences d'écart entre les repères 28 et 98, de chaque côté de la fissure de dilatation du sommet de 1973 à 1992. Puisque la différence d'écart entre les repères est parallèle au changement d'altitude du pingo, les mesures de l'écart entre les repères à travers une fissure de dilatation sommitale peuvent donner des indications sur la croissance d'un pingo.

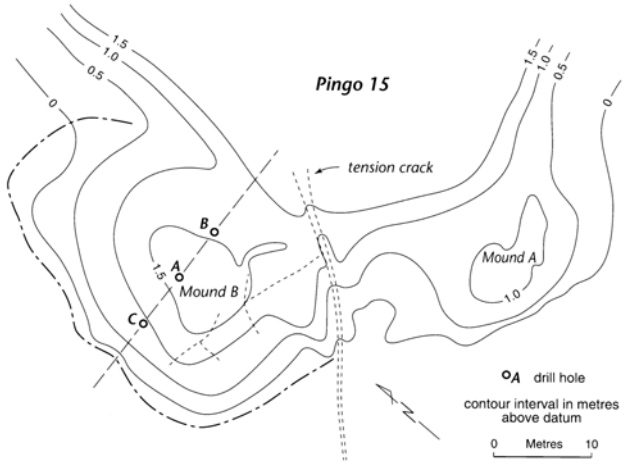

FIGURE 46. Frost Mounds A and B formed by hydrofracturing and peripheral rupture of Pingo 15 with the intrusion of water into permafrost. The contour map was prepared in June 1988.

Les buttes cryogènes A et B ont été formées par fracturation hydraulique et rupture périphérique du pingo n^o 15 avec l'arrivée d'eau dans le pergélisol. La topographie a été établie en juin 1988.

water injected into Mound A, including that lost by spring flow which was measured for a brief period, exceeded 500 m^3 or about 1% of the total volume of Pingo 15 as measured above the periphery. Mound A subsided substantially in 1975. Surveys from 1976 to 1992 have shown no significant changes in Mound A nor were any changes noted on a brief site visit in 1996. Therefore, Mound A has become a perennial appendage to Pingo 15, a satellite or baby pingo.

3. Mound B

Mound B, which grew between July 1980 and July 1983, is larger but otherwise similar to Mound A (Fig. 46). Mound B, in 1983, was about 33 m in length, 20 to 25 m in width, and the highest point was more than 2 m above the adjoining lake flat. The volume of Mound B was several times that of Mound A and were it not for the loss of water that accompanied the growth of Mound B, the growth of Pingo 15 from 1980 to 1983 would have been much greater than it actually was (Fig. 45). Surveys showed that Mound B remained unchanged from 1983 to 1992 and no changes could be seen on a brief site visit in 1996. Therefore Mound B, like Mound A, has become a frozen appendage of Pingo 15.

On 30 June 1988 Holes A, B, and C were drilled in Mound B to a depth sufficient to penetrate through any intrusive ice and water down to mineral soil beneath (Figs. 46, 48). Water samples were collected for analyses, the sample locations being shown in Figure 48 and the analyses being given in Table V. Sample 1 of intrusive ice and Sample 2 of water were collected from Hole A. No water was encountered beneath the ice of Hole B. In Hole C Samples 3 and 4 of intrusive ice were collected as drilling was in progress. Sample 5 of water, with a little contained ice, was collected as soon as possible after the drill penetrated the water lens. After the drill rods were withdrawn water rose up the 7.5 cm diameter drill hole and then overflowed slowly onto the ground surface for more than an hour. Sample 6, of overflow water, was collected shortly after overflow reached the surface. The temperature of the overflow water was - 2.35°C. Samples 2, 5, and 6 of water were much more saline than Samples 1, 3, and 4 of ice because of solute rejection in the freezing process. Furthermore, the water temperature of Sample 2, collected at a depth of about 4 m below the ground surface, was - 2.65°C on 30 June 1988, a temperature a degree lower than the freezing temperature of most sea water. On 30 June 1988, when water Sample 2 was collected, the maximum temperature rise from the downward penetrating summer warming wave had not yet reached the 4 m depth of Sample 2, as estimated from [6] and temperature lags elsewhere. The thermal diffusivities (α) of the frozen sand and ice are unknown, but if diffusivities of $\alpha = 1 \times 10^{-6}$ m^2/s and $\alpha = 2 \times 10^{-6}$ m^2/s are used (*e.g.* Williams and Smith, 1989), the time lag (t_z) at a 4 m depth would be in the range of 10 to 7 weeks. Because Sample 2 was collected on 30 June before the near surface ground temperature had

FIGURE 47. Photograph of Pingo 15 showing Frost Mound A on the right, Frost Mound B on the left, with a person standing on the top of each mound for scale. July 1988.

Photographie du pingo n^{o} 15 qui montre la butte cryogène A à droite et la butte B à gauche. Les personnes sur les trois sommets donnent l'échelle (juillet 1988).

reached its maximum, which is usually in late July, the temperature at the site of Sample 2 would have increased until sometime in September or October. At Pingo 15, the amplitude (A) for the mean annual near surface ground temperature is unknown, but a conservative value of 15°C will be used in equation [6], as estimated from Garry Island data (Mackay, 1974b, 1993a; Mackay and MacKay, 1974) to give an amplitude from about 4 to 6°C at the 4 m depth of Sample 2. Consequently, as the warm summer temperature wave progressed downward from July to September, the temperature at the site of Sample 2 would have risen above - 2.65°C with the result that some of the ice above Sample 2 would have melted and the salinity of the Sample 2 water would have decreased slightly. Conversely, in the winter and spring, the temperature in the ice above Sample 2 would have decreased, minimum temperatures might drop below - 10°C, some water would freeze, and the salinity of the water at the site of Sample 2 would increase. Thus, the ice thickness, water salinity, and water temperature of Mound B would oscillate during the year being dependent upon the downward propagation of the seasonal temperature waves.

The three ice and three water samples from Mound B have been analyzed for $\delta^{18}O$ and δD (analyses by the University of Waterloo) and the results plotted in Figure 49. The three ice and three water samples group into separate clusters, the water samples being much more negative than the ice samples. The co-isotope slope is about 5.2. There have been numerous attempts to correlate and explain the co-isotope slopes of ice and water frozen under a variety of conditions (*e.g.* Gordon *et al.*, 1988; Jouzel and Souchez, 1982; Souchez and Jouzel, 1984; Souchez and De Groote, 1985; Mackay and Dallimore, 1992; Burn and Maxwell, 1993) but the slopes have usually been difficult to interpret. The water and ice in Mound B were subjected to several stages of fractionation: fractionation associated with permafrost growth and pore water expulsion at the bottom of downward aggrading permafrost; fractionation in the growth of intrusive ice by downward freezing in the Pingo 15 sub-pingo water lens; and freezing of water in Mound B from the sub-pingo lens water of Pingo 15. Furthermore, the stable isotope ratios for Mound B would, as discussed above, vary seasonally, depending upon the time of year when the samples were collected.

BENCH MARK SEPARATIONS

The separations between pairs of bench marks on the north slope of Pingo 15 were measured in 1974, 1988, and 1992. In proceeding upslope from BM 95, the distances between successive pairs of bench marks all decreased to

TABLE V

Water quality analyses for Pingo 15, Mound B for June 30 and July 1, 1988. The sample locations are given in Figure 48. Analyses by Chemex Labs Ltd., Vancouver, B.C.

Sample	pH	Total hardness mg/L $CaCO_3$	Conductivity λS/cm	Chloride dissolved mg/L	Silica mg/L SiO_2	Ca dissolved mg/L	Mg dissolved mg/L	Na dissolved mg/L	K dissolved mg/L
1. Ice	7.6	190	760	270	1.0	23	15	60	0.16
2. Water at - 2.65°C	7.1	1,600	66,900	29,200	48.0	340	3,440	1,380	1.40
3. Ice	8.0	300	1,410	355	2.6	43	37	150	0.20
4. Ice	7.7	270	1,410	385	1.6	40	38	150	0.16
5. Water	7.2	1,400	60,600	29,200	64.0	118	2,190	10,000	0.88
6. Overflow water at - 2.35°C	7.2	1,400	60,000	21,400	96.0	83	2,690	11,200	1.04

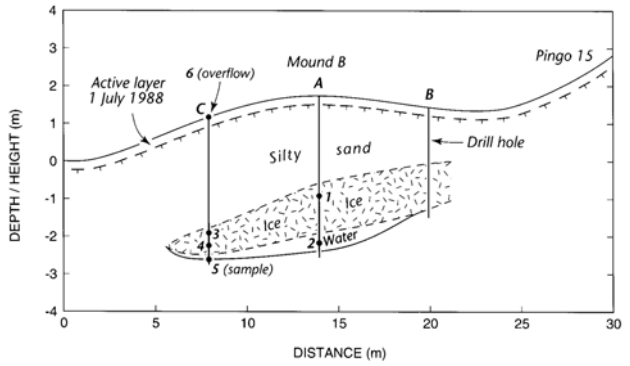

FIGURE 48. Vertical profile of Frost Mound B (see Fig. 46 for the location of the profile). The numbers refer to sample sites for water quality analyses as given in Table V.

La butte cryogène B vue en coupe (voir la fig. 46 pour la localisation). Les chiffres correspondent aux sites d'échantillonnage de l'analyse donnés au tableau V.

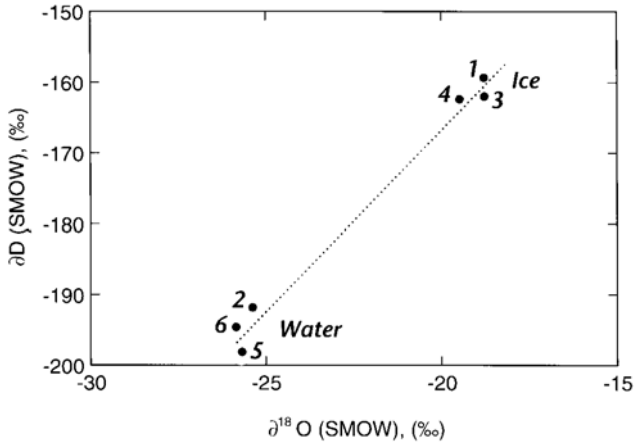

FIGURE 49. Co-isotope plot of $\delta^{18}O$ (SMOW) and δD for the sample sites given in Figure 48 and Table V. The co-isotope slope is about 5.2.

Graphique résultant de l'analyse $\delta^{18}O$ (SMOW) et δD des échantillons d'eau et de glace de la figure 48 et du tableau V. La pente isotopique est d'environ 5,2.

the top at BM 98 (Table VI) whereas the bench mark heights increased progressively upslope in the same period. The decreases in separations indicated that the downslope component of the bench mark tilts increased progressively with height. The decrease pattern was similar to that previously given for Pingo 9.

In 1974 BM 28 was about 3.5 m from the edge of the summit dilation crack and that of BM 98 on the opposite side was about 1.5 m (Fig. 44). The width of the summit dilation crack, as measured at ground level, was about 6.5 m. In the period from 1974 to 1992 the distance between the top of BM 28 and BM 98 increased 0.56 m, the height of BM 28 increased by 0.56 m, and the height of BM 98 increased by 0.27 m. In the same 1974 to 1992 period the distance between BM 98 and BM 94 on the pingo periphery decreased 0.28 m (Table VI). Therefore, about half of the 0.56 m increase in separation between BM 28 and BM 98 can be accounted for by the outward movement of BM 98. Consequently, the tops of both BM 28 and BM 98 moved outwards (*i.e* in opposite directions) toward the pingo periphery, with BM 98 moving the most, because it was closest to the pingo slope. Moreover, the pingo slope by BM 98 is much steeper than that by BM 28. The increase in width of the summit dilation crack resulted primarily from the growth of dilation crack ice beneath the bottom of the summit dilation crack, as shown by the frequent occurrence of fresh cracks in both winter and summer.

TABLE VI

Bench mark separations and bench mark height differences for Pingo 15 (Fig. 44a,b) for 1974, 1988, 1992 and 1974 to 1992

Benchmark separation	1974 (m)	1988 (m)	1992 (m)	1974 to 1992 (m)
BM 94 to BM 95	23.09	22.98	22.94	- 0.15
BM 95 to BM 96	6.95	6.90	6.88	- 0.07
BM 96 to BM 97	3.69	3.65	3.64	- 0.05
BM 97 to BM 98	4.88	4.87	4.87	- 0.01
BM 94 to BM 98	38.61	34.40	38.33	- 0.28
BM 98 to BM 28	11.70	12.07	12.26	+ 0.56
Bench mark height differences	1974 (m)	1988 (m)	1992 (m)	1974 to 1992 (m)
BM 94 to BM 95	3.08	3.14	3.15	0.07
BM 95 to BM 96	2.92	2.92	2.96	0.04
BM 96 to BM 97	1.69	1.83	1.86	0.17
BM 97 to BM 98	1.98	2.05	2.10	0.12
BM 94 to BM 98	9.67	9.74	9.87	0.20
BM 98 to BM 28	1.35	1.48	1.64	0.29

PINGO 16

Pingo 16 grew up in the bottom of the same drained lake as Pingo 15, and about 50 m to the east. Pingo 16 is oval shaped, with a long axis of 80 m, a short axis of 50 m, and a height of about 6 m, or half that of Pingo 15. In 1969 two bench marks were installed, one on the summit, the other on a lower slope. No growth was recorded in annual surveys from 1969 to 1974 nor in intermittent surveys from 1975 to 1992. In 1969 the dilation cracks of Pingo 16 terminated at the pingo periphery rather than continuing out onto the adjacent lake flats, an indication that Pingo 16 had probably long ceased growing.

PINGO 17

Pingo 17 has grown up in the bottom of the same drained lake as Pingos 13 and 14. Although field studies were started in 1971 at Pingos 13 and 14, they did not start at Pingo 17 until 1974 when spring flow, growing frost mounds, and recent faulting were discovered on the southwest side of Pingo 17, so temporary bench marks were installed at the pingo top. In 1975 datum BM 68 was established on high land about 200 m south of Pingo 17, BM 69 was located on the highest point of Pingo 17 (Fig. 50), and five other bench marks were arranged in a line along the major dilation crack that bisects the pingo (Fig. 40). At BM 69 a 2 m drill hole penetrated pure ice from 0.7 to 2 m and at BM 72 pure ice from 0.5 to 2 m, both drill holes bottoming in ice at 2 m. The occurrence of pure ice at depths just below the active layer, is unusual, but it seems unlikely that the ice was at the top of the pingo ice core. The growth pattern of Pingo 17 resembles that of Pingos 13 and 14, with an increase to the early 1980's, a levelling off in the mid-1980's, and a slight increase in the late 1980's to the last survey in 1991 (Fig. 34).

SUB-PINGO WATER LENS

Pingo 17 is underlain by a large sub-pingo water lens which has contributed to frequent hydrofracturing as shown by short and long period oscillations in the pingo height, repetitive normal faulting, and springs that have flowed intermittently for decades. For example, in the year from June 1977 to June 1978 the height of BM 69 on the summit increased 0.47 m. A one year height increase of 0.47 m cannot be attributed to the growth of ice (Fig. 4) but is readily explained by the rapid addition of water to the sub-pingo water lens.

DILATION CRACKS

The dilation crack pattern of Pingo 17 is unusual because there are semi-concentric cracks in addition to the normal straight summit and radial dilation cracks (Fig. 40).

1. Dilation cracking

In the 1975 to 1991 period the summit dilation crack between BM 69 and BM 70 cracked in both summer and winter. The winter cracks were measured for their widths and probed for their depths. In April 1978 one crack was probed to a depth of 10 m below ground level at which depth the probe jammed, so the bottom of the crack was more than 10 m below the dilation crack trough. As the pingo top was 12 m above the level of the adjacent lake flat, the bottom of the crack was then either just above or possibly even below the level of the adjacent drained lake flat. Crack widths varied, but in one winter a 20 cm wide crack was measured just below the maximum depth of summer thaw. Even though the crack might have narrowed from re-expansion of the top of permafrost during the spring warming period before snowmelt could enter the crack to freeze, the 20 cm crack width implied the addition of a thick vertical wedge of dilation crack ice that penetrated downwards many metres into the pingo ice core. Although the rifle-like sounds produced by thermally induced ice-wedge cracking during a rapid drop in winter temperature have been known for more than 100 years (Leffingwell, 1915; Washburn, 1980; Mackay, 1993a, 1993b) it is interesting to note that dilation cracking can also be heard, although not previously reported, to the best of the writer's knowledge. Specifically, on 9 June 1978 two assistants and the writer heard a nearby muffled report, suspected to be that of dilation cracking, while working near BM 69 and BM 70. Since the separation between BM 69 and BM 70 had been measured two days previously, remeasurement showed that the bench mark separation had increased 0.4 cm, an amount beyond measurement error. The muffled report can be attributed, with confidence, to dilation cracking which was mechanically induced, not thermally, as in ice-wedge cracking.

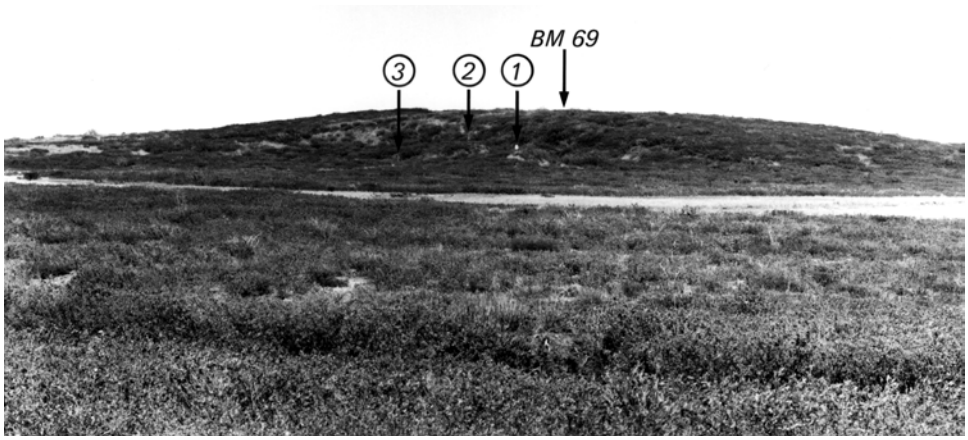

FIGURE 50. Pingo 17 with BM 69 on the top. The numbers 1 and 2 refer to Frost Mounds A and E in Figure 53; the number 3 locates a site of winter spring flow from peripheral pingo rupture. June 1985.

Le pingo n^{0} 17 avec le repère 69 au sommet. Les chiffres 1 et 2 correspondent aux buttes cryogènes A et E de la figure 53, et le chiffre 3 localise l'emplacement d'un écoulement hivernal d'une source résultant d'une rupture en périphérie du pingo.

2. Semi-concentric dilation cracks

Most of the semi-concentric dilation cracks on the west side of Pingo 17 (Fig. 40) have resulted from normal faulting with the upthrow side towards the pingo summit (Fig. 51). The crack pattern suggests that the pingo has undergone periods of uplift and subsidence from addition to and loss of water from the sub-pingo water lens, similar to what appears to have happened with some hydraulic (open) system pingos (*cf.* Worsley and Gurney, 1996). Because pingo growth increases from the periphery to the summit, the upthrow side would then tend to be towards the pingo summit.

OVERBURDEN STRETCHING

Between 1975 and 1991 the height of BM 69 at the pingo summit increased about 1.50 m and the separation between BM 69 and BM 70 increased about 0.90 m (Fig. 52). In 1991 the ground surface width of the dilation crack between BM 69 and BM 70, with allowance for slight slumping, was about 5 m and the pingo top was about 12 m above the surrounding lake flats. The correlation between the increase in pingo height and dilation crack width for 1975 to 1991 was approximately linear. Thus, the data from Pingos 9, 15, and 17 show that an estimate as to whether or not a pingo is growing can be made by repeated measurements of the separation between bench marks on either side of a summit dilation crack and probably the rate of pingo growth with height by measuring separations on downslope trending dilation cracks. The separation approach to an assessment as to whether a pingo is, or is not, growing is much easier to measure than it is to carry out a levelling survey, but the precise amount of growth cannot be determined.

SPRING FLOW

In the summer of 1974 two springs issued from dilation crack “x” (Fig. 40) located just south of BM 69 (Mackay, 1977a, 1978, 1979). The larger of the two flows came from a spring orifice that was 4 m above the lake flats. A steel surveyors tape was pushed 7 m into the orifice before jamming so the water source was well within the pingo. The mean daily discharge from 27 July to 2 August 1974 exceeded 2 L/s for a weekly total of more than 1200 m^3. The basal area of Pingo 17 is about 130,000 m^2 so the weekly loss of water from the larger spring alone was equivalent to that of a 1 cm thick layer of water beneath the entire pingo and the depth would have been proportionately greater if the area of the water lens were much smaller than that of the pingo basal area. Moreover, as the period of flow was considerably longer than one week and there was also flow from the smaller spring, the loss would have been several centimetres if spread over the entire area of the sub-pingo water lens. There was also abundant evidence from old dead willows and ground birch downstream from the two springs to show that there had been intermittent flow for at least the preceding 10 to 20 years.

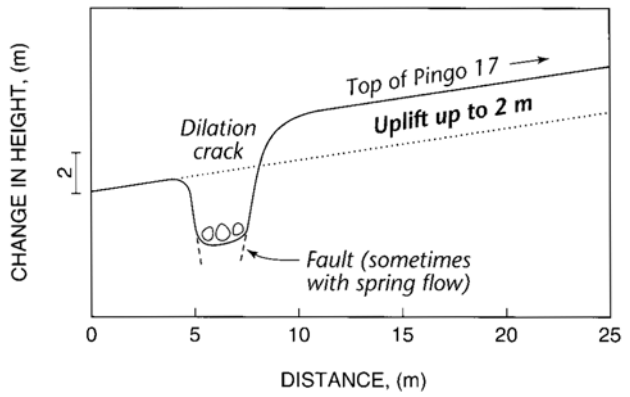

FIGURE 51. Profile of a typical dilation crack along a normal fault of Pingo 17. The upthrow side is towards the pingo summit.

Fissure de dilatation typique vue en coupe le long d’une faille normale du pingo n^o 17. Le bord soulevé est situé du côté du sommet.

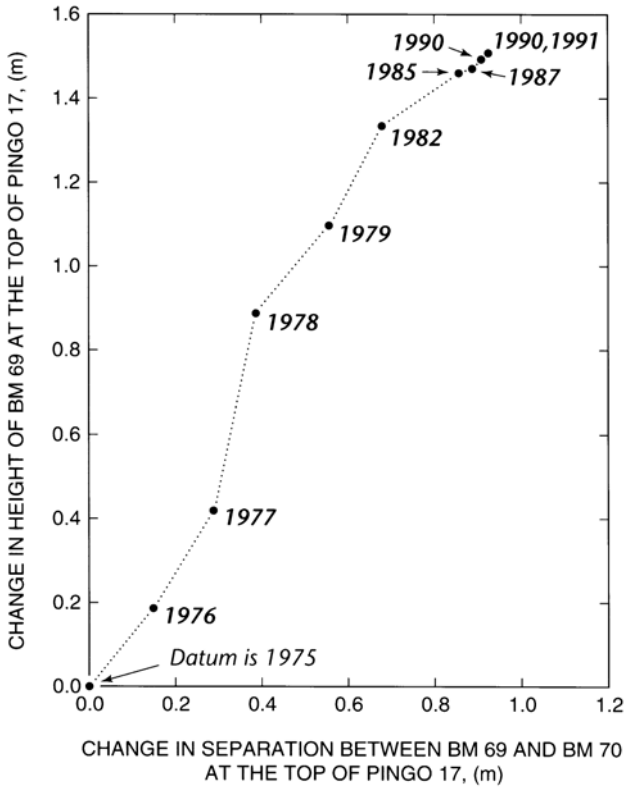

FIGURE 52. Change in height of BM 69 at the top of Pingo 17 plotted against the change in separation between BM 69 and BM 70 on the opposite side of the summit dilation crack for the 1975 to 1991 period. The graph shows that the uplifts of BM 69 and BM 70 were not vertical during pingo growth, because the trajectories subtended an angle of about 30° for the 1975 to 1991 growth period. The graph also shows that the growth of a pingo can be approximated by the change in separation across a summit dilation crack as with Pingo 15.

Différences d’altitude du repère 69 au sommet du pingo n^o 17 comparées aux différences d’écart entre les repères 69 et 70 situés de chaque côté de la fissure de dilatation située au sommet, pour la période 1975-1991. Le graphique montre que les montées des repères 69 et 70 ne se sont pas faites à la verticale durant la croissance du pingo, en raison d’une trajectoire à un angle d’environ 30° pour la période 1975-1991. Le graphique montre aussi que la croissance d’un pingo peut être estimée approximativement d’après la différence d’écart entre les deux côtés d’une fissure de dilatation sommitale, comme dans le cas du pingo n^o 15.

In view of the periodic nature of the spring flow, the bench marks on the top of Pingo 17 were levelled at frequent intervals in order to correlate the effect of spring flow with changes in pingo height. Frequent levelling showed that increases in the pingo height correlated inversely with spring flow in an on-and-off valve effect (Mackay, 1977). Five years (1974 to 1979) of intermittent summer and winter observations showed that every spring at some time flowed rhythmically in bursts of a few days, alternating with periods of quiescence, as if there was a build-up of water pressure in the sub-pingo water lens, then pressure release from spring flow, followed by another build-up of water pressure. The temperature of the spring water was usually between - 0.06 and - 0.08°C.

FROST MOUNDS

In the summer of 1974 frost mounds in various stages of growth and collapse were observed in the area downslope from dilation crack “x” (Fig. 40).

1. Frost Mound A

Frost Mound A (Fig. 50, no. 1; Fig. 53) commenced growth prior to the summer of 1973 because it was on 1973 air photographs. The intrusion of water was in late fall, before the active layer had frozen through to permafrost, because the intrusive ice in 1974 was at the bottom of the active layer. In the summer of 1974 the frost mound was elongated downslope with a length of about 40 m and a maximum width of about 20 m. The mound was mapped and wooden dowels inserted into the active layer to serve as markers for future surveys (Fig. 53a, b). In the following winter (1974/75) there was renewed spring flow associated with normal faulting along dilation crack “x” (Fig. 40), the upthrow side being towards the pingo summit. The fault was delineated by a line of broken willow branches, which had been weighted down by snow, beneath which the active layer had been ruptured. The frost mound subsided differentially, and slowly, during the next decade. In June 1985 a hole was drilled on top of Mound A near BM 17 (Fig. 53a) when the active layer was 0.50 m deep. The material from the surface down was: a brown organic rich mud to 0.50 m; an icy grey mud from 0.50 to 0.75 m; then intrusive ice from 0.75 m to the bottom of the hole at 1.10 m. A second hole by BM 3 (Fig. 53a), just downslope from the end of Mound A, penetrated frozen mud at 0.55 m, then an icy clay to 1.20 m. Therefore, if there were no future additions of intrusive ice, the mound would continue to subside by slow thaw of the icy grey mud and the intrusive ice beneath. From 1974 to 1991 the top of the mound changed little in height as measured above local datum (Fig. 53a, BM 1) but the mound had increased, by the intrusion and later freezing of water, about 0.3 m in height at BM 3, 6, 14, and 75. When last seen in the summer of 1996, when the mound was more than 20 years old, the top of the mound was collapsing.

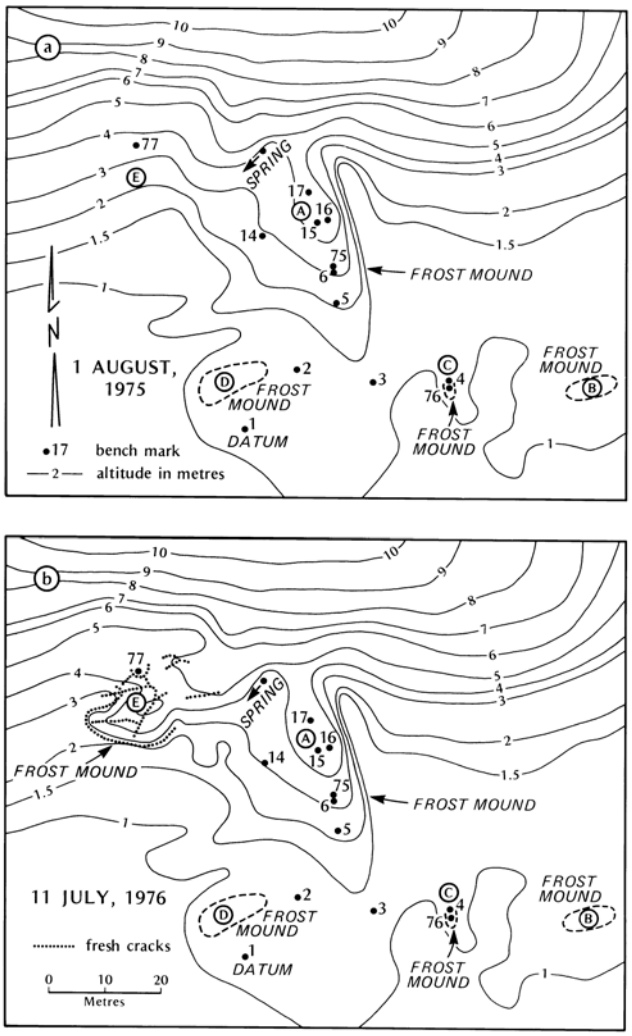

FIGURE 53. a) A map of the “area of spring flow” (Fig. 40) of Pingo 17 for August 1975. b) Map of the same area as in Figure 53a but for July 1976. See text for a discussion of the changes in the individual frost mounds and for the new frost mound at E.

a) Carte de la zone d’écoulement du pingo n^{o} 17 (fig. 40) en août 1975 ; b) carte de la même partie en juillet 1976. Voir le texte qui explique les changements survenus dans les buttes cryogènes et l’apparition de la nouvelle butte en E.

2. Frost Mound B

Frost Mound B (Fig. 53a,b) grew in the winter of 1973/74 to a height of nearly 1 m by the intrusion and freezing of water near the bottom of the active layer. Thaw of the intrusive ice continued in the summers from 1974 to 1977 by which time the intrusive ice had melted and Frost Mound B was no more.

3. Frost Mound C

Frost Mound C (Fig. 53a,b) grew in the winter of 1973/74, like Frost Mound B, but only to a height of 0.6 m. The stratigraphy for a hole drilled on 20 June 1977 between BM 4 and BM 76 was: a 0.26 m active layer; intrusive ice from 0.26 to 0.64 m; and an icy mud to the bottom of the hole at 1.0 m.

On 5 July 1979, after the mound had collapsed, the stratigraphy was: a 0.33 m active layer and an icy mud to the bottom of the hole at 0.9 m. On 1 July 1985 the stratigraphy was: a 0.4 m deep active layer; a brown mud from 0.4 to 0.6 m; then an icy mud to the bottom of the hole at 1.1 m. The sequence of events was then as follows: the intrusive ice which was present on 20 June 1977 had melted by 5 July 1979 with equivalent ground subsidence; by the summer of 1985 the active layer had deepened to 0.6 m by the thaw of all of the icy mud that was formerly present, after thaw, to that depth.

4. Frost Mound D

Frost Mound D (Fig. 53a,b) grew from the intrusion and freezing of water near the bottom of the active layer in the winter of 1973/74, like Mounds B and C, but the mound grew only to a height of 0.5 m. Mound collapse from the thaw of the intrusive ice was complete by 1976.

5. Frost Mound E

In the summer of 1974 intrusive ice from a previous frost mound was exposed at location E (Fig. 50, no. 2; Fig. 53a,b). The intrusive ice was overlain by only 0.2 m of thawed soil so the intrusion of water took place early in the freeze-back period of 1973. The ice, which was about 0.9 m thick, was composed of alternating bands of clear and bubbly ice. Probing showed that the intrusive ice continued downslope over a large area for more than 10 m at a fairly constant depth of about 0.2 m beneath the ground surface. In the winter of 1974/75 a fresh fault scarp 13 m long had developed about 7 m upslope from the ice exposure of 1974 along the trend of dilation crack “x” (Fig. 40). The scarp was delineated by a line of broken willow branches and a ruptured active layer with the upthrow side towards the pingo summit similar to that near Mound A. On 1 August 1975 a hole was drilled 2 m upslope from the scarp and BM 77, a 1.5 cm diameter aluminum rod, was inserted in the hole. The hole stratigraphy was: 0 to 0.7 m, thawed then frozen dark grey mud; mainly intrusive ice from 0.7 to 1.45 m; and nearly pure intrusive ice from 1.45 to 2.0 m, the bottom of the hole. In the winter of 1975/76 there was renewed faulting along the trend of dilation crack “x” and a new frost mound had grown just downslope from BM 77. The mound was 4 m high, nearly circular in plan, and with a diameter of 15 to 20 m. The stratigraphy was: a 0.25 m thick soil overburden; 1.2 m of clear intrusive ice; a 1.3 m high air filled cavity left by the escape of water before freeze-back was complete; then icy mud. A vertical entrance shaft was dug into the mound and inspection showed that the cavity had the same shape as the mound, but, of course, the dimensions were much smaller. BM 77 had been broken in half at freeze-back with the top of the rod being in the frozen active layer and the bottom in new intrusive ice (Fig. 54). Drilling to a depth of 4 m beside BM 77 showed that 0.75 m of new intrusive ice had grown in the winter of 1975/76. A comparison of the contour maps made in the summers of 1975 and 1976 (Fig. 53a,b) showed that the 0.75 m of new intrusive ice had grown beneath a large area. From 1976 to 1979 there was further spring flow (Fig. 55) associated with the scarp of dilation crack “x”.

FIGURE 54. BM 77 (Fig. 53b) broken by the growth of 0.75 m of intrusive ice in the winter of 1975/76 as a result of renewed normal faulting along “dilation crack x” (Fig. 40). The arrow points to the location where the top of BM 77 was broken off. The broken top is labelled “77” and is horizontal at the bottom of BM 77. The water source was along the fault as shown in Figure 55.

Le repère 77 (fig. 53b) brisé par une poussée de 0,75 m de glace intrusive durant l’hiver 75-76 en raison de l’apparition d’une faille normale le long de la fissure de dilatation x (fig. 40). La flèche montre l’endroit où la partie supérieure du repère 77 a été brisée, partie maintenant située au pied du repère 77. La source se situait le long de la faille (fig. 55).

FIGURE 55. Spring flow issuing along the line of the normal fault along “dilation crack x” (Fig. 40) of Pingo 17 in May 1978 (Mackay, 1987, Fig. 12). Episodic flow along the fault line produced the frost mounds in Figure 53.

Écoulement d’eau de source le long de la ligne de faille normale développée le long de la fissure de dilatation x (fig. 40) du pingo n^{o} 17, en mai 1978 (Mackay, 1987, fig. 12). Un écoulement épisodique le long de la ligne de faille a entraîné la formation des buttes cryogènes de la figure 53.

WATER QUALITY

Water quality analyses have been obtained for spring flow by Mound A and ice from Mound E for 27 and 28 July 1974. The salinity of the spring water, whose source was in the subpingo water lens beneath Pingo 17, was much higher than that for the ice of Mound E which also had the same water source.

For example, the total hardness (mg/L $CaCO_3$) of spring water was 488 as compared to the 7.4 for the mound ice and the respective conductivities (µS/cm) were 1330 for spring water and 40 for ice. The much greater purity of the mound ice reflected, as elsewhere, solute rejection in the freezing process. The salinity of the spring water which issued from the sub-pingo water lens was, in turn, much less than that of drill-hole flow from the sub-pingo water lens of Pingo 14 (Mackay, 1979, p. 40), even though Pingos 14 and 17 are close together and share the same groundwater system. The much higher salinity of the drill-hole flow from the sub-pingo water lens of Pingo 14 suggests that the residence time there was longer, so that there was more enrichment from solute rejection in the growth of intrusive ice, than for Pingo 17, where the residence time was shorter because of frequent pingo rupture and recharge from less saline groundwater.

PINGO 18 (IBYUK PINGO)

Pingo 18 (Ibyuk Pingo), whose summit rises about 49 m above the surrounding drained lake flat (Fig. 56), is the highest known pingo in Canada. The world's highest known pingo is Kadleroshilik Pingo which is 40 km southeast of Prudhoe Bay, Alaska. Its height, as given on a 1975 topographic map (Beechy Point (A-2), Alaska, scale 1: 63,360), is about 54 m above the adjacent lake plain or about 5 m higher than Ibyuk Pingo. Porsild (1938, Fig. 3) photographed Ibyuk Pingo in 1935. A comparison of Porsild's photograph with Ibyuk Pingo of today shows only a slight change, such as slumping near the bottom of the north facing slope. The writer made his first field observations on Ibyuk Pingo in June 1954. In May 1955, Müller (1959, 1962) carried out detailed observations on Ibyuk Pingo, and, since then, there have been several short reports (*e.g.* Fyles *et al.*, 1972; Rampton and Walcott, 1974). In 1973 two datum bench marks were located on stable terrain inland from the former lake shore and eight bench marks were installed from the pingo base to the pingo top (Fig. 56). The first 10 years of survey, 1973 to 1983, showed that Ibyuk Pingo was growing slowly (Mackay, 1986b). The survey has now been extended to 1994 to give a 21 year record.

PINGO CANADIAN LANDMARK

The Ibyuk Pingo area, which includes two other large pingos (Split Hill Pingo and Peninsula Point Pingo) and a well known exposure of massive ground ice, has been established by the Canadian Parks Service as a Pingo Canadian Landmark, National Historic Landmark. In the 1950 hydrographic chart of the area, Ibyuk Pingo was referred to as "Crater Summit Pingo" but subsequently the name was changed to Ibyuk Pingo (Arctic, 1959, 12; 125). According to detailed enquiries made of old inhabitants, the name "Ibyuk" refers to "two mounds which are close together," Ibyuk Pingo to the south and Split Pingo to the north. According to tradition recounted by elders, the two large and conspicuous pingos were formerly used as navigation aids by people travelling along the coast (C. Nuligaq, personal communication, 9 June 1993).

STRATIGRAPHY

The overburden above the ice of Ibyuk Pingo is 15 m thick and comprises, from the surface downward (Fig. 57): Unit A, about 4 m of lake silts; Unit B, about 2 m of a diamicton with glacially striated boulders; and Unit C, 9 m of sand with a few driftwood logs (Müller, 1959, 1962). The bottom of the ice core is then at least 15 m below the level of the adjacent lake flats. A 47 m deep hole drilled in 1973 (by the Geological Survey of Canada under the supervision of Dr. V.N. Rampton) to the north of Ibyuk Pingo penetrated through 6 m of clay and ice (Units A and B) and then into sands (Unit C). The sediments of Unit A are interpreted as lacustrine; Unit B as debris flow material into a shallow thermokarst lake; and Unit C as glaciofluvial sands (Fyles *et al.*, 1972). Ibyuk Pingo has grown up in the bottom of a large drained lake that measures 800 by 1400 m. Radiocarbon dating of organic material in the pingo overburden indicates that Ibyuk Lake was probably in existence before 12 ka BP and drainage was after 1.65 ka BP (Fyles *et al.*, 1972; Mackay, 1986b). Therefore, there was ample time for a large and deep unfrozen basin to develop beneath the lake.

PINGO GROWTH

The volume of Ibyuk Pingo above the lake flats is about 1 Mm^3 and the area of the drained lake bottom about 1 Mm^2. If the porosity of the lake bottom sands is assumed to be 30% and the volume of expelled pore water was somewhat less than the theoretical 9%, permafrost aggradation to a depth of 50 m

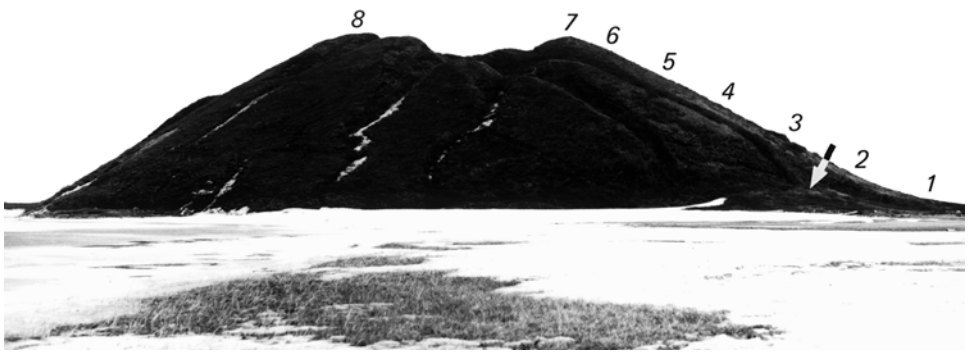

FIGURE 56. Pingo 18 (Ibyuk Pingo) showing the locations of BM 1 to 8. The arrow marks a slump formed by wave undercutting during a rise in sea level that accompanied a storm surge.

Le pingo n^o 18 (Ibuyk) et les repères 1 à 8. La flèche montre un glissement occasionné par le sapement des vagues au cours d'une hausse du niveau marin lors d'une tempête.

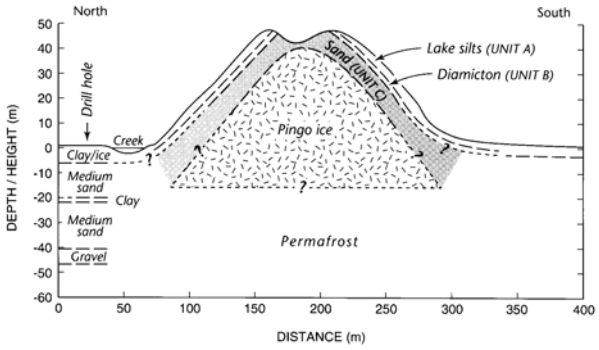

FIGURE 57. Inferred cross section of Pingo 18 (Ibyuk Pingo) based partly on Müller (1959).

Coupe présumée du pingo n^{o} 18 (Ibyuk) en partie fondée sur Müller (1959).

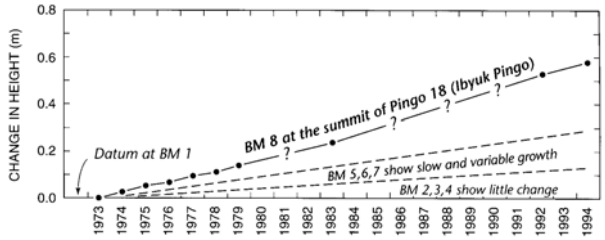

FIGURE 58. Changes in heights of the bench marks on Pingo 18 (Ibyuk Pingo) for the 1973 to 1994 period.

Différences d'altitude des repères du pingo n^{o} 18 (Ibyuk) pour la période 1973-1994.

would have been ample to supply the required volume of expelled pore water for the growth of Ibyuk Pingo. The growth of Ibyuk Pingo from 1973 to 1994 is plotted in Figure 58. The annual surveys from 1973 to 1979 showed that only the upper part of Ibyuk Pingo was growing, within the limits of survey precision, so subsequent surveys were spaced at longer intervals, as logistics permitted. BM 1, at the base of the pingo, remained stable for the 1973 to 1994 survey period. The interpretations of the survey data for BM 2, 3, and 4 are uncertain, because the changes in the 21 year period were so small that the results might have been affected more by factors such as bench mark tilt, downslope movement of the active layer, or permafrost creep rather than by pingo growth. BM 5, 6, and 7 showed slight increasing growth with height. The growth of BM 8, at the top, averaged 2.7 cm/a for the 21 year period. Because only the upper half of the pingo shows measureable growth, the growth must then be restricted to a small area beneath the pingo centre. Ibyuk Pingo may be 1 ka or more years old (Mackay, 1986).

DILATION CRACKS

1. Summit crater

Ibyuk Pingo, in profile, resembles a classic volcano with a summit depression, commonly referred to as a "crater", a descriptive term that will be used here (Fig. 56). As Ibyuk Pingo grew, the overburden would have stretched about 35 m had it not failed in tension which, with thaw, produced the summit crater. The depth to pingo ice in the summit crater is variable, but, in places, the overburden is only several metres thick (*e.g.* Müller, 1959). The bottom of the crater is overgrown with willows that surround a small pond which has varied greatly in both size and depth since the pond was first seen by the writer in 1954.

2. Radial dilation cracks

Inconspicuous radial dilation cracks trend downslope and some merge into ice wedges on the lake flats. Unlike most dilation cracks, a few have raised ridges on the lower pingo slopes. Dilation crack ice has been exposed in at least two of the cracks in the past several decades. Thaw of the dilation crack ice has created tunnel like features that have extended back several metres into the ice. In 1979, meltwater had eroded a tunnel 4.5 m deep, as measured normal to the slope, into the ice of one dilation crack. In 1992 another hole, 1 m in depth, had developed downslope from the 1979 tunnel which had collapsed to form an elongated depression. Erosion and slumping along the downslope trending dilation cracks present potential hazards to the stability of the pingo.

PINGO COLLAPSE

In view of the "Landmark" status of Ibyuk Pingo, the potential for natural collapse is augmented by its proximity to the nearby settlement of Tuktoyaktuk, N.W.T. (Fig. 2) with its potential as a tourist attraction and so to human disturbances. The beginning of collapse could be triggered by at least three methods: mass wasting, wave erosion, and thermokarst melting.

1. Mass wasting

Slumping occurs along sections of the north and east slopes where gradients of 40 to 45° are common, particularly where bare slopes in sand are exposed. At one site on the east slope slumping has already removed Units A and B to expose the loose sands of Unit C (Fig. 59). Furthermore, in summer, a few active individuals have been observed sliding and jumping down the steep bare sandy slopes to accelerate naturally induced mass wasting. The gentler and partially vegetated south and west slopes are less vulnerable, but slumping has occurred, as shown by the development of some terracettes.

2. Wave erosion

The creek that flows along the north side of Ibyuk Pingo is tidal and so are many of the ponds in the drained lake bottom. Although the tidal range is only about 0.4 m (Henry and Heaps, 1976) storm surges from strong northwest winds can raise the water level 1 to 2 m above mean sea level. A maximum storm surge of 2.4 m above mean sea level has been reported for Tuktoyaktuk (Harper *et al.*, 1988; Marsh and Schmidt, 1993), the data coming from the height of driftwood. During even a moderate storm, Ibyuk Pingo becomes an island and severe storms can erode the seaward facing north slope. There is a prominent slide, resulting from undercutting by wave erosion, that extends along the pingo base on the west side (Figs. 56, 60). The slide can be seen in Por-

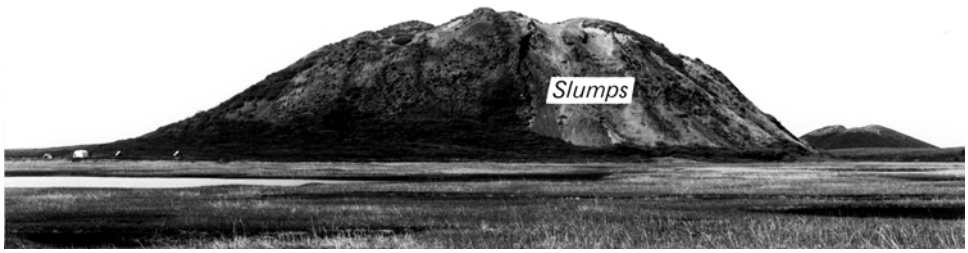

FIGURE 59. Photograph of Pingo 18 (Ibyuk Pingo) taken in the opposite direction to that of Figure. 56. If slumping continues unabated on the numerous steep slopes, pingo ice may become exposed and so endanger the stability of the pingo. July 1992.

Photographie du pingo n^{o} 18 (Ibyuk) prise dans le sens opposé à celle de la figure 56. Si les glissements se poursuivent de façon soutenue sur les pentes abruptes, la glace du pingo pourrait être mise au jour et la stabilité du pingo être ainsi compromise (juillet 1992).

sild's 1935 photograph (Porsild, 1938, Fig. 3). At present, two large driftwood logs, more than 10 m in length and 0.3 m in diameter, are lodged on slide debris at least 2.2 m above mean sea level, an indication of the severity of a storm surge. With respect to the effect of climate warming on sea level, one best estimate suggests a rise of about 0.5 m by the year 2070 (Warrick and Oerlemans, 1990). If there is such a rise in sea level and storm surges continue unabated, Ibyuk Pingo will be subjected to even greater wave erosion than at present.

3. Thermokarst effects

Pingo ice underlies the pingo crater at such a shallow depth that a minor disturbance, particularly if enhanced by stream flow from snowmelt or drainage of the crater pond, could readily initiate local thaw. In addition, pingo ice might be exposed by further slumping in Unit C on some of the very steep east facing slopes or by more erosion along some of the radial dilation cracks. When the preceding are combined with the likelihood of a deeper active layer from climate warming, the summit crater is a potential thermokarst hazard.

PINGO 19

Pingo 19 has provided us with excellent illustrations of two processes that contribute to pingo collapse, namely headwall retreat of exposed pingo ice (i.e. thermokarst collapse) and active layer slides (*i.e.* mass wasting). Pingo 19, prior to the beginning of collapse, was 26 m high and about 130 m in diameter. Pingo collapse apparently began in the mid 1970's because no pingo ice can be detected in a 1973 air photo (A23476-200); no ice was seen from a distance of several kilometres in 1975; but by 1978 considerable ice was exposed to view. Pingo 19 was surveyed in August 1979. The vertical thaw face in pingo ice was from 3 to 5 m high, about 30 m long, and as the thaw face had already retreated about 10 m upslope towards the pingo centre, thaw had probably started by 1977. The thaw face, or headwall, in pingo ice was mapped in 1979, 1980, 1982, 1983, and 1985 during which period the headwall retreated about 30 m upslope at a rate of about 4 m/a (Mackay, 1988c). In plan view, the thaw face was concave downslope towards the pingo periphery. The organic and mineral overburden above the pingo ice was only 1 to 2 m thick.

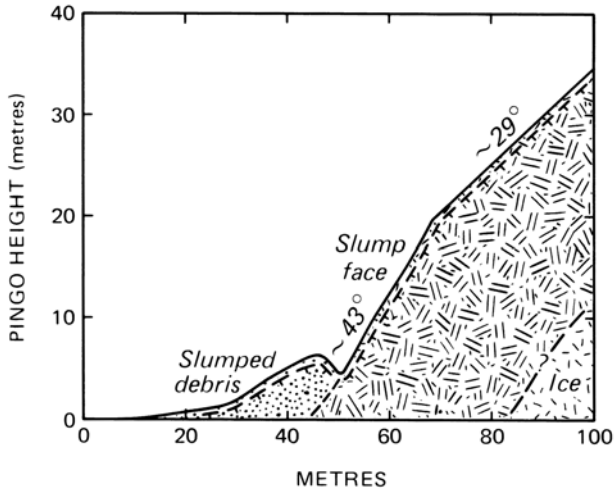

FIGURE 60. Cross section of the slump shown by the arrow in Figure 56. The slump was caused by wave erosion when there was a rise of sea level that accompanied a severe storm surge. The failure surface was in permafrost.

La coupe du glissement indiqué par la flèche de la figure 56. Le glissement a été occasionné par le sapement des vagues au cours d'une hausse du niveau marin survenue pendant une tempête.

The contact between the pingo overburden and the underlying pingo ice was typical of the thaw contact that usually accompanies pingo growth, summit dilation cracking, and thinning of the overburden above the pingo ice. Overhangs in the overburden were numerous, because of the binding effect of roots. As overhangs collapsed, the falling debris either slid down the ice face or dropped to the bottom of the scarp where it moved downslope to build a steep fan-delta into the bordering lake (Fig. 61).

The rate of headwall retreat of pingo ice or ice-rich ground depends upon many factors such as the orientation, slope angle, volumetric latent heat, and weather conditions (Mackay, 1966b; Lewkowicz, 1987). The 4 m/a headwall retreat for pingo ice at Pingo 19 was slightly less than that measured for ground-ice slumps in nearby areas. At Garry Island (Fig. 2) the headwall retreat of a ground-ice slump for the 1964 to 1971 period was about 7 m/a (Kerfoot and Mackay, 1972) and about 6 m/a for the 1935 to 1985 period for an ice-rich slump near Pingo 24 (Mackay, 1986a). Thus

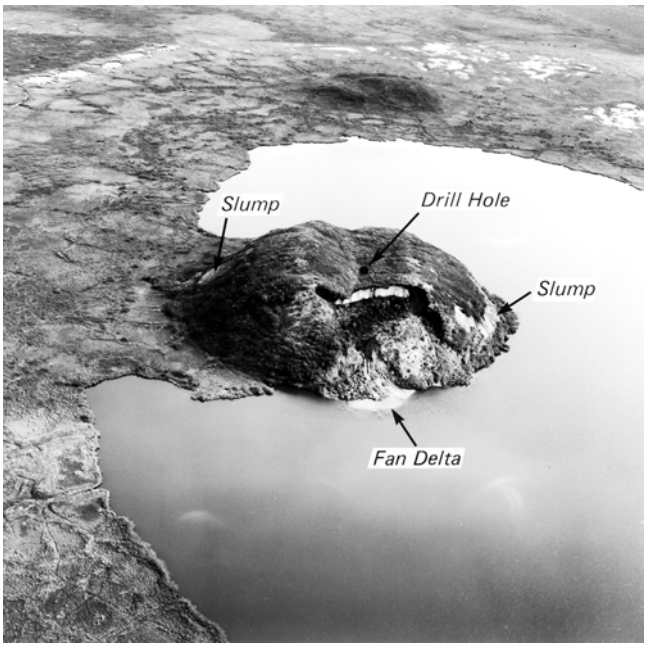

FIGURE 61. Photograph of Pingo 19, taken in 1980, about two years after part of the ice core was exposed to thaw. Most of the slopes exceeded 30°, and some exceeded 40°. Much dilation crack ice underlay the summit crater.

Photographie du pingo n^{o} 19, prise en 1980, environ deux ans après que le noyau de glace ait été exposé au dégel. La plupart des pentes dépassaient 30° et certaines dépassaient 40°. Une grande partie de la glace issue de fissures de dilatation repose sous le cratère du sommet.

the 4 m/a rate for the headwall retreat at Pingo 19 gives an indication of the rapidity with which pingo ice can thaw, provided the thawed material can move downslope so that the thaw face remains exposed to ablation. However, once a mantle of debris covers an ice-rich thaw face, it may take decades before there is a resumption of headwall retreat.

1. Active layer slides

When Pingo 19 was surveyed in 1979, recent active layer slides were numerous on the steep pingo slopes. Active layer slides, also known by other terms such as active-layer detachment slides, active layer failures, or skin flows, are shallow landslides with the failure surface usually near the bottom of the active layer or at the top of permafrost. Active layer slides are often triggered by the thaw of ice-rich material at the bottom of the active layer or top of permafrost, common causes being an unusually warm summer, a very heavy rainfall near the end of the summer, or an increased thaw depth from a disturbance to the vegetation cover (Mackay and Mathews, 1973; McRoberts and Morgenstern, 1974; Lewkowicz, 1990; Harris and Lewkowicz, 1993). In addition, at Pingo 19 active layer slides have been facilitated by the numerous steep slopes of 40 to 45°. The thickness of the slide material has been typically less than 1 m and so has coincided, approximately, with the thickness of the late summer active layer. The freshness of many slides suggests that their recency may be climate induced.

2. Dilation cracks

During the growth of Pingo 19 there was extensive dilation cracking at the pingo summit. The increase in length of the pingo overburden during growth was about 13 m and this corresponds closely with the amount of dilation crack ice formerly exposed in the thaw scarp at the pingo summit (Figs. 61, 62). Numerous radial dilation cracks trend down the pingo slopes. On the landward side, the average spacing of 9 dilation cracks was 10 to 15 m. The radial cracks extend about 10 to 15 m onto the lake flats where they either disappear or merge into an ice-wedge polygon complex.

3. Stratigraphy and temperatures

In August 1980 a 55 m deep hole was drilled in the centre of the pingo crater (Fig. 62) and two thermistors were installed at the bottom of the hole. The bottom of the pingo ice was penetrated at a depth of about 10 m below the level of the adjacent lake flats and frozen sand was beneath the pingo ice. Thus, when allowance is made for the thickness of the pingo overburden and the depth of the residual pond in which Pingo 19 grew, the ice core appears to be of intrusive ice because, if there was much segregated ice, the bottom of the ice core would then lie much more than 10 m below the adjacent lake flats. In 1980 the temperature at the bottom of the drill hole was - 2.8°C and there was little temperature variation in the next five years. The mean annual ground surface temperature (Tg) in the area is estimated to be about - 7 to - 8°C (Mackay, 1979). The temperatures given in Figure 62 have been based upon a linear interpolation between an assumed mean annual ground surface temperature of - 7°C and the known 1980 temperature of - 2.8°C at the bottom of the drill hole. If the temperatures are projected downward, the implication is that ice-bonded permafrost below the pingo is more than 60 m deep, as measured beneath the lake flats, or else that permafrost has frozen through to the bottom of the pre-drainage unfrozen basin. In any event, Pingo 19 is probably hundreds of years old for there to have been time for growth of its intrusive ice core and also the thick ice-bonded permafrost beneath it.

PINGO 20

Pingo 20, prior to partial collapse, was about 15 to 20 m in height. Pingo growth probably started before 1900, as estimated from the ages of willows and the ice-wedge polygons on the drained lake flat. Slight thermokarst collapse can be seen on a 1943 air photo (5-4-43-11A-3-176L-88). The pingo was photographed by the writer in 1970 when it appeared unchanged from the 1943 air photo. Although the pingo was seen frequently after 1970, it was not until the early 1980's that there were good ice exposures which were examined yearly from 1983 to 1988. The overburden of peaty lacustrine clay was about 3 m thick beneath which there were at least 30 alternating bands of clear and bubbly ice which, detailed study showed, were seasonal growth bands (Fig. 7) which were used, like tree rings and varved sediments, for a study of growth processes (Mackay, 1990). All of the seasonal bands had been tilted by pingo growth. Attempts were made to correlate the 30 year seasonal band widths with the more than 500

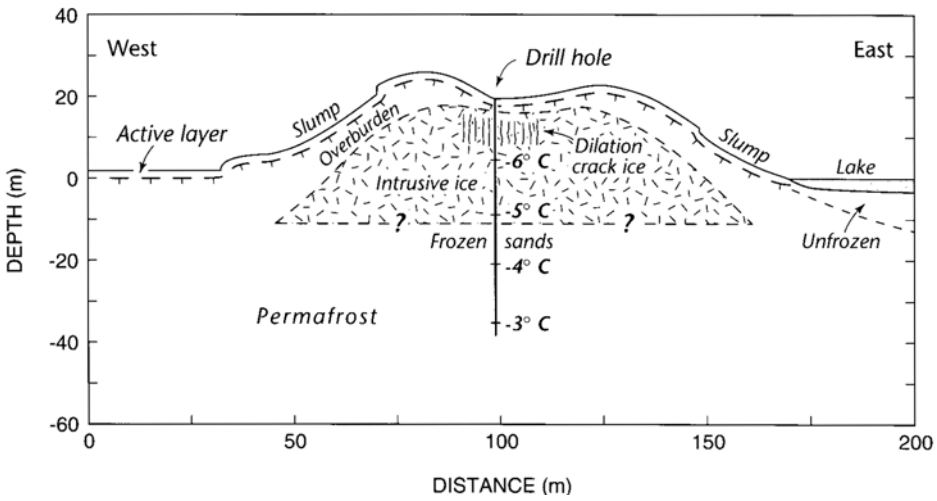

FIGURE 62. Inferred cross section of Pingo 19 as determined, in part, by drilling. The temperature at the bottom of the drill hole on 19 July 1980 was - 2.8°C.

Coupe présumée du pingo n^{o} 19 telle que déterminée, en partie, par les forages. La température au fond du trou de forage était de – 2,8 °C, le 19 juillet 1980.

years of Mackenzie Delta tree-ring data (Giddings, 1947; Parker, 1976) but the cross-correlations were inconclusive. By 1989, slumping had buried the last vestige of pingo ice (Fig. 63). When the pingo was seen in June 1996 a pond occupied much of the pingo crater. If the pond does not drain, thermokarst collapse will probably continue for many years. The collapse pattern of Pingo 20 is suggestive of what Pingo 19 might eventually look like, prior to complete collapse, given ponding in the summit crater.

PINGO 21 (WHITEFISH SUMMIT PINGO)

Pingo 21 (Whitefish Summit Pingo) is about 2 km along the coast to the west of Pingos 8, 9, 10, and 11. Pingo 21 was, prior to wave erosion, about 16 m high and 150 m in diameter. In 1935 (air photo A5026-35R) Pingo 21 was about 200 m inland from the coast; by 1967 (air photo A19978-18) waves were beginning to erode the seaward periphery; and by 1973 half of the pingo had been eroded away. Thus, from 1935 to 1973 coastal recession was about 300 m for a rate of about 7 m/a, a rate similar to that estimated for the nearby coast at Pingos 8, 9, 10, and 11 to the east (Mackay, 1986a). In 1973 the exposed section (Fig. 64) showed from the ground surface downward: 3.5 m of a stony clay; 0.35 m of fine sand; 3 m of nearly pure ice, probably segregated ice in sands; and frozen sand to the bottom of the exposure (Gell, 1976; Mackay, 1979). Since the pingo, prior to erosion, was about 16 m high but only 3 m of ice were exposed above the sand in 1973, at least 10 m of ice underlay the sand. By 1996, Pingo 21 had been effectively eroded by coastal retreat.

PINGO 23

Pingo 23 is a large, old, collapsed pingo (Fig. 65) which appears unchanged from its appearance on a 1935 air photo (A5025-50C). A prominent rampart surrounds a central pond. The rampart rises to 12 m above the surrounding lake flat. The maximum pond depth in 1984 was 5.4 m. Pingo 23 is probably one thousand or more years old as estimated from the well developed ice-wedge polygons on the adjacent drained lake flat (Mackay, 1988c). The outward facing rampart slope retains considerable evidence of extensive slumping from when the pingo was higher, because remains of old slumps, many forming benches 3 to 8 m wide, blanket nearly two-thirds of the outer rampart. About 30 radial dilation cracks trend down the outer rampart slope and many grade into ice wedges on the lake flat. None of the dilation cracks on the ramparts appear active, nor should any be active.

FIGURE 63. Pingo 20 in 1989. By 1996 a pond occupied the pingo crater, a sign of gradual thermokarst collapse.

Le pingo n^{o} 20 en 1989. En 1996, une mare occupait le cratère du pingo, un signe d'affaissement graduel.

In 1986 four holes were drilled along a diameter as shown in Figure 65. Pingo ice was penetrated in three of the four holes (Mackay, 1988c). The bottom of the pingo ice was about 25 m below the adjacent lake flat. Therefore the overburden thickness, like that of Pingo 18, probably exceeded 10 m. Since the maximum height of the rampart is 12 m and one drill hole penetrated 10 m of ice, the rampart would be very subdued or even absent if all of the pingo ice were to thaw. Here it should be stressed that Pingo 23, like the numerous other collapsed pingos, is still underlain by permafrost. Therefore, if all the permafrost in the area were to thaw from climate change, it is doubtful if many recognizable traces of Pingo 23 would remain.

FIGURE 64. Photograph of Pingo 21 (Whitefish Summit Pingo) taken in 1973. The exposed section, from the ground surface downward, was: 3.5 m of a stony clay; 0.35 m of fine sand; 3 m of nearly pure ice; and frozen sands to the bottom of the exposure.

Photographie du pingo n^{o} 21 (Whitefish Summit) prise en 1973. La partie exposée était formée, à partir de la surface, de 3,5 m d'argile pierreuse, de 0,35 de sable fin, de 3 m de glace presque pure et de sable gelé à la base.

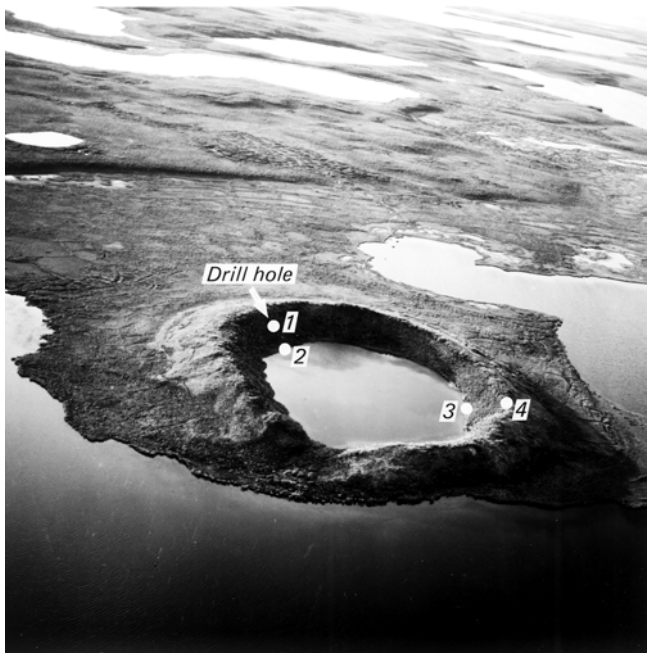

FIGURE 65. Photograph of Pingo 23, a partially collapsed pingo, showing a central pond surrounded by a rampart. Pingo ice, with a maximum thickness of 10 m, was encountered in three of the four drill holes. The bottom of the pingo ice was about 25 m below the adjacent lake flats. Because considerable ice still underlies the ridges, probably very little of the rampart would remain if there was complete degradation of permafrost surrounding and beneath the pingo.

Photographie du pingo n^{o} 23, en partie affaissé, montrant une mare centrale entourée d'une levée. La glace du pingo, d'une épaisseur maximale de 10 m, a été enregistrée dans trois des quatre trous de forage. La base du pingo était située à environ 25 m sous le fond du lac. Comme il y a beaucoup de glace sous les levées, il est probable que ces dernières disparaîtront presque totalement avec la dégradation complète du pergélisol autour et sous le pingo.

PINGO 25

Pingo 25, known locally as Peninsula Point Pingo (Fig. 66), is a wave-eroded pingo on the coast 7 km southwest of Tuktoyaktuk, N.W.T. Pingo 25 is joined by a 1 km long sandbar to an intensively studied exposure of massive ground ice (Mackay, 1971, 1986a; Fujino *et al*., 1988; Mackay and Dallimore, 1992; Moorman *et al*., 1996). Pingo 25 shows up in a 1935 air photo (A5023-87R) when an estimated 50 m had already been wave-eroded. The writer first saw Pingo 25 in 1954 when a contour map was made of the pingo and the exposed steep seaward bluff studied. Although about one third of the pingo had been eroded by 1954, the sea bluff had not yet reached the pingo summit which rose about 25 m above sea level. As an estimate, the basal diameter of Pingo 25, prior to erosion, was about 200 m. Pingo 25 was resurveyed in 1983 (Mackay, 1986a).

Pingo 25 was seen repeatedly from 1954 to 1996 and at no time was a good vertical section of pingo ice exposed. Almost without exception, the seaward exposures consisted of stratified sands that paralleled, in general, the pingo slopes; the sections often showed disturbances from faulting; and the few exposures of pingo ice that were seen were usually restricted to wave cut sections close to sea level or else exposed briefly higher up following slumping. In the fall of 1987 the bluff was undercut in a storm so that ice was exposed in the winter of 1987 and in the summer of 1988. Above the intrusive ice near sea level, but with the transition obscured by slumping, there was a complex of intrusive ice in bands that ranged from horizontal to vertical and also abundant segregated ice that had grown in sands (Mackay and Dalimore, 1992). In addition, there were several ice dikes that extended upward. One dike merged with the bottom of an ice wedge several metres below the ground surface. Another ice dike, which was underlain by segregated ice in sands, trended upward at an angle to the bedding for several tens of metres (Fig. 67). Pingo 25 is composed of glaciofluvial sands beneath a veneer of diamicton (Rampton and Bouchard, 1975; Mackay and Dalimore, 1992), the same stratigraphy as for the massive ground ice exposure 1 km to the east. Therefore it is interesting to note that ice dikes extend upward above both the segregated ice of Pingo 25 and that of the massive ground ice exposure, thus suggesting that both dikes formed from hydrofracturing and the upward intrusion of water which then froze to form the dikes. The appearance of ice dikes above injection or segregated ice has been observed elsewhere, as in the former USSR (*e.g.* Karpov, 1981) and at Garry Island, N.W.T.

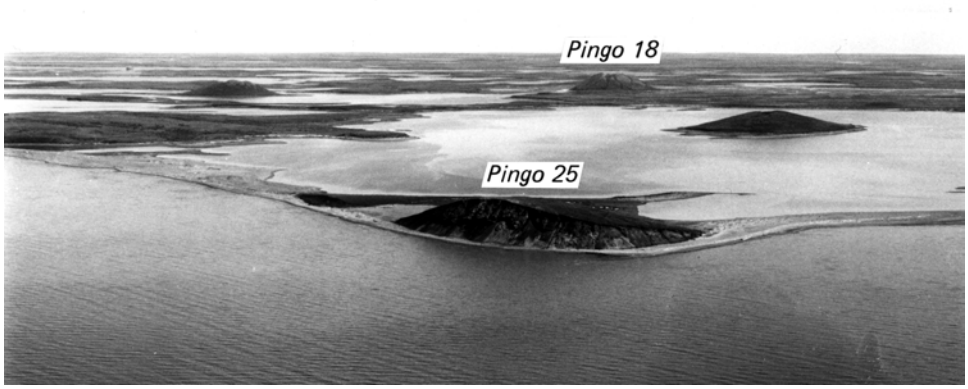

FIGURE 66. Photograph in 1981 of Pingo 25 (Peninsula Point Pingo) with Pingo 18 (Ibyuk Pingo) in the background. Pingo 25 is a wave-eroded pingo along the coast a few kilometres to the southwest of Tuktoyaktuk, N.W.T. Between 1954 and 1996 the wave-eroded bluff was seen in most summers but pingo ice was rarely seen.

Photographie du pingo n^{o} 25 (Peninsula Point) prise en 1981 et du pingo n^{o} 18 (Ibyuk) à l'arrière plan. Le pingo n^{o} 25, érodé par la mer, est situé le long de la côte, à quelques kilomètres de Tuktoyaktuk. Entre 1954 et 1996, l'escarpement érodé pouvait être observé presque à tous les étés, mais la glace du pingo a rarement été observée.

PINGO 26

Pingo 26 is about 20 m high and slightly oval with a 120 m long axis. Pingo 26 has been wave-eroded during a period of many decades when sea level was raised by storm surges from the northwest. To all appearances, Pingo 26 has grown up in the alluvium of the modern Mackenzie Delta, because the pingo periphery is flooded by storm waves as is the contiguous Delta. However, Pingo 26 has grown up in an eroded part of Richards Island which is underlain by Pleistocene or older sediments (Hill, 1996). The overburden of Pingo 26 comprises about 5 m of lacustrine sediments. The near surface sediments date back to about 3 ka BP and that just above pingo ice back to about 9 ka BP (Mackay and Stager, 1966). Exposures of intrusive ice have been seen along the wave-eroded periphery. In 1963 a 5 m deep hole drilled on the pingo periphery penetrated only intrusive ice. Because the pingo overburden was more than 5 m in thickness and there was probably more ice beneath the bottom of the hole, melting of all of the pingo ice would produce a pond, similar to that prior to pingo growth. There was very little additional erosion between 1963 and 1996.

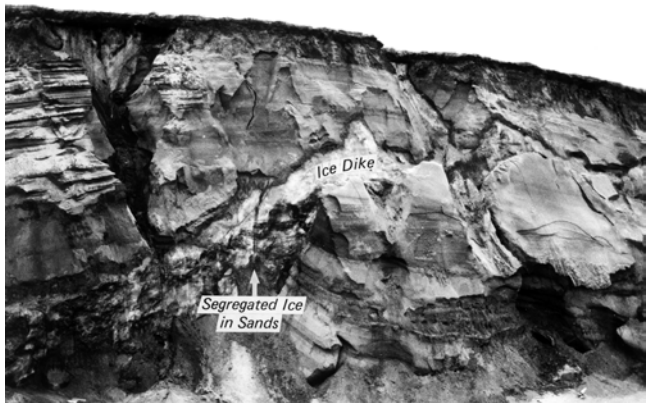

FIGURE 67. Photograph of Pingo 25 showing a rare exposure of pingo ice comprising an ice dike with a length of several tens of metres and segregated ice in sands beneath one portion of the dike. July 1988.

Photographie du pingo n^{o} 25 montrant une rare image de glace mise à nu comprenant un filon de glace d'une longueur de plusieurs mètres et de glace cristallisée dans le sable sous une partie du filon.

DISCUSSION AND CONCLUSION

THE TIME ELEMENT

In the 1969 to 1996 period growth data were obtained on a total of 15 pingos, 11 with records of 20 or more years. In view of the many rapid advances in surveying methods, those used by the writer are partially outdated. Nevertheless, the time required to determine whether or not a pingo is growing and how it is growing remains unchanged. For this reason, a very accurate survey for a brief period, such as a week, month or year, would usually be very misleading if extrapolated over a longer period such as 5, 10, or 20 years, with the possible exception of some large and old growing pingos.

PINGO GROWTH VARIABILITY

The growth patterns of pingos show such a high degree of variability that broad generalizations are difficult to make. For example, three of the pingos under study ruptured during the observation period, seven pingos were underlain by sub-pingo water lenses, and five of the pingos showed up-and-down oscillations. If it had been possible to carry out the pingo surveys more frequently and for a longer period, the number of pingos that ruptured, had sub-pingo water lenses, and oscillated up-and-down would be greater. Therefore, broad generalizations on the growth pattern of the Tuktoyaktuk Peninsula Area pingos should be taken within the context of the time and variability within which the data were obtained.

LAKE DRAINAGE

The field evidence shows that nearly 100% of the Tuktoyaktuk Peninsula Area pingos have grown up in the bottoms of lakes most of which have probably drained rapidly, in a

matter of days, weeks, or months but not in a period measured in decades or centuries. Therefore, the initiation of pingo growth, with few exceptions, has resulted from a discrete event, namely lake drainage.

PERMAFROST AGGRADATION

1. Lake bottom heave

When permafrost aggrades downward in a recently exposed drained lake bottom underlain by sands, the survey of bench marks installed across the lake bottom in conjunction with temperature measurements and/or drilling gives an indication of the growth of ice at depth. If the lake bottom heave is approximately equal to the volume expansion of pore water to pore ice, most of the pore water has frozen in place. Conversely, if there is negligible heave as temperatures at depth decrease below 0°C, there is then pore water expulsion with groundwater flow.

2. Freezing point depression

The freezing point depression for the pore water beneath ice-bonded permafrost at the drained lake site of Pingos 8, 9, 10, and 11 ranged from - 0.10 to - 0.25°C; at Pingo 12 the temperatures were fairly constant at about - 0.10°C or slightly below; at Pingos 13, 14, and 17 temperatures were about - 0.10°C or below; and at Pingo 15 the temperatures ranged from - 0.20°C for drill-hole flow beneath ice-bonded permafrost to - 2.65°C for water entrapped beneath Mound B. Saline permafrost is probably present beneath some thousands of drained lakes in the Tuktoyaktuk Peninsula Area irrespective of whether pingos have grown up in the drained lake bottoms.

3. Convective heat transport from groundwater flow

In the growth of the Tuktoyaktuk Peninsula Area pingos intrapermafrost groundwater at a negative temperature flows from beneath areas of thick permafrost towards areas of pingo growth. Therefore, the thermal regime of the drained lake bottom cannot be calculated from conventional methods of heat conduction, because of the addition of convective heat transfer from groundwater flow. Consequently, the thermal regime at a growing pingo site requires a three-dimensional conductive-convective heat transfer approach, and not the one-dimensional convective approach commonly used in permafrost studies. The net effect of convective heat transfer from groundwater flow at a negative temperature, because of a freezing point depression, is to accelerate the rate of permafrost growth in the direction of groundwater flow.

SUB-PINGO WATER LENSES

The evidence for the existence of sub-pingo water lenses at some stage of pingo growth beneath many of the pingos of the Tuktoyaktuk Peninsula Area comes from four main sources: 1) the widespread occurrence of intrusive ice, with seasonal growth bands, which requires freezing of a sub-pingo water lens; 2) confirmation of sub-pingo water lenses by drilling; 3) the up-and-down growth patterns of some pingos; and 4) pingo rupture with spring flow and the growth of frost mounds. The presence of a sub-pingo water lens beneath a pingo represents an unstable condition, because if the addition of water exceeds the growth of intrusive ice over a period of many years, the pingo will rupture, but if the addition of water is less than the growth of intrusive ice, the ice will freeze to the bottom and growth of intrusive ice will cease. The frequent occurrence of spring flow and the growth of frost mounds at the periphery of a pingo indicate hydrofracturing from the pressure of a sub-pingo water lens.

SEGREGATED ICE IN SANDS

Although intrusive ice is the most abundant type of ice in the early growth stage of many of the Tuktoyaktuk Peninsula Area pingos, segregated ice is also present. Coarse grained soils, such as sands, in general, are considered to be non frost-susceptible. However, when permafrost aggrades downward in saturated sands, such as in much of the Tuktoyaktuk Peninsula Area, the pore water below the freezing front is under a high uplift pressure with the hydraulic head often many metres above ground level. Therefore, under such conditions, segregated ice has grown in otherwise non-frost susceptible sands in the Tuktoyaktuk Peninsula Area. In contrast to the Tuktoyaktuk Peninsula Area pingos, many of the pingos in the frost-susceptible fine-grained alluvium of the distal part of the Mackzenzie Delta, immediately to the west of the Pleistocene sediments of Richards Island, have abundant segregated ice.

CLIMATE CHANGE

1. Seasonal growth bands in pingo ice

Because the seasonal growth bands in pingo ice result from the downward propagation of the seasonal temperature waves, potentially, information on the time and climatic conditions of pingo growth might be obtained by cross-correlations of the seasonal bands among different pingos and also with the 500 year, or longer, tree-ring record for the nearby Mackenzie Delta area. Thus, a study of seasonal growth bands in relation to other data might assist in determining the time of pingo growth for some pingos, their rates of pingo growth, various aspects of solute rejection, and the climate at the time of growth.

2. Recent climate change

In the interpretation of the survey results given in this paper, the tacit assumption has been made that the effects of recent climate change have been too small to affect the results. For large old pingos, this assumption is reasonable, but not for young growing pingos such as Pingos 7 and 9. Nevertheless, since 1969, when detailed pingo surveys were started, there have been noticeable changes in the vegetation cover of many pingos, which is to be expected with young pingos but less so with old pingos. At Pingo 6 (Aklisuktuk), there has been a rapid increase in the height and density of the willow cover in the crater since the mid 1970's. At Pingos 13, 14, and 17 the spread of willows and ground birch has been so rapid since the early 1980's that several campsites and many trails formerly used in surveys have had to be abandoned. At Inuvik, N.W.T., a field study following the 1968 forest-tundra fire has shown that vegeta-

tion growth at an unburnt site increased rapidly after the late 1970's. In addition to the increase in the vegetation cover, which can be attributed to climate effects, there has also been a reduction in the activity of mud hummocks near many pingo sites, specifically near Pingos 4, 8, 9, 10, and also at field sites at Garry Island, N.W.T.

PALEO-PINGOS

The field studies of both collapsing and collapsed pingos suggest some criteria that might be helpful in determining whether a collapse feature in a non-permafrost area was formerly a pingo. Natural exposures and trenching across a rampart might show: peripheral normal faults with the upthrow side towards the central depression; signs of radial dilation cracking, the casts of dilation-crack ice, and extensions of radial cracks into the surrounding area; mass wasting and/or fluvial deposits in the ramparts derived from a former higher source within the area of the central depression. Undisturbed material, similar stratigraphically to that in the surrounding area, should underlie the fill in the central depression at a depth greater than the thickness of any pingo overburden. If the undisturbed sediments below the fill are frost-susceptible soils, then an ice core would have been of segregated ice, and disturbances from ice segregation would likely be present elsewhere in the area. If the soils at depth in the central depression are coarse grained and there was a potential water source under pressure to form intrusive ice, the depth of fill might then approximate the thickness of the overburden. Elongate or crescent-shaped hydrostatic pingos are inherently unstable and so such features, if pingos, would likely be smaller than those of a more circular shape. However, in frost-susceptible soils, long gently curving pingos, some resembling eskers and railroad embankments, have been observed in the field.

ACKNOWLEDGEMENTS

I would like to express my thanks to the numerous individuals and organizations that have supported my field studies for more than four decades. The field work was started in 1951 under the former Geographical Branch, Department of Mines and Technical Surveys, Ottawa. Research grant support initially came mainly from the National Research Council, Canada, and later from the Natural Sciences and Engineering Research Council, Canada. Much of the field work on pingos has been supported by the Geological Survey of Canada, the Polar Continental Shelf Project, Department of Natural Resources, Canada, and the Inuvik Research Laboratory, Inuvik, NWT. Many colleagues, friends, and field assistants have been of invaluable help. I would like to extend special thanks to: P.A. Batson, P. Benham, D. Blythe, R. Boyd, N. Buckley, C.R. Burn, K.E. Champion, A. Collett, P. Davidson, C. Diana, D.F. Dickins, J. Dwyer, B. Enderton, W.A. Gell, J.M. Gill, G. Gruson, S.E.B. Irwin, M. Jakob, E. Jetchick, W. Kay, N. King, A. Kriss, G.O. Lougheed, D.K. MacKay, D.G. McPhee, R.A. Myers, N. Oke, A. Olney, A.J. Podrouzek, V.W. Sim, J.K. Stager, J.K. Stathers, G. Thompson, R.W. Toews, M. Wark, B. Woods, P. Wright. Professor J.J. Solecki has translated numerous Russian publications that have made access to some of the abundant Russian literature possible. The cartography is by Paul Jance. The two referees have given constructive comments. Lastly, I would like to thank my late wife Violet Mackay for helping me in countless ways for more than four decades of field research.

REFERENCES

Abed, A.M., Makhlouf, I.M., Amireh, B.S. and Khalil, B., 1993. Upper Ordovician glacial deposits in southern Jordan. Episodes, 16: 316-328.

Åkerman, H.J. and Malmström, B., 1986. Permafrost mounds in the Abisko area, northern Sweden. Geografiska Annaler, 68A: 155-165.

Allen, D.M., Michel, F.A. and Judge, A.S. 1988. The permafrost regime in the Mackenzie Delta, Beaufort Sea region, N.W.T. and its significance to the reconstruction of the palaeoclimatic history. Journal of Quaternary Science, 3(1): 3-13.

An, Z., 1980. Formation and evolution of permafrost ice mound on Qing-Zang Plateau (in Chinese). Journal of Glaciology and Cryopedology, 2(2): 25-30.

Anderson, R.M., 1913. Natural history appendix, p. 436-527. *In* V. Stefansson, My Life with the Eskimo. Macmillan, New York.

Arvidson, W.D. and Morgenstern, N.R., 1977. Water flow induced by soil freezing. Canadian Geotechnical Journal, 14: 237-245.

Babinski, Z., 1982. Pingo degradation in the Bayan-Nuurin-Khotnor Basin, Khangai Mountains, Mongolia. Boreas, 11: 291-298.

_____ 1994. Pingo formation and degradation in the Bajan-Nuurin-Khotnor Basin (Khangai Mountains, Mongolia) (in Polish). Przeglad Geograficzny, 66: 133-150.

Bahat, D., 1991. Tectonofractography. Springer-Verlag, Berlin, 354 p.

Balduzzi, F., 1959. Experimental investigation of soil freezing (in German). Mitteilungen der Versuchsanstalt für Wasserbau und Erdbau, 44. Translated by D.A. Sinclair. National Research Council of Canada, Ottawa, 1960, TT-912, 43 p.

Balkwill, H.R., Roy, K.J., Hopkins, W.S. and Sliter, W.V. 1974. Glacial features and pingos, Amund Ringnes Island, Arctic Archipelago. Canadian Journal of Earth Sciences, 11: 1319-1325.

Beskow, G., 1935. Soil freezing and frost heaving with special application to roads and railroads (in Swedish). The Swedish Geological Society, Series C, No. 375, 26th Year Book 3. Translated by J.O. Osterberg. Published by the Technological Institute, Northwestern University, Evanston, 1947, 145 p.

Beuf, S., Biju-Duval, B., De Charpal, O., Rognon, P., Gariel, O. and Bennacef, A., 1971. Les grès du Paléozoïque inférieur au Sahara. Publications de l'Institut français du Pétrole, Collection Science et technique du pétrole, 18, Technip, Paris, 464 p.

Biju-Duval, B., Deynoux, M. and Rognon, P., 1981. Late Ordovician tillites of the Central Sahara, p. 99-107. *In* M.J. Hambrey and W.B. Harland, eds., Earth's Pre-Pleistocene glacial record. Cambridge University Press.

Bik, M.J.J., 1969. The origin and age of the prairie mounds of southern Alberta, Canada. Biuletyn Peryglacjalny, 19: 85-130.

Bleich, K.E., 1974. On the formation of pingos in the Mackenzie Delta, N.W.T. (in German). Polarforschung, 44(1): 60-66.

Bobov, N.G., 1969. The formation of beds of ground ice (in Russian). Izvestiya Akademii Nauk, SSSR, seriya geograficheskaya, 6: 63-68. *In* Soviet Geography: Review and Translation, 1970, 11: 456-463.

Bostrom, R.C., 1967. Water expulsion and pingo formation in a region affected by subsidence. Journal of Glaciology, 6: 568-572.

Brown, R.J.E. and Péwé, T.L, 1973. Distribution of permafrost in North America and its relationship to the environment: A review, 1963-1973. *In* North American Contribution Permafrost Second International Conference, Yakutsk, U.S.S.R. National Academy of Sciences, Washington, D.C., p. 71-100.

Brown, R.J.E. and Kupsch, W.O., 1974. Permafrost terminology. National Research Council Canada, Ottawa, NRCC 14274, 62 p.

Burn, C.R. and Maxwell, M.G., 1993. Proper determination of the $\delta^{18}O$ - δD relationship for ice and water by least-squares cubic regression. Canadian Journal of Earth Sciences, 30: 109-112.

Carter, L.D. and Galloway, J.P., 1979. Arctic Coastal Plain pingos in National Petroleum Reserve in Alaska. *In* K.M. Johnson and J.R. Williams, eds., The United States Geological Survey in Alaska: Accomplishments during 1978. Geological Survey Circular 804-B: 33-35.

Chen, X., Jiang, P. and Wang, Y. 1980. Pore water pressure of saturated gravel during freezing (in Chinese). Journal of Glaciology and Cryopedology, 2(4): 33-37.

Corry, C.E., 1988. Laccoliths; mechanics of emplacement and growth. Geological Society of America Special Paper 220, 110 p.

Craig, B.G., 1959. Pingo in the Thelon Valley, Northwest Territories; radiocarbon age and historical significance of the contained organic material. Bulletin of the Geological Society of America, 70: 509-510.

Cui, Z., 1982. Basic characteristics of periglacial landforms in the Qinghai-Xizang Plateau. Scientia Sinica (Series B), 25: 79-91.

Danilov, I.D., 1983. Methods of Cryolithological Research (in Russian). Moscow, Nedra, 200 p.

De Gans, W., 1988. Pingo scars and their identification, p. 299-322. *In* M.J. Clark, ed., Chapter 13, Advances in Periglacial Geomorphology. John Wiley, Chichester.

Ferrians Jr., O.J., 1988. Pingos in Alaska: A review. *In* K. Sennest, ed., Permafrost Fifth International Conference Proceedings. Tapir Publishers, Trondheim, 1: 734-739.

Fitzsimons, S.J., 1989. Reinterpretation of pingos in Antarctica. Quaternary Research, 32: 114-116.

Flemal, R.C., 1976. Pingos and pingo scars: Their characteristics, distribution, and utility in reconstructing former permafrost environments. Quaternary Research, 6: 37-53.

Fotiev, S.M., 1978. Effect of long-term cryometamorphism of earth materials on the formation of groundwater (in Russian). Third International Conference on Permafrost, Edmonton, Alberta. Part I: English translations of twenty-six of the Soviet Papers, NRCC 18119, Ottawa, 1980, p. 177-194.

French, H.M. and Dutkiewicz, L., 1976. Pingos and pingo-like forms, Banks Island, Western Canadian Arctic. Biuletyn Peryglacjalny, 26: 211-222.

Fujino, K., Sato, S., Matsuda, K., Sasa, G., Shimizu, O. and Kato, K., 1988. Characteristics of the massive ground ice body in the western Canadian Arctic (11). *In* K. Senneset, ed., Permafrost Fifth International Conference Proceedings. Tapir Publishers, Trondheim, 1: 143-147.

Fyles, J.G., Heginbottom, J.A. and Rampton, V.N., 1972. Quaternary geology and geomorphology, Mackenzie Delta to Hudson Bay. 24th International Geological Congress, Montreal, Excursion A30, 23 p.

Gasanov, S.S., 1978. Cryolithogenesis as an independent hydrothermal type of sedimentary process (in Russian). Third International Conference on Permafrost, Edmonton, Alberta. Part 1: English translations of twenty-six of the Soviet Papers, NRCC 18119, Ottawa, 1980, p. 225-244.

Gell, W.A., 1976. Underground ice in permafrost, Mackenzie Delta-Tuktoyaktuk Peninsula, N.W.T. Ph.D. thesis, University of British Columbia, Vancouver, 258 p.

——— 1978. Fabrics of icing-mound and pingo ice in permafrost. Journal of Glaciology, 20: 563-569.

Geurts, M.-A. and Dewez, V., 1985. Le pingo d'Aishihik, sud-ouest du Yukon: caractères morphogénétiques et cadre temporel. Géographie physique et Quaternaire, 39: 291-298.

Giddings Jr., J.L., 1947. Mackenzie River Delta chronology. Tree-Ring Bulletin, 13(4): 26-29.

Gordon, J.E., Darling, W.G., Whalley, W.B. and Gellatly, A.F. 1988. δD-$\delta^{18}O$ relationships and the thermal history of basal ice near the margins of two glaciers in Lyngen, north Norway. Journal of Glaciology, 34: 265-268.

Gretener, P.E., 1969. On the mechanics of the intrusion of sills. Canadian Journal of Earth Sciences, 6: 1415-1419.

Gurney, S.D. and Worsley, P., 1997. Genetically complex and morphologically diverse pingos in the Fish Lake area south west Banks Island, N.W.T. Canada. Geografiska Annaler, 79A: 41-56.

Gussow, W.C., 1954. Piercement domes in Canadian Arctic. The Bulletin of the American Association of Petroleum Geologists, 38: 2225-2226.

——— 1962. Energy source of intrusive masses. Transactions of the Royal Society of Canada, Third Series, 56(3): 1-19.

Guth, P.L., Hodges, K.V. and Willemin, J.H., 1982. Limitations on the role of pore pressure gravity sliding. Geological Society of America Bulletin, 93: 606-612.

Hallet, B., 1978. Solute redistribution in freezing ground. *In* Third International Conference on Permafrost, Edmonton, Alberta, Canada. National Research Council of Canada, Ottawa, 1: 85-91.

Hamilton, T.D. and Obi, C.M., 1982. Pingos in the Brooks Range, Northern Alaska, U.S.A. Arctic and Alpine Research, 14: 13-20.

Harper, J.R, Henry, R.F. and Stewart, G.G., 1988. Maximum storm surge elevations in the Tuktoyaktuk Region of the Canadian Beaufort Sea. Arctic, 41: 48-52.

Harris, S.A., French, H.M., Heginbottom, J.A., Johnston, G.H., Ladanyi, B., Sego, D.C. and van Everdingen, R.O., 1988. Glossary of permafrost and related ground-ice terms. Permafrost Subcommittee, Associate Committee on Geotechnical Research, National Research Council of Canada, Ottawa, Technical Memorandum, 142: 156 p.

Harris, C. and Lewkowicz, A.G., 1993. Form and internal structure of active-layer detachment slides, Fosheim Peninsula, Ellesmere Island, Northwest Territories, Canada. Canadian Journal of Earth Sciences, 30: 1708-1714.

Henry, R.F. and Heaps, N.S., 1976. Storm surges in the southern Beaufort Sea. Journal of the Fisheries Research Board of Canada, 33: 2362-2376.

Hill, P.R., 1996. Late Quaternary sequence stratigraphy of the Mackenzie Delta. Canadian Journal of Earth Sciences, 33: 1064-1074.

Hill, P.R, Mudie, P.J., Moran, K. and Blasco, S.M., 1985. A sea-level curve for the Canadian Beaufort Shelf. Canadian Journal of Earth Sciences, 22: 1383-1393.

Hill, P.R, Héquette, A. and Ruz, M-H., 1993. Holocene sea-level history of the Canadian Beaufort Shelf. Canadian Journal of Earth Sciences, 30: 103-108.

Hobbs, P.V., 1974. Ice physics. Clarendon Press, Oxford, 838 p.

Holmes, G.W., Hopkins, D.M. and Foster, H.L., 1968. Pingos in Central Alaska. U.S. Department of the Interior, Geological Survey Bulletin 1241-H, 40 p.

Hughes, O.L., 1969. Distribution of open-system pingos in Central Yukon Territory with respect to glacial limits. Geological Survey of Canada, Paper 69-34, 8 p.

Ingersoll, L.R., Zobel, O.J. and Ingersoll, A.C., 1954. Heat conduction with engineering, geological, and other applications. University of Wisconsin Press, Madison, 325 p.

Jouzel, J. and Souchez, R.A., 1982. Melting-refreezing at the glacier sole and the isotopic composition of the ice. Journal of Glaciology, 28: 35-42.

Judge, A.S., Taylor, A.E. and Burgess, M., 1979. Canadian Geothermal data collection - northern wells 1977-78. Energy, Mines and Resources Canada, Earth Physics Branch, Ottawa, Geothermal Series, 11: 187 p.

Karpov, E.G., 1981. New information about thick layered deposits of underground ice in the northern reaches of the Yenisei Region (in Russian). Academy of Sciences of the U.S.S.R., Section of Glaciology, 41: 67-70.

Kerfoot, D.E. and Mackay, J.R., 1972. Geomorphological process studies, Garry Island, N.W.T. p. 115-130. *In* D.E. Kerfoot, ed., Mackenzie Delta Area Monograph. 22nd International Geographical Congress, Canada. Brock University, St. Catharines.

Khakimov, K.R., 1957. Problems in the theory and practice of artificial freezing of soil (in Russian). Publishing House of the Academy of Science USSR, Moscow. Translated by the National Technical Information Service, U.S. Department of Commerce, AD 711 891, 1970, 178 p.

Konrad, J.M., 1990. Theoretical modelling of massive icy beds. *In* Permafrost - Canada: Proceedings of the Fifth Canadian Permafrost Conference. Université Laval. Centre d'études nordiques, Québec, and National Research Council, Canada, Ottawa, Collection Nordicana, 54: 31-35.

Lachenbruch, A.H., 1962. Mechanics of thermal contraction cracks and ice-wedge polygons in permafrost. Geological Society of America, Special Paper 70, 69 p.

Lagerbäck, R. and Rodhe, L., 1986. Pingos and palsas in northernmost Sweden - preliminary notes on recent investigations. Geografiska Annaler 68A: 149-154.

Leffingwell, E. de K., 1915. Ground-ice wedges, the dominant form of ground-ice on the north coast of Alaska. Journal of Geology, 23: 635-654.

——— 1919. The Canning River Region Northern Alaska. United States Geological Survey Professional Paper 109, 251 p.

Lewkowicz, A.G., 1987. Headwall retreat of ground-ice slumps, Banks Island, Northwest Territories. Canadian Journal of Earth Sciences, 24: 1077-1085.

——— 1990. Morphology, frequency and magnitude of active-layer detachment slides, Fosheim Peninsula, Ellesmere Island, N.W.T. *In* Permafrost - Canada: Proceedings of the Fifth Canadian Permafrost Conference. Université Laval. Centre d'études nordiques, Québec, and National Research Council Canada, Ottawa, Collection Nordicana, 54: 111-118.

Mackay, J.R., 1958. The Anderson River map-area, N.W.T. Geographical Branch, Mines and Technical Surveys, Ottawa, Memoir 5, 137 p.

——— 1962. Pingos of the Pleistocene Mackenzie Delta Area. Geographical Branch, Mines and Technical Surveys, Ottawa, Geographical Bulletin, 18: 21-63.

——— 1963. The Mackenzie Delta Area, N.W.T. Geographical Branch, Mines and Technical Surveys, Ottawa, Memoir 8, 202 p.

——— 1966a. Pingos in Canada. *In* Permafrost International Conference, 1963, Lafayette, Indiana. National Academy of Sciences-National Research Council, Washington, D.C., Publication, 1287: 71-76.

——— 1966b. Segregated epigenetic ice and slumps in permafrost, Mackenzie Delta Area, N.W.T. Geographical Branch, Mines and Technical Surveys, Ottawa, Geographical Bulletin, 8: 59-80.

——— 1971. The origin of massive icy beds in permafrost, Western Arctic Coast, Canada. Canadian Journal of Earth Sciences, 8: 397-422.

——— 1973. The growth of pingos, Western Arctic Coast, Canada. Canadian Journal of Earth Sciences, 10: 979-1004.

——— 1974a. Ice-wedge cracks, Garry Island, Northwest Territories. Canadian Journal of Earth Sciences, 11: 1366-1383.

——— 1974b. Performance of a heat transfer device, Garry Island, N.W.T. Geological Survey of Canada, Paper 74-1, Part B: 252-254.

——— 1975a. Some resistivity surveys of permafrost thicknesses, Tuktoyaktuk Peninsula, N.W.T. Geological Survey of Canada, Paper 75-1, Part B: 177-180.

——— 1975b. Freezing processes at the bottom of permafrost, Tuktoyaktuk Peninsula Area, District of Mackenzie (107 C). Geological Survey of Canada, Paper 75-1, Part A: 471-474.

——— 1977a. Pulsating pingos, Tuktoyaktuk Peninsula, N.W.T. Canadian Journal of Earth Sciences, 14: 209-222.

——— 1977b. Permafrost growth and subpermafrost pore water expulsion, Tuktoyaktuk Peninsula, District of Mackenzie. Geological Survey of Canada, Paper 77-1A: 323-326.

——— 1978. Sub-pingo water lenses, Tuktoyaktuk Peninsula, Northwest Territories. Canadian Journal of Earth Sciences, 8: 1219-1227.

——— 1979. Pingos of the Tuktoyaktuk Peninsula Area, Northwest Territories. Géographie physique et Quaternaire, 33: 3-61.

——— 1981. Aklisuktuk (Growing Fast) Pingo, Tuktoyaktuk Peninsula, Northwest Territories, Canada. Arctic, 34: 270-273.

——— 1983. Pingo growth and subpingo water lenses, p. 762-766. *In* Permafrost: Fourth International Conference, Proceedings, Fairbanks, Alaska. National Academy Press, Washington, D.C.

——— 1984. The direction of ice-wedge cracking in permafrost: Downward or upward? Canadian Journal of Earth Sciences, 21: 516-524.

——— 1985a. Permafrost growth in recently drained lakes. *In* Current Research, Part B, Geological Survey of Canada, Paper 85-1B: 177-189.

——— 1985b. Pingo ice of the western Arctic coast, Canada. Canadian Journal of Earth Sciences, 22: 1452-1464.

——— 1986a. Fifty years (1935 to 1985) of coastal retreat west of Tuktoyaktuk, District of Mackenzie. *In* Current Research, Part A, Geological Survey of Canada, Paper 86-1A: 727-735.

——— 1986b. Growth of Ibyuk Pingo, Western Arctic Coast, Canada, and some implications for environmental reconstructions. Quaternary Research, 26: 68-80.

——— 1987. Some mechanical aspects of pingo growth and failure, western Arctic coast, Canada. Canadian Journal of Earth Sciences, 24: 1108-1119.

——— 1988a. Catastrophic lake drainage, Tuktoyaktuk Peninsula area, District of Mackenzie. *In* Current Research, Part D, Geological Survey of Canada, Paper 88-1D: 83-90.

——— 1988b. The birth and growth of Porsild Pingo, Tuktoyaktuk Peninsula, District of Mackenzie. Arctic, 41: 267-274.

——— 1988c. Pingo collapse and paleoclimatic reconstruction. Canadian Journal of Earth Sciences, 25: 495-511.

——— 1990. Seasonal growth bands in pingo ice. Canadian Journal of Earth Sciences, 27: 1115-1125.

——— 1992a. Lake stability in an ice-rich permafrost environment: Examples from the Western Arctic Coast, p. 1-26. *In* R.D. Robarts and M.L. Bothwell, eds., Arctic ecosystems in semi-arid regions: Implications for resource management. N.H.R.I. Symposium Series 7, Environment Canada, Saskatoon.

——— 1992b. The frequency of ice-wedge cracking (1967-1987) at Garry Island, western Arctic coast, Canada. Canadian Journal of Earth Sciences, 29: 236-248.

——— 1993a. Air temperature, snow cover, creep of frozen ground, and the time of ice-wedge cracking, western Arctic coast. Canadian Journal of Earth Sciences, 30: 1720-1729.

——— 1993b. The sound and speed of ice-wedge cracking, Arctic Canada. Canadian Journal of Earth Sciences, 30: 509-518.

——— 1995. Active layer changes (1968 to 1993) following the forest-tundra fire near Inuvik, N.W.T., Canada. Arctic and Alpine Research, 27: 323-336.

——— 1997. A full-scale field experiment (1978-1995) on the growth of permafrost by means of lake drainage, western Arctic coast: A discussion of the method and some results. Canadian Journal of Earth Sciences, 34: 17-33.

Mackay, J.R. and MacKay, D.K., 1974. Snow cover and ground temperatures, Garry Island, N.W.T. Arctic, 27: 288-296.

Mackay, J.R. and Dallimore, S.R., 1992. Massive ice of the Tuktoyaktuk area, western Arctic coast, Canada. Canadian Journal of Earth Sciences, 29: 1235-1249.

Mackay, J.R. and Stager, J.K., 1966. The structure of some pingos in the Mackenzie Delta Area, N.W.T. Geographical Branch, Mines and Technical Surveys, Ottawa, Geographical Bulletin, 8: 360-368.

Mackay, J.R. and Mathews, W.H., 1973. Geomorphology and Quaternary History of the Mackenzie River Valley near Fort Good Hope, N.W.T., Canada. Canadian Journal of Earth Sciences, 10: 26-41.

Marion, G.M., 1995. Freeze-thaw processes and soil chemistry. U.S. Army Corps of Engineers, Cold Regions Research and Engineering Laboratory, Hanover, N.H. Special Report 95-12, 23 p.

Marsh, B., 1987. Pleistocene pingo scars in Pennsylvania. Geology, 15: 945-947.

Marsh, P. and Schmidt, T., 1993. Influence of a Beaufort Sea storm surge on channel levels in the Mackenzie Delta. Arctic, 46: 35-41.

McRoberts, E.C. and Morgenstern, N.R., 1974. The stability of thawing slopes. Canadian Geotechnical Journal, 11: 447-469.

——— 1975. Pore water expulsion during freezing. Canadian Geotechnical Journal, 12: 130-141.

Michel, B. and Ramseier, R.O., 1971. Classification of river and lake ice. Canadian Geotechnical Journal, 8: 36-45.

Middleton, G.V. and Wilcock, P.R., 1994. Mechanics in the earth and environmental sciences. Cambridge University Press, Cambridge, 459 p.

Miller, R.D., 1980. Freezing phenomena in soils, p. 254-299. *In* D. Hillel, ed., Applications of soil physics. Academic Press, New York.

Mitchell, G.F., 1971. Fossil pingos in the south of Ireland. Nature, 230: 43-44.

Moorman, B.J., Michel, F.A. and Wilson, A., 1996. ^{14}C dating of trapped gasses in massive ground ice, Western Canadian Arctic. Permafrost and Periglacial Processes, 7: 257-266.

Muller, S.W., 1945. Permafrost or permanently frozen ground and related engineering problems. Military Intelligence Division, Office, Chief of Engineers, U.S. Army, Washington, D.C. (Second printing with corrections), 231 p.

Müller, F., 1959. Observations on pingos (in German). Meddeleser om Grønland, 153, 127 p. Translated by D.A. Sinclair, National Research Council of Canada, Ottawa, TT-1073, 1963, 117 p.

——— 1962. Analysis of some stratigraphic observations and radiocarbon dates from two pingos in the Mackenzie Delta Area, N.W.T. Arctic, 15: 278-288.

Parameswaran, V.R. and Mackay, J.R., 1996. Electrical freezing potentials measured in a pingo growing in the western Canadian Arctic. Cold Regions Science and Technology, 24: 191-203.

Parker, M.L., 1976. Improving tree-ring dating in Northern Canada by X-ray densitometry. Syesis, 9: 163-172.

Pelletier, B.R., (ed.), 1987. Marine atlas of the Beaufort Sea: Geology and geophysics. Geological Survey of Canada, Miscellaneous Report 40.

Pickard, J., 1983. Pingos in Antarctica. Quaternary Research, 20: 105-109.

Pihlainen, J.A., Brown, R.J.E. and Legget, R.F., 1956. Pingo in the Mackenzie Delta, Northwest Territories, Canada. Bulletin of the Geological Society of America, 67: 1119-1122.

Pissart, A., 1967. Les pingos de l'île Prince Patrick (76 °N-120 °W). Geographical Branch, Mines and Technical Surveys, Ottawa, Geographical Bulletin, 9: 189-217.

Pissart, A. and French, H.M., 1976. Pingo investigations, north-central Banks Island, Canadian Arctic. Canadian Journal of Earth Sciences, 13: 937-946.

Poley, D.F., 1982. A detailed study of a submerged pingo-like-feature in the Canadian Beaufort Sea. B.Sc. Thesis, Dalhousie University, Halifax, 96 p.

Pollard, D.D., 1968. Deformation of host rocks during sill and laccolith formation. Ph.D. Thesis, Stanford University, 134 p.

——— 1973. Derivation and evaluation of a mechanical model for sheet intrusions. Tectonophysics, 19: 233-269.

Pollard, D.D. and Johnson, A.M., 1973. Mechanics of growth of some laccolithic intrusions in the Henry Mountains, Utah. 11. Bending and failure of overburden layers and sill formation. Tectonophysics, 18: 311-354.

Porsild, A.E., 1938. Earth mounds in unglaciated Arctic northwestern America. Geographical Review, 28: 46-58.

Rampton, V.N., 1988. Quaternary geology of the Tuktoyaktuk Coastlands, Northwest Territories. Geological Survey of Canada, Memoir 423, 98 p.

Rampton, V.N. and Mackay, J.R., 1971. Massive ice and icy sediments throughout the Tuktoyaktuk Peninsula, Richards Island, and nearby areas, District of Mackenzie. Geological Survey of Canada Paper 71-21, 16 p.

Rampton, V.N. and Walcott, R.I., 1974. Gravity profiles across ice-cored topography. Canadian Journal of Earth Sciences, 11: 110-122.

Rampton, V.N. and Bouchard, M., 1975. Surficial geology of Tuktoyaktuk, District of Mackenzie. Geological Survey of Canada Paper 74-53, 17 p. and map.

Richardson, J., 1828. *In* J. Franklin, 1828. Narative of a second expedition to the shores of the polar sea in the years 1825, 1826, and 1827. John Murray, London, p. xli.

——— 1851. Arctic searching expedition. Longman, Brown, Green and Longmans, London, Vol. 1, 413 p.

Rummel, F., 1987. Fracture mechanics approach to hydraulic fracturing stress measurements, p. 217-240. *In* B.K. Atkinson, ed., Fracture Mechanics of Rock. Academic Press, London, Chapter 6.

Ryckborst, H., 1975. On the origin of pingos. Journal of Hydrology, 26: 303-314.

Scott, W.J., 1975. Preliminary experiments in marine resistivity near Tuktoyaktuk, District of Mackenzie. Geological Survey of Canada, Paper 75-1, Part A: 141-145.

Scott, W.J. and Hunter, J.A., 1977. Applications of geophysical techniques in permafrost regions. Canadian Journal of Earth Sciences, 14: 117-127.

Scotter, G.W., 1985. A pingo in the Mala River Valley, Baffin Island, Northwest Territories, Canada. Arctic, 38: 244-245.

Seppälä, M., 1988. Rock pingos in northern Ungava Peninsula, Quebec, Canada. Canadian Journal of Earth Sciences, 25: 629-634.

Shearer, J.M., Macnab, R.F., Pelletier, B.R. and Smith, T.B., 1971. Submarine pingos in the Beaufort Sea. Science, 174: 816-818.

Shumskii, P.A., 1959. Principles of Geocryology. Part 1, General Geocryology, Chapter lX, Ground (subsurface) ice (in Russian), p. 274-327. Academy of Sciences of the U.S.S.R, V.A. Obruchev Institute of Permafrost Studies, Moscow. Translated by C. De Leuchtenberg, National Research Council Canada, Ottawa, TT-1130, 1964, 118 p.

——— 1964. Principles of structural glaciology. (translated from Russian). Dover Publications, New York, 497 p.

Shumskii, P.A. and Vtyurin, B.I., 1966. Underground ice. *In* Permafrost International Conference, 1963, Lafayette, Indiana. National Academy of Science - National Research Council, Washington, D.C., Publication 1287: 108-113.

Soloviev, P.A., 1973. Thermokarst phenomena and landforms due to frost heaving in Central Yakutia. Biuletyn Peryglacjalny, 23: 135-155.

Song, H. and Xia, Y., 1988. Fossil-pingo lake peatlands in the Sanjang Plain (in Chinese). Journal of Glaciology and Geocryology, 10(1): 76-83.

Souchez, R.A. and Jouzel, J., 1984. On the isotopic composition in δD and $\delta^{18}O$ of water and ice during freezing. Journal of Glaciology, 30: 369-372.

Souchez, R.A. and De Groote, J.M., 1985. δD-$\delta^{18}O$ relationships in ice formed by subglacial freezing: paleoclimatic implications. Journal of Glaciology, 31: 229-232.

Stager, J.K., 1956. Progress report on the analysis of the characteristics and distribution of pingos east of the Mackenzie Delta. The Canadian Geographer, 7: 13-20.

St-Onge, D.A. and Pissart, A., 1990. Un pingo en système fermé dans des dolomies paléozoïques de l'Arctique canadien. Permafrost and Periglacial Processes, 1: 275-282.

Taber, S., 1930. The mechanics of frost heaving. Journal of Geology, 38: 303-317.

Takashi, T., Yamamoto, H., Ohrai, T. and Masuda, M., 1978. Effect of penetration rate of freezing and confining stress on the frost heave ratio of soil. *In* Proceedings, Third International Conference on Permafrost, Edmonton, Alberta, Canada. National Research Council of Canada, Ottawa. 1: 737-742.

Tarnocai, C. and Netterville, J.A., 1976. Some characteristics of a pingo in the Simpson Peninsula, N.W.T. Canadian Journal of Earth Sciences, 13: 490-492.

Taylor, G., 1945. Arctic Survey. 111. A Mackenzie Domesday: 1944. Canadian Journal of Economics and Political Science, 11: 189-233.

Taylor, A.E. and Judge, A.S., 1977. Canadian Geothermal data collection - northern wells 1976-77. Energy, Mines and Resources Canada, Earth Physics Branch, Ottawa, Geothermal Series, No. 10, 194 p.

Tolstikhin, N.I. and Tolstikhin, O.N., 1974. Groundwater and surface water in the permafrost region (in Russian). *In* P.I. Melinkov and O.N. Tolstikhin, eds., Chapter IX, General Permafrost Studies, USSR Academy of Sciences, Siberian Branch, Novosibirsk. English translation published by Environment Canada, Inland Waters Directorate, Ottawa, 1976. Technical Bulletin No. 97, 25 p.

Tsytovich, N.A. and Sumgin, M.I., 1937. Principles of frozen ground mechanics (in Russian). Moscow, Izdatel'stvo Akademii Nauk SSSR, 423 p.

Tsytovich, N.A. 1955. Influence of freezing conditions on the porosity of water saturated sands (in Russian). *In* Voprosy geologii Azii (Problems of the Geology of Asia), USSR Academy of Sciences Press, 2: 612-628.

——— 1959. Principles of Geocryology (Permafrost Studies), Part 11: Engineering Geocryology, Pore water expulsion (in Russian). Chapter 3. Academy of Sciences of the U.S.S.R., V.A. Obruchev Institute of Permafrost Studies, Moscow.

——— 1975. The mechanics of frozen ground (translated from the Russian). Scripta Book Company, Washington, D.C., 426 p.

Tsytovich, N.A., Vyalov, S.S., and Shusherina, E.P., 1959. Physico-mechanical properties, p. 108-152. *In* Tsytovich *et al.* eds., Principles of Geocryology, Part 1. General Geocryology. Chapter V. Physical phenomena and processes in freezing, frozen and thawing soils (in Russian). Academy of Sciences of the U.S.S.R., V.A. Obruchev Institute of Permafrost Studies, Moscow. Translated by G. Belkov, National Research Council of Canada, Ottawa, TT-1164, p. 24-25.

Vaslet, D., 1990. Upper Ordovician glacial deposits in Saudi Arabia. Episodes, 13: 147-161.

Vtyurin, B.I., 1975. Underground ice in the U.S.S.R. (in Russian). Nauka, Moscow, 212 p.

Walker, D.A., Walker, M.D., Everett, K.R. and Weber, P.J., 1985. Pingos of the Prudhoe Bay Region, Alaska. Arctic and Alpine Research, 17: 321-336.

Walker, M.D., Everett, K.R., Walker, D.A. and Birkeland, P.W., 1996. Soil development as an indicator of relative pingo age, Northern Alaska, U.S.A. Arctic and Alpine Research, 28: 352-362.

Wang, S. and Yao, H., 1981. On the pingos along both banks of the Qing-Shui River on Qinghai-Xizang Plateau (in Chinese). Journal of Glaciology and Cryopedology, 3(3): 58-62.

Wang, B. and French, H.M., 1995. Permafrost on the Tibetan Plateau, China. Quaternary Science Reviews, 14: 255-274.

Warrick, R. and Oerlemans, J. 1990. Sea level rise, p. 268-281. *In* J.T. Houghton, G.J. Jenkins, and J.J. Ephraums, eds., Climate Change. The IPCC Scientific Assessment, Cambridge University Press.

Washburn, A.L., 1980. Geocryology: A survey of periglacial processes and environments. John Wiley, New York, 406 p.

Watson, E., 1977. The periglacial environment of Great Britain during the Devensian. Philosophical Transactions Royal Society of London, B, 280: 183-198.

Williams, P.J. and Smith, M.W., 1989. The frozen earth: Fundamentals of geocryology. Cambridge University Press, 306 p.

Worsley, P. and Gurney, S.D., 1996. Geomorphology and hydrogeological significance of the Holocene pingos in the Karup Valley area, Traill Island, northern east Greenland. Journal of Quaternary Science, 11: 249-262.

Yoshikawa, K. and Harada, K., 1995. Observations on nearshore pingo growth, Adventdalen, Spitsbergen. Permafrost and Periglacial Processes, 6: 361-372.

Young, F.G., Myhr, D.W. and Yorath, C.J., 1976. Geology of the Beaufort-Mackenzie Basin. Geological Survey of Canada, Paper 76-11: 63 p.

Zhestkova, T.N., 1982. Formation of the cryogenetic structure of frozen ground (in Russian). Akademia Nauk SSSR, Izdatel'stva, Nauka, Moscow, 216 p.